TEXAS Geosciences
The University of Texas at Austin
Jackson School of Geosciences

6th Annual
Jackson School of Geosciences
Student Research Symposium

February 4, 2017

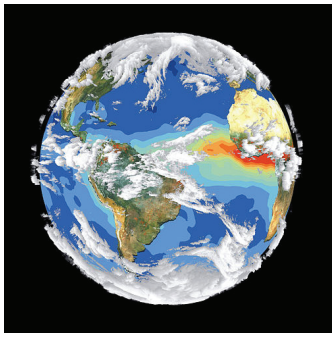


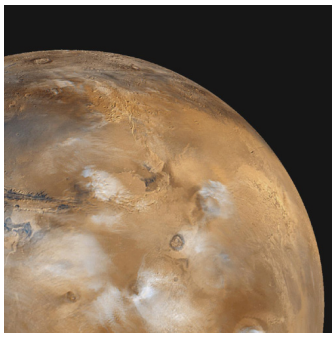

ConocoPhillips

Jackson School of Geosciences
GSEC
Graduate Student Executive Committee

Welcome to the 6th Annual Jackson School Research Symposium

It is with great pleasure we welcome you all to the 6th Annual Jackson School Research Symposium at UT-Austin! This symposium would not have been possible without the hard work of student volunteers, the support of faculty/research scientists, and generous support from ConocoPhillips. Thank you for taking part in supporting our students and growing research program within the Jackson School. Enjoy the posters!

Schedule of Presentations and Events

Breakfast, A.M. session poster set-up.....8:30 a.m.

Early Career Graduate (ECG) posters.....9:00-11:30 a.m.

Late Career Masters (LCM) posters.....9:00-11:30 a.m.

Lunch, A.M. session poster take-down.....11:30 a.m.

P.M. session poster set-up.....12:30 p.m.

Undergraduate (U) posters….....1:00-3:30 p.m.

Late Career PhD (LCPhD) posters.....1:00-3:30 p.m.

Happy hour/judging.....3:30 p.m.

Awards/closing.....4:00 p.m.

Table of Contents

A.M. POSTER LAYOUT

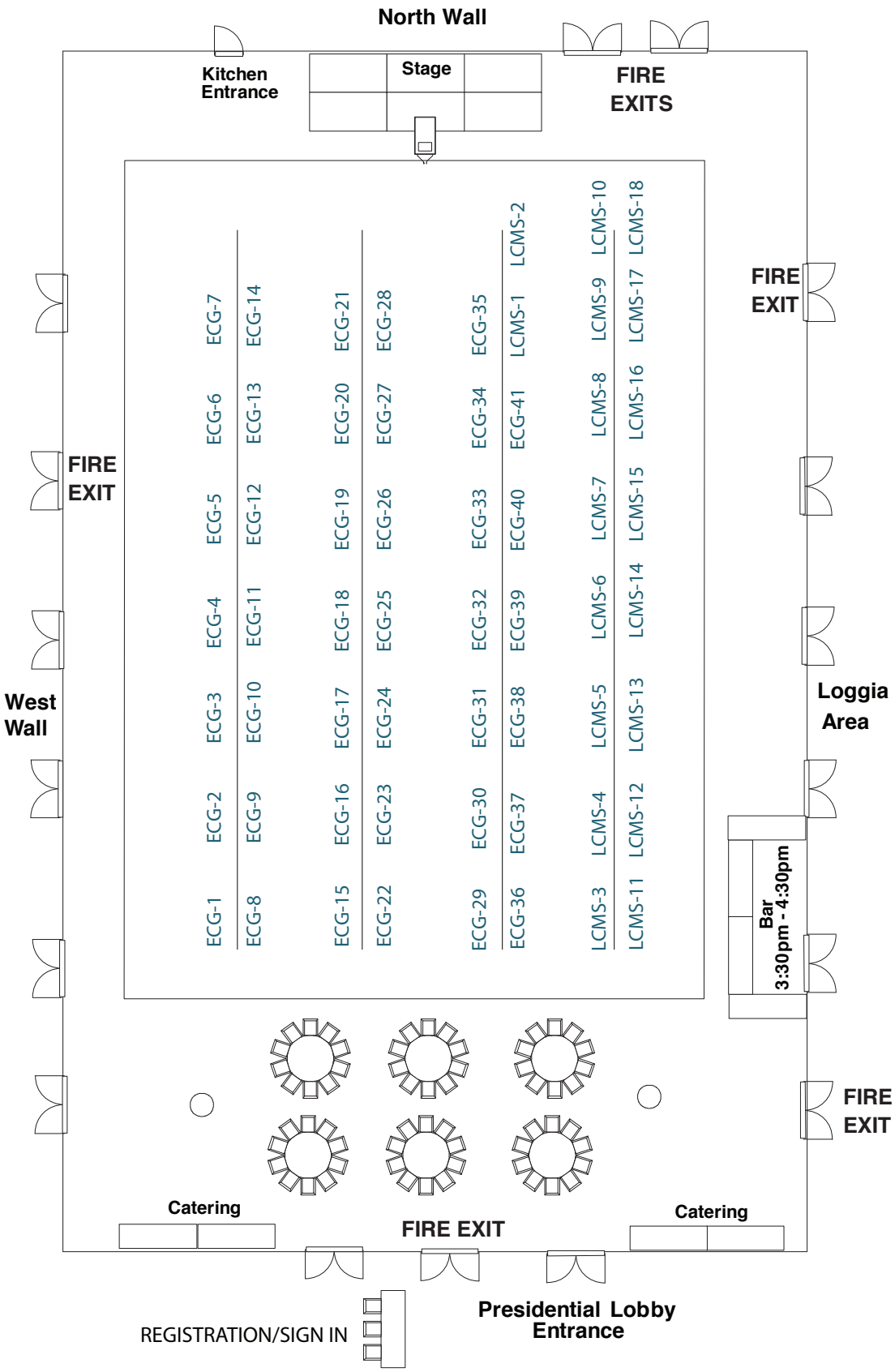

P.M. POSTER LAYOUT

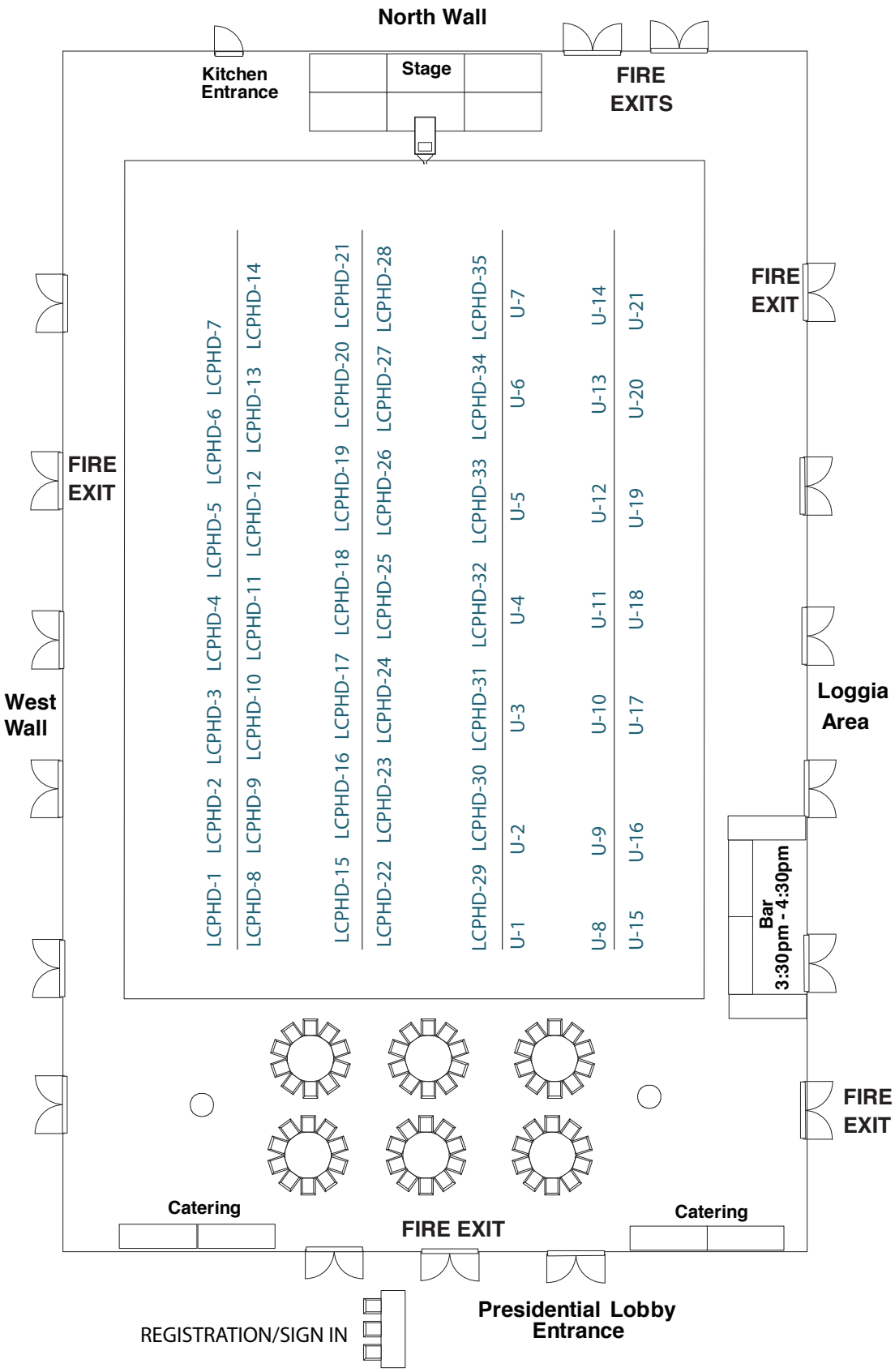

ECG

Hydroclimate of North Island of New Zealand During the Last 45,000 Years

Natallia Piatrunia
Piatrunia, N., University of Texas at Austin
Shanahan, T., University of Texas at Austin
Augustinus, P., University of Auckland
Atkins, D., University of Auckland
Huang, Y., Brown University

Southern Hemisphere climate variability and its connection with past changes in the Northern Hemisphere remains poorly understood. While climate conditions in the polar regions are well-studied, the spatial and temporal resolution of existing Southern Hemisphere mid-latitude records is limited. New Zealand provides an ideal location for the preservation of high-resolution multi-proxy records in lacustrine cores and the analysis of mid-latitude climate throughout the Holocene and beyond. Here, we present a 45,000-year record of terrestrial plant wax dD (a proxy for precipitation and moisture source) and branched GDGT-derived temperatures from Lake Pupuke, on the North Island of New Zealand (36°78.30'S, 174°76.70'E). We find that during the last glacial the North Island experienced colder and drier conditions, with temperatures that were > 3.5°C cooler than those experienced during the Holocene. Plant wax dD values vary substantially during the glacial interval, with the most enriched values occurring at ~21 kyr and 24.5 and 35.5 kyr. Shifts to more arid conditions during these intervals were potentially associated with intensification of the SH westerlies and the northward migration of the subtropical (STF), subpolar (SPF) and polar fronts (PF). The Lake Pupuke record suggests that deglaciation of New Zealand initiated at ~19 kyr, with gradual increases in temperature. Temperature increases abruptly during the Bolling-Allerod warming – coincident with changes in the Northern Hemisphere.

Keywords: plant wax dD, branched GDGTs, hydroclimate, lacustrine sediments, New Zealand

CCG
ECG

Aberrant bivalves and tenacious corals of the Early Jurassic, Morocco: Survivors of extinction and oceanic anoxia

Hannah-Maria Brame
Ettinger, N., The University of Texas at Austin, Austin, TX
Martindale, R., The University of Texas at Austin, Austin, TX
Bodin, S., Ruhr-Universität Bochum, Institut für Geologie, Mineralogie und Geophysik, Bochum, Germany

Reef ecosystems are particularly sensitive to environmental changes, specifically global warming and ocean acidification. Concerns regarding the future sustainability of modern reefs have prompted paleontologists to investigate how ancient reefs have responded to similar environmental stresses in the past. Analyses of reef ecosystems in deep time provide an opportunity to evaluate the causes of ecosystem collapse and the timing and dynamics of recovery. Although a direct analogue for modern reefs may not exist, examination of intervals of major reef turnover in Earth's history can provide an invaluable context for evaluating the potential long-term trajectory of modern reef ecosystems. Furthermore, it is critical to examine the full range of possible reef ecologies, including those that persist within unique post-extinction environments (i.e. survivors).

The Early Jurassic is characterized by pronounced environmental disruptions; in the late Pliensbachian and early Toarcian there is the emplacement of the Karoo-Ferrar large igneous province, rapidly increased atmospheric CO2 concentrations, global warming, sea-level rise, and associated perturbations to global geochemical cycles. In the oceans, the early Toarcian is marked by 1) the deposition of organic-rich black shales (Toarcian Oceanic Anoxic event [T-OAE]), which record pulses of oceanic anoxia, 2) possible ocean acidification, 3) a multi-phased mass extinction at the Pliensbachian-Toarcian boundary/T-OAE, and 4) a significant metazoan reef crisis. During the Early Jurassic, a group of large, aberrant bivalves ("Lithiotids") arise and proliferate in nearshore marine environments, often forming substantial gregarious buildups and "biostromes". Unlike most boundary sections, in Morocco, Lithiotids persist across the Pliensbachian-Toarcian boundary and are frequently associated with corals.

For this study, detailed lithostratigraphic data were collected for two sections of late Pliensbachian and early Toarcian strata in the Western High Atlas that record extensive Lithiotid buildups and biostromal growth along a mixed carbonate-siliciclastic ramp. All five Lithiotid genera are documented here and display diverse growth forms and colony architectures. Notably, the occurrence of Lithiotids (and co-occurrence with corals) is rarely observed within the early Toarcian, and this study documents Lithiotid-coral associations bracketing the Pliensbachian/Toarcian boundary. The Moroccan sites studied here provide spectacular, expanded stratigraphy for the study of the proliferation and collapse of unique Lithiotid-coral reef ecosystems not possible elsewhere in the world. Continued examination of this interval has the potential to expand our understanding of the ecology of aberrant reef-forming bivalves and the reef dynamics of intervals of characterized by environmental perturbations.

Keywords: Jurassic, Lithiotids, bivalves, corals, ecology, Morocco, extinction

CCG
ECG

The Impact of Landscape Nitrogen Dynamics on Water Quality in Texas

Seungwon Chung
Chung, S., Jackson School of Geosciences, The University of Texas at Austin, Austin, TX
Yang, Z., Jackson School of Geosciences, The University of Texas at Austin, Austin, TX

Nutrient transport and processes are significantly modified by human activities. Land use and land cover have impacts on nutrient inputs and pathways in the terrestrial ecosystems and on nutrient loading in rivers and other water bodies. Nutrient transport plays a critical role in water quality across watersheds. This study presents a modeling framework for integrating terrestrial nitrogen inputs (Net Anthropogenic Nitrogen Inputs, NANI), a land surface model (The community Noah land surface model with multi-parameterization options, Noah-MP-CN) and a river routing model (Routing Application for Parallel computation of Discharge, RAPID) to simulate nitrogen transport in river networks. The Noah-MP-CN model was originally developed for weather and climate prediction, but recent modifications to the Noah-MP-CN model introduce large capabilities for nitrogen dynamics and hydrological simulations in river networks. A two-year case study is conducted in the San Antonio and Guadalupe basins during dry and wet years (2009 and 2010, respectively). The Noah-MP-CN model provides daily nitrogen loads to the river reaches through runoff. Nitrogen loadings are transported through streamflow to downstream of river basins under the impact of in-stream processes. The modeled nitrate concentrations are evaluated with the observed data at the United States Geological Survey (USGS) gauge stations near the outlets of river basins.

Keywords: nitrogen transport, nitrogen dynamics, anthropogenic nitrogen inputs

CCG
ECG

Origin of Novel Color Phenotypes: Contribution of Structural Properties of Biochemical Networks

Sarah Davis
Davis, S., Department of Geological Sciences, The University of Texas at Austin, Austin, TX
Morrison, E., Department of Ecology and Evolutionary Biology, The University of Arizona, Tucson, AZ
Badyaev, A., Department of Ecology and Evolutionary Biology, The University of Arizona, Tucson, AZ

Examining the phenotypic variation observed within a species is an opportunity to understand the mechanisms that underlie the overall stability of a trait. In this study, we investigate what determines the likelihood for phenotypic change and the magnitude of this change within a species. Feather coloration in many birds is produced through complex biochemical networks that modify ingested, dietary compounds to produce final colorful carotenoids which are deposited within the feather matrix. Within-species color variation can be caused by variation in either the structure of this network or the way it is used to regulate flux of compounds. Here we test the contribution of structural properties across individuals from 21 populations of house finches (*Haemorphous mexicanus*) in Montana and Arizona to study the stability of color-producing enzymatic pathways that underlie population divergence in color phenotypes. With the largest carotenoid network of any studied species, the house finch provides an ideal system to address the relative contribution of differences in how the expression of this network changes during population divergence. Using high performance liquid chromatography, we extracted and identified the carotenoid compounds from over 3,000 feather samples. We analyzed the relationship between the presence of different compounds across the populations and their topological positions within the network. We then determined what mechanisms are driving these patterns of diversification—whether populations diverge along the same or different pathways within the network. We found that populations were more distinct in the presence of derived vs dietary compounds, suggesting that evolution of biochemical synthesis accompanied recent population divergence in ecologically distinct locations.

Keywords: Phenotypic variation, population divergence, biochemical network, carotenoids, feather coloration

CCG
ECG

Postcranial Anatomy of Kayentatherium wellesi: Swimming Adaptations in a Mammal Relative from the Early Jurassic

Eva Hoffman
Hoffman, E., Jackson School of Geosciences, The University of Texas at Austin, Austin, TX
Rowe, T., Jackson School of Geosciences, The University of Texas at Austin, Austin, TX

An increasingly rich fossil record has shed new light on ecomorphological diversification during the early evolution of the mammalian lineage. The earliest mammals and their relatives were not confined to a generalized insectivorous niche; instead, recent fossil evidence suggests the repeated evolution of morphological specializations reflecting a variety of ecological roles. Adaptations for a semiaquatic lifestyle have been described previously in docodontans, a Mesozoic mammaliaform clade. Our interpretation of previously undescribed postcranial material from *Kayentatherium wellesi*, a tritylodontid from the Early Jurassic of Arizona, indicates that semiaquatic habits were also present in a more basal mammaliamorph lineage, and thus may have had a broader importance than previously recognized in the evolutionary history of Pan-Mammals. In *Kayentatherium*, morphological features of the tail and hindfoot, including bifurcate transverse processes of the caudal vertebrae and an expanded semicircular base of the first metatarsal, indicate convergence with modern semiaquatic mammals such as beaver and platypus. Comparative and functional inference suggest that *Kayentatherium* was an adept swimmer. Phylogenetic analysis, aided by inclusion of new postcranial characters, is needed to resolve the position of tritylodontids within Eucynodontia, so that the evolution of semiaquatic behavior can be understood in the full context of mammalian evolutionary history.

Keywords: paleontology, vertebrate paleontology, morphology, mammals, mammalia, mammaliamorpha, tritylodontidae, semiaquatic, swimming

CCG
ECG

A Coral-based Reconstruction of Interannual Climate Variability at Vanuatu during the Medieval Climate Anomaly (950-1250 CE)

Allison Lawman
Lawman, A., Institute for Geophysics, The University of Texas at Austin, Austin, TX
Quinn, T., Institute for Geophysics, The University of Texas at Austin, Austin, TX
Partin, J., Institute for Geophysics, The University of Texas at Austin, Austin, TX
Taylor, F., Institute for Geophysics, The University of Texas at Austin, Austin, TX
Thirumalai, K., Institute for Geophysics, The University of Texas at Austin, Austin, TX
Wu, C., Department of Geoscience, National Taiwan University, Taipei, Taiwan
Shen, R., Department of Geoscience, National Taiwan University Taipei, Taiwan

The Medieval Climate Anomaly (MCA: 950-1250 CE) is identified as a period during the last 2 millennia with Northern Hemisphere surface temperatures similar to the present. However, our understanding of tropical climate variability during the MCA is poorly constrained due to a lack of proxy records that cover this time period. We investigate sea surface temperature (SST) variability during the MCA using geochemical records developed from well preserved fossilized corals from the tropical southwest Pacific (Tasmaloum, Vanuatu; 15° 37' S, 166° 54.5' E). We present Sr/Ca from a 1.68-m-long *Porites lutea* coral head collected from Tasmaloum, Vanuatu. An absolute U/Th date of 1127.1 ± 2.7 CE indicates that the selected fossil coral lived during the MCA. To put the results from the fossil coral into context relative to the modern day, we also present a modern 164-year-long Sr/Ca record from Sabine Bank, Vanuatu, located ~90 km to the SW of Tasmaloum. Preliminary assessment of >100 years of monthly resolved Sr/Ca data from the fossil coral yields a median value of 26.1°C, and an average annual cycle of 3.4°C based on modern Sr/Ca-SST calibrations. We find that the median SST at Vanuatu was 1.3 ± 0.7°C cooler relative to the modern, and that the magnitude and variability of the SST annual cycle are larger that what is observed in gridded SST datasets and modern coral Sr/Ca-SST reconstructions for Vanuatu. Future work will focus on further quantifying the uncertainty in our SST estimates by replicating these results with another fossil coral that grew during MCA.

Keywords: paleoclimatology, paleoceanography

CCG
ECG

Latitudinal Relationship between Ecosystem Water Use Efficiency and Vegetation Attributes in North American Forest Ecosystem

Lingcheng Li
Li, L., Jackson School of Geoscience, The University of Texas at Austin, Austin, TX
Wei, J., Jackson School of Geoscience, The University of Texas at Austin, Austin, TX
Yang, Z., Jackson School of Geoscience, The University of Texas at Austin, Austin, TX

Ecosystem water use efficiency (EWUE) is the ratio of carbon gain (i.e. gross primary production GPP) to water loss (i.e. evapotranspiration ET). EWUE implicates interactions between the global carbon cycle and the global water cycle. In this study, we examine relationships between EWUE and a wide range of vegetation attributes (VAs) for the North American forest ecosystems. Results show that the slope of ????????????????/????????????? is larger at high latitudes than at low latitudes. It is mainly because of the smaller slope of *?ET/?*????????????? at high latitudes, which is caused by the smaller ratio of transpiration to evapotranspiration. The latitudinal relationship between EWUE and VA can be used as a benchmark to evaluate land surface models.

Keywords: Water Use Efficiency, Vegetation Attributes, North American Forest Ecosystem

CCG
ECG

Cranial osteology of extinct and extant gerrhonotine lizards

Simon Scarpetta
Scarpetta, S., University of Texas at Austin
Ledesma, D., University of Texas at Austin

Gerrhonotinae is an extant clade of anguid lizards with a rich Cenozoic fossil record in the Americas and a diverse assemblage of species that still inhabit regions of North America and much of Central America. My preliminary analysis of x-ray computer tomography (CT) scans of a previously known but as of yet unidentified Pliocene lizard specimen from the Palm Spring Formation in Anza Borrego Desert State Park in southern California has determined it to be a potentially new species of gerrhonotine most likely belonging to the genus *Elgaria*. More specific taxonomic and phylogenetic affiliation has yet to be determined. Species belonging to the genera *Elgaria* are currently found in western and central North America, often in mesic habitats. Despite the relative familiarity of some species to biologists and paleontologists, comprehensive studies of the cranial anatomy of *Elgaria* are currently lacking. Description of the bones in the skull supplies useful data for examining morphological variation and phylogeny, and thus provides an excellent tool for any morphological study. Here, I aim to describe the anatomy of the skulls of the nine species of *Elgaria* as well as select other gerrhonotine taxa, especially species from the genus *Gerrhonotus* as well as the genera *Mesaspis*, *Barisia*, and *Abronia*. This method will provide novel anatomical information for many of the almost 60 modern gerrhonotine species, greatly expanding the currently limited cranial osteological data available. Comprehensive cranial descriptions will supply the framework for diagnosing phylogenetic placement of fossils, in particular the Anza Borrego gerrhonotine specimen. I will employ traditionally prepared skeletons as well as CT scans; the latter enables me to generate data about rare specimens of many gerrhonotine species for which no skeletal data exists.

Keywords: Morphology, Gerrhonotinae, X-ray computed tomography, fossils

CCG
ECG

The role of carbon use efficiency and isotopic fractionation during microbial respiration to the down-profile increase in the carbon isotope ratio of soil organic matter

Lily Serach
Serach, L., Department of Geological Sciences, The University of Texas at Austin, Austin, TX

The increases in the stable C isotope ratio (δ13C) of soil organic carbon (SOC) with depth common in well-drained soils are widely accepted as being due to the C isotope fractionation between CO2 and SOC during microbial respiration. However, results from previous studies that investigate C isotope fractionation during respiration are conflicting. Respired CO2 with 13C values lower, higher and not significantly different than the associated SOC have been reported in the literature. This project aims to quantify the contribution of isotopic fractionation during microbial respiration to the down-profile shift in δ13C values by means of a long-term (2 year) incubation of topsoil (0-2cm). The topsoil used in the incubations was collected from undisturbed temperate and tropical forests. At each location, soil profiles from 0-20 cm depth were also collected and the down profile trends in concentrations and δ13C values of bulk organic carbon were measured. The CO2-SOC carbon isotope enrichment factor εCO2-SOM required to explain each profile was then calculated. We compared these calculated εCO2-SOM values with empirical values determined from soil incubations. εCO2-SOM values were determined from incubations as the difference between δ13C values of headspace CO2 and bulk SOC. We have thus far measured these δ13C values at 1,4 and 7 months, allowing us to track if and when empirical εCO2-SOM values reach the magnitude required to explain the profiles. Thus far, all empirical εCO2-SOM values are either too small or of the wrong sign to explain the profiles, suggesting that a mechanism other than C isotope fractionation during microbial respiration may be responsible. Therefore, we are also investigating the possibility that the anthropogenic increase in concentrations of atmospheric CO2, through its influence on δ13C values of C3 plants, explains a substantial portion of the typical down profile increase in SOC δ13C values.

Keywords: soil, 13C, carbon, soil organic matter, stable isotopes

CCG
ECG

Distribution of branched glycerol dialkyl glycerol tetraethers in soils on the Northeastern Qinghai-Tibetan Plateau and possible production by nitrite-reducing bacteria

Chijun Sun
Sun, C., Department of Geological Sciences, The University of Texas at Austin, Austin, TX
Zhang, C., State Key Laboratory of Marine Geology, Tongji University, Shanghai, China
Li, F., State Key Laboratory of Marine Geology, Tongji University, Shanghai, China
Wang, H., State Key Laboratory of Loess and Quaternary Geology, Institute of Earth Environment, Chinese Academy of Sciences, Xi'an, China
Liu, W., State Key Laboratory of Loess and Quaternary Geology, Institute of Earth Environment, Chinese Academy of Sciences, Xi'an, China

Branched glycerol dialkyl glycerol tetraethers (bGDGTs) are ubiquitous and abundant in soils, but their sources remain elusive. Recent studies demonstrate that the distributions of bGDGTs are sensitive to various environmental factors. In an effort to understand how and to what extent soil moisture (expressed as soil water content (SWC) or mean annual precipitation (MAP), pH and temperature may impact the distribution of bGDGTs, and to shed more light on the biological sources of bGDGTs in cold and arid regions, we investigated the distribution of bGDGTs as well as bacterial 16S rRNA gene and functional genes involved in the N cycle (including *amoA*, *nirS* and *nirK*) in 41 surface soil samples from around Lake Qinghai and east of Qaidam Basin on the Northeastern Qinghai-Tibetan Plateau. We found that lower soil moisture reduced the fractional concentrations of cyclic bGDGTs and thus the cyclisation ratio of branched tetraethers (CBT) index correlated negatively with SWC and MAP, suggesting that soil moisture is an important factor controlling bGDGT distributions in soils in this arid and semi-arid region. Two subgroups of bGDGTs were assigned on the basis of cluster analysis, and bGDGT indices behaved differently in the two groups, hinting at different biosynthetic mechanisms for bGDGTs under different environmental conditions. Real time PCR results showed that *nirS* and *nirK* genes correlated significantly with the concentration of bGDGTs, suggesting that the *nirS*- or *nirK*-encoding bacteria involved in denitrification might potentially be an additional biological source for soil bGDGTs (besides Acidobacteria). Moreover, our results also support the application of new indices based on 5-methyl bGDGTs and 6-methyl bGDGTs in reconstructing past temperature and pH variations in this region.

Keywords: bGDGTs, Soil water content, CBT, nirS- or nirK-encoding bacteria, Real time PCR, Cluster analysis

CCG
ECG

A Preliminary Report on the Arvicoline Rodents from the Pleistocene Sites of Conard Fissure, Arkansas and Cumberland Cave, Maryland

Charles Withnell
Withnell, C., The University of Texas at Austin, Austin, TX

Arvicoline rodents (voles, lemmings, and muskrats) are some of the most common fossils found in North American Pleistocene mammal sites. Their rapid evolution and reputedly distinct dental characteristics make them excellent specimens for biochronological analyses. A lot of work in the Pleistocene has been done in the western, and Great Plains regions of North America. However not a lot of work has been done in the eastern portion of of the continent in the last 60 years. The utility of continent wide North American Land Mammal Ages (NALMAs) is something that a lot of researchers take at face value and do not look further into. At sites lacking absolute age control it is important to find other means for establishing the age range. Two such sites are the Conard Fissure, Arkansas and Cumberland Cave, Maryland. Here I present the preliminary results of two of the sites that will provide the foundation for my dissertation. For my dissertation I am going to examine several sites from the eastern United States to attempt to correlate and test the assumption of continent wide NALMAs for the Pleistocene. I will catalog and identify all the arvicoline rodents from the sites for the respective museums, establish taxonomic affinity whenever possible, and attempt to establish a more refined biochronologic age range. Primarily I will be using the lower first molar (m1) and upper third molar (M3) because these have proven to be the most useful for establishing generic as well as species differentiation. Traditional morphological classification of the morphotypes will be utilized and possibly untraditional methods such as morphometrics to better distinguish between morphotypes. The overall objective of this study is to test provinciality, and the validity of continent wide NALMAs during the Pleistocene.

Keywords: Arvicoline rodents, biochronology, Pleistocene, vertebrate paleontology

CCG
ECG

What Controls the Duration of El Niño and La Niña Events?

Xian Wu
Wu, X., Institute for Geophysics, The University of Texas at Austin, Austin, TX
Okumura, Y., Institute for Geophysics, The University of Texas at Austin, Austin, TX
DiNezio, P., Institute for Geophysics, The University of Texas at Austin, Austin, TX

The El Niño-Southern Oscillation (ENSO) in the tropical Pacific is the largest source of interannual climate variability around the world. El Niño events tend to decay rapidly after peaking near the end of the calendar year while La Niña events often persist through the following year and re-intensify in boreal winter. The temporal evolution of individual El Niño and La Niña, however, varies considerably from event to event. To understand the factors affecting the duration of ENSO events, we analyze a suite of observational data as well as a long control simulation of the Community Climate System Model version 4. Both the observational and model analyses show that strong and early-onset El Niño events tend to decay rapidly, while weaker and late-onset El Niño events tend to last longer. The equatorial western Pacific winds after the peaking of El Niño are also key factors for the duration of El Niño. The duration of La Niña events tends to be dominated by the amplitude of preceding El Niño events and not affected by the western Pacific winds as significantly as that for El Niño.

Keywords: El Niño-Southern Oscillation

EG
ECG

Semiautomatic Seismic to Well Ties

Sean Bader
Bader, S., Bureau of Economic Geology

The seismic to well tie is a subjective, labor-intensive, workflow depending on the interpreter's experience and intuition. It is also the key link between borehole measurements and seismic data. Several efforts have been made to automatically tie wells by focusing on local reflectors instead of maximizing a global correlation coefficient. One of these methods, local similarity, is used to automatically tie well data to seismic data so well ties are more consistent and accurate. These ties are quality checked and updated using predictive painting to interpolate log data to a single location along seismic structure. This method is tested on the Teapot Dome seismic dataset where multiple wells are accurately tied to the seismic data and log data are interpolated between wells. These interpolated data are tested with a blind well test and show promising results.

Keywords: synthetic well, well tie, interpolation

EG
ECG

Sequence Stratigraphy and Structure of the Wolfcampian Hueco Platform on the Southwestern Margin of the Delaware Basin

Taylor Canada
Canada, T., Jackson School of Geoscienes, Bureau of Economic Geology, The University of Texas at Austin, Austin, TX
Kerans, K., Jackson School of Geoscienes, Bureau of Economic Geology, The University of Texas at Austin, Austin, TX
Zahm, C., Bureau of Economic Geology, The University of Texas at Austin, Austin, TX

The Wolfcamp resource play has become one of the most important and most active oil and gas targets in the U.S. during the recent industry downturn. Presently, over 25% of all active rigs in the U.S. are targeting the Wolfcamp in the Delaware Basin per Baker Hughes. Despite this current production interest, the Wolfcampian strata in the Delaware Basin lack a detailed platform-to-basin sequence stratigraphic model. Kerans and Ruppel (1994), Fitchen (1997), and Kerans and Tinker (1999) have developed a framework for the Leonardian-Guadalupian outcrops surrounding the western and northern margins of the Delaware Basin but this model has not yet been extended to the Bone Spring in detail nor has the Wolfcampian section below been addressed in an integrated shelf-to-basin framework. Late Carboniferous-early Permian Ouachita-Marathon tectonic activity has created a complex setting with active compression, strong differential subsidence, and near-peak icehouse eustacy during Wolfcamp deposition in the Delaware Basin. This complexity coupled with limited outcrop availability has created a challenging setting for characterizing Wolfcampian strata on the platform and in the basin.

The primary record of Wolfcampian platform-to-slope carbonate production in the southwestern Delaware Basin is the Hueco Formation exposed in the Sierra Diablo, Baylor, and Wylie Mountains. Fitchen (1997) and Playton and Kerans (2002) characterized the Hueco Formation in the Sierra Diablo Range as including platform interior, platform margin, and slope carbonate deposits and established a tentative sequence stratigraphic framework for the area. The Sierra Diablo and Baylor Mountains have since become inaccessible but the Wylie Mountains represent an accessible and extensive Hueco platform succession. This succession will be characterized in the context of its stratigraphic and structural events to understand sequence development and the effects of Ouachita-Marathon tectonism on platform evolution. This study can then be tied to the Hueco sections studied in the Sierra Diablo Range to construct a platform-to-basin model for Wolfcampian deposition on the southwestern margin of the Delaware Basin.

Stratigraphic section logging and fault mapping in the field will be supplemented by a drone captured 3D outcrop model to understand 3D platform architecture and its response to syn- and post-depositional tectonic activity. Preliminary data collected by Kerans and Zahm from the western escarpment of the Wylie Mountains in August 2016 indicate a suite of platform interior carbonate facies showing a high degree of lateral heterogeneity and a range of intertidal to subtidal environments. The outcrop is also extensively faulted and will be mapped in detail to determine the timing and effects of these faults on platform growth.

Keywords: Carbonate sedimentology, sequence stratigraphy, sedimentology, reservoir characterization

EG
ECG

Computed Tomography (CT) Scanning of a Berea Sandstone at Different Resolutions to Compare Results in Density, Porosity, and Elastic Properties

Eric Goldfarb
Goldfarb, E., Jackson School of Geosciences, The University of Texas at Austin, Austin, Texas
Ikeda, K., Jackson School of Geosciences, The University of Texas at Austin, Austin, Texas
Spikes, K., Jackson School of Geosciences, The University of Texas at Austin, Austin, Texas
Tisato, N., Jackson School of Geosciences, The University of Texas at Austin, Austin, Texas

Porosity, permeability, and elastic properties are rock effective properties that are used for modelling flow and volume for groundwater, subsurface contamination, and hydrocarbons. A plethora of laboratory and field methods are used to estimate these properties, and when combined they are time consuming and expensive, and typically investigate only very small rock volumes. In addition, they can permanently damage a sample which may not be in abundance. Digital rock physics (DRP) is a field of study where a sample is converted to a digital model that could be used to numerically calculate rock properties. X-ray computed tomography (CT) is a non invasive DRP method, but has a major pitfall with its processing requirements. The most common DRP processing method requires segmenting each data point, or voxel, into a specific mineral and assigning properties from the literature. To work effectively, segmentation requires very high resolution voxels (i.e., sub-micrometric in size) in order to detail the features that control the rock effective properties such as cracks and grain contacts. The downside with this requirement is that DRP samples are at most 2 mm cubed, and often less, in order to prevent terabytes of memory for computer processing being required. The project team is presenting a new method to obtain physical properties of rocks via DRP without using segmentation. A Berea sandstone was scanned with a resolution of 16.7 microns per voxel. Using targets (sometimes called ghosts) with known densities, a calibration curve was created to convert the measured X-Ray intensity to density in g/cm^3. A density to porosity conversion used their inverse relationship for monomineralic rocks. For each voxel, permeability and elastic properties came from the Kozeni-Carman relationship, and the modified upper Hashin-Shtrikman bound, respectively. Effective permeability, V_p and V_s of the entire volume were estimated by numerically simulating water fluid flow and propagation of ultrasonic waves. Voxels were then averaged together to simulate poorer resolutions and the estimate of voxel properties was recalculated. The properties from the segmentation-less method are consistent at a range of resolutions up to 300 microns per voxel. Therefore, a more representative sample of 20 times the size could be scanned at $1/20^{th}$ the resolution, to obtain a result of the same size digital dataset, without a loss of information. This overcomes a major obstacle for traditional segmented scanning, which limits sample sizes.

Keywords: Computed Tomography, Digital Rock Physics, Berea, Porosity, Permeability, Elastic Properties.

EG
ECG

Stratigraphic Interpretation of Neogene Sediment Transport and Channels of the Mississippi Fan, Southeastern Gulf of Mexico

Mario Gutierrez
Gutierrez, M., Institute for Geophysics, J. J. Pickle Research Campus, University of Texas at Austin, Austin, Texas, USA
Snedden, J., Institute for Geophysics, J. J. Pickle Research Campus, University of Texas at Austin, Austin, Texas, USA

The Neogene depositional extent of the Mississippi Fan in the Southeastern Gulf of Mexico has been one of the most thoroughly studied modern deepwater fan systems due to the motivation of the active hydrocarbon exploration efforts on underlying stratigraphic units. After the regional sediment depocenter into the Gulf of Mexico shifted eastward during the early Neogene, the largely mud-dominated submarine fan developed into the dominant sediment provider into the Gulf. The Pliocene and Pleistocene are periods of the highest sediment flux throughout the life of the fan, creating over 4 Kilometer thick stratigraphic units in some places of the fan.

Sediment transport and channel development of the proximal extent fan has been documented with 2-D seismic surveys and well data since the 1980's, with development in seismic acquisition technology and complementary data integration refining the stratigraphic and structural interpretations. The geologic constraint of this study is focused on the distal extent of Pliocene and Pleistocene stratigraphy of the Mississippi Fan. The availability of reprocessed 2-D lines of the Yucatan and DeepEast surveys, select well control, and associated (biostratigraphic, petrographic, well log) data establishes an integrated stratigraphic framework of the canyon and older proximal lobes of the fan. This study will calibrate past interpretations with the availability of a new 3-D survey and multibeam data to identify distinct stratigraphic units within the fan and the corresponding seismic facies related to channel, MTD, levee, and lobes facies.

This interpretation, along with calibration of Cenozoic up dip wells, will produce high resolution maps of the youngest to modern distal extent of this fan in the Lund Production Area. This will result in a more detailed understanding of the Pliocene and Pleistocene deep water system development of the Mississippi Fan. The study also has implications which can potentially be applied to the study of other global mud-dominated submarine fans, as well as the current economic interests of hydrocarbon exploration in the Gulf of Mexico.

Keywords: Gulf of Mexico, Stratigraphy, Deep-water, Submarine Fan

EG
ECG

Modelling of the Relationship Between 2D and 3D Effective Elastic Properties

Ken Ikeda
Ikeda, K., Jackson School of Geoscience, The University of Texas at Austin, Austin, TX
Mavko, G., Rock Physics Laboratory, Department of Geophysics, Stanford University, Stanford, CA
Aliyeva, S., Rock Physics Laboratory, Department of Geophysics, Stanford University, Stanford, CA
Tisato, N., Jackson School of Geoscience, The University of Texas at Austin, Austin, TX

Digital rock physics allows calculating physical properties of rocks from analytical-method datasets such as optical microscopy or X-ray micro-computed tomography. However, the numerical process of deriving physical properties from two-dimensional (2D) analytical datasets is straightforward and requires fewer computational resources than from three-dimensional (3D) analytical datasets. Moreover, 2D images like those obtained from rock thin sections under optical microscopy are widely used, inexpensive and could be easily prepared. Nevertheless, the elastic properties estimated from 2D slices are typically lower than those obtained from 3D models because of geometry differences. For instance, a 2D circular cross-sectional shape obtained from a spherical inclusion behaves like a 3D infinitely long cylindrical tube that under plane strain conditions is more compliant than a sphere. This study investigates how the effective elastic properties of a 3D dataset can be accurately estimated by performing numerical experiments on a minimal number of 2D slices extracted from the 3D domain. Here, we test a quartz cubic volume containing several spherical water saturated pores (i.e., Finney Pack model). The materials are assumed to be isotropic and linear-elastic. The effective elastic properties of the samples are then evaluated with Finite Element Methods (FEM). Effective medium theories such as Hashin-Shtrikman bounds and differential effective medium (DEM) provide an upper and lower limit for effective moduli of the composite materials. In the numerical model, Finney Pack, we observe a strong linearity between the square root of the harmonic average of 3D and 2D moduli, and porosity which could be used to explain the relation between 2D and 3D effective bulk and shear moduli. Ultimately, geologists might be able to extract physical properties (i.e., elastic moduli) from rock thin-sections beside rock mineralogy.

Keywords: Digital Rock Physics, Elastic Properties

EG
ECG

Steady-State Liquid Permeability Tests in the Wolfcamp Formation, Permian Basin, West Texas

Sebastian Ramiro Ramirez
Ramiro-Ramirez, S., Institute for Geophysics, The University of Texas at Austin, Austin, TX
Bhandari, A., Institute for Geophysics, The University of Texas at Austin, Austin, TX
Polito, P., Bureau of Economic Geology, The University of Texas at Austin, Austin, TX
Flemings, P., Institute for Geophysics, The University of Texas at Austin, Austin, TX

We performed steady-state liquid permeability tests on a core plug from the Wolfcamp Formation at different confining pressures (Pc = 2000 to 9500 psia) while maintaining a constant mean pore pressure (Pp = 1000 psia). In the first loading cycle, the permeability decreased from 83.3 μD to 0.42 μD, and in the second loading cycle it decreased from 3.55 μD to 0.02 μD. We interpreted that this permeability decrease resulted from the closure of microfractures induced by either coring or core sampling. If most of these microfractures closed at the end of the second pressure loading cycle, we can infer that the matrix permeability of the sample is near 0.02 μD. We maintained a constant average pore pressure during both pressure cycles by setting the upstream and downstream ends of the core to constant flow rate and constant pressure respectively. When the test reached steady-state conditions (i.e., pressure difference between both ends of the core plug, ΔP, does not change over time) we plugged the corresponding ΔP value into Darcy's law for fluid flow in porous media to calculate the permeability. Very limited literature, if any, exists on liquid permeability experiments in tight rocks such as the Wolfcamp Formation. Here, we developed a novel testing protocol to obtain reliable liquid permeability results that will improve reservoir depletion plans in unconventional resource plays.

Keywords: Permeability, Petrophysics, Unconventional, Permian Basin

EG
ECG

Stress-Dependent Static-to-Dynamic Transforms of Anisotropic Mancos Shale

Matthew Ramos
Ramos, M., Jackson School of Geosciences, The University of Texas at Austin, Austin, TX
Espinoza, D., Department of Petroleum and Geossytems Engineering, The University of Texas at Austin, Austin, TX
Laubach, S., Jackson School of Geosciences, The University of Texas at Austin, Austin, TX

Shale mechanical behavior varies widely within and between formations, with layering-induced anisotropic rock properties complicating drilling, formation evaluation, and hydraulic fracturing. Core scale characterization of shale mechanical properties is valuable for understanding rock behavior in the laboratory, however measurement frequency and strain magnitude often limit upscaling to the wellbore and reservoir scales. The development of stress dependent static-to-dynamic transforms of shales provides a means for upscaling laboratory derived anisotropic rock properties, as well as understanding how these relationships may vary with changing stresses and induced damage. In this study, we conduct simultaneous triaxial stress tests and ultrasonic wave propagation monitoring to quantify static and dynamic stiffness anisotropy in Mancos Shale. Measurements of Mancos Shale plugs taken perpendicular, parallel, and at 45° to bedding allow for determination of the 5 independent stiffness parameters necessary to describe this pseudo transversely isotropic material, from which anisotropic quasi-static and dynamic Young's moduli and Poisson's ratios are calculated. Relationships between static and dynamic anisotropic effective moduli are presented as static-to-dynamic transforms, where the directional and stress dependences of stiffness are evaluated.

Results show anisotropic and nonlinear stress, strain, and damage dependences of static and dynamic moduli. In general, increases in confining stress caused increased Young's moduli for all plug orientations, but only impact Poisson's ratios corresponding to loading parallel to bedding. Increases in deviatoric stress cause increased Young's moduli until roughly 70% of peak stress, and increasing static Poisson's ratio in all loading orientations, with little change in dynamic values. Comparison between naturally fractured and intact Mancos samples show increased ratios of dynamic to static Young's moduli for fractured samples at the same confining stress, where intact samples have ratios between 2:1 to 4:1 and naturally fractured samples exhibit ratios between 4:1 and 8:1. Naturally fractured samples exhibit lower static and dynamic Young's moduli, which increase with deviatoric stress until failure, whereas intact samples decrease beyond 70% of peak stress. Overall, higher ratios of dynamic to static moduli are likely related to lower mechanical competence (due to natural fractures), and increasing ratios with increasing deviatoric stress is linked to stress-induced damage during testing.

X-ray microtomography imaging was utilized to evaluate natural fracturing and correlate mechanical behavior with microstructural changes after deviatoric loading to failure. Image analysis shows interaction between stress-induced fracturing with bedding planes and pre-existing natural fractures. Understanding the potential linkages between the dynamic and static responses of naturally fractured and intact anisotropic rocks in the laboratory provide opportunities to upscale stress-strain behavior to the wellbore environment and better utilize dipole sonic and time-lapse well logs to decrease mechanical uncertainty of unconventional reservoirs.

Keywords: Triaxial Testing, Shale, Anisotropy, Ultrasonic, Fractures

EG
ECG

Deposition and Sequence Stratigraphy of the East Texas Smackover Formation

Peter Schemper
Schemper, P., Primary Researcher
Fu, Q., Advisor
Loucks, B., Advisor

A study of the Smackover formation and its facies assemblages in East Texas, Van Zandt county using core descriptions and log data.

Keywords: Smackover

EG
ECG

Sediment-routing reconstruction and provenance analysis of Permian (Guadalupian) strata, southern Delaware Basin, west Texas

Graham Soto-Kerans
Soto-Kerans, G., Graduate Student, Jackson School of Geosciences, Austin, TX
Covault, J., Bureau of Economic Geology, The University of Texas at Austin, Austin, TX
Janson, X., Bureau of Economic Geology, The University of Texas at Austin, Austin, TX
Stockli, D., Department of Geological Sciences, Jackson School of Geosciences, Austin, TX

The Glass Mountains of west Texas mark the terminus of the Pennsylvanian (Oklahoma)-Early Permain (west Texas) Ouachita-Marathon suture, merging the supercontinents of Gondwana and Laurentia. Subsequent filling of the Delaware Basin facilitated the deposition of large amounts of Guadalupian (~272-260 Ma) mixed carbonate-siliciclastic strata. These strata have been interpreted to be sourced from northern crystalline basement uplifts of the Ancestral Rocky Mountains (Paleoproterozoic basement provenance). However, recent U-Pb detrital-zircon provenance analysis of Guadalupian strata in the northwestern Delaware Basin show significant age signals from Paleozoic, Neoproterozoic, and Mesoproterozoic age basement. These results suggest source areas to the south and southeast, including Yucatan-Maya and Mixteca terranes (likely via eolian sediment transport) as well as recycled Appalachian detritus (mixed fluvial and eolian transport). We integrate new and published detrital zircon U-Pb ages from across the Delaware Basin in order to reconstruct sediment routing and provenance of Guadalupian strata. We sampled the Road Canyon, Word, Vidrio, and Altuda formations in the Glass Mountains located at the southern tip of the Delaware Basin in order to develop an evaluation of sediment routing in an area not observed by previous studies. Combining our data from the south with the data compiled in the other regions of the Delaware Basin, we will be able to interpret a more spatially complete provenance analysis. We hypothesize that our results will align with previous studies, and our geochronologic data will include large proportions of Paleozoic, Neoproterozoic and Mesoproterozoic ages from southern and southeastern source areas. Moreover, we anticipate further dilution of age signals from the Ancentral Rocky Mountains and greater affinity to southern source areas due to our southern location in the Delaware Basin. Our integrated provenance analysis will provide new insight into Permian source-to-sink relationships, calibration of paleocurrents and provenance across the Delaware Basin, and better constrained regional paleogeography. Furthermore, results of this study should aid in the understanding of sediment dispersal patterns in analogous ancient foreland basin depocenters.

Keywords: Provenance, Detrital Zircon, Geochronology, Permian Basin, Delaware Basin, Sediment Routing, Guadalupian, Permian

MG
ECG

Pore-Scale Analysis of Methane Hydrate Formation and Dissociation in Brine using Micro-Raman Spectroscopy

Tiannong Dong
Dong, T., Institute for Geophysics, The University of Texas at Austin, Austin, TX
Lin, J., Department of Geological Sciences, The University of Texas at Austin, Austin, TX
Flemings, P., Institute for Geophysics, The University of Texas at Austin, Austin, TX
Polito, P., Department of Geological Sciences, The University of Texas at Austin, Austin, TX

Most investigations of methane hydrate formation and dissociation have been performed at macroscopic scales without direct microscopic observations. We use micro-Raman spectroscopy to study these phenomena at the pore scale (1-μm resolution) and link to macroscopic observations. We synthesize methane hydrate in a porous sample of medium-grained glass beads or industrial sand, packed in a stainless-steel cell with a sapphire window and pore fluids containing 3.5–7.0 wt% NaCl brine and methane gas at 12.36 MPa and 1 degree C. Methane hydrate is a nonstoichiometric crystalline solid composed of water and methane molecules. Converting water and methane into hydrate or dissociating hydrate are first-order phase transitions, and the phase boundary is a function of pressure, temperature, and salinity in the surrounding. In a closed system, when hydrate forms from water and methane in brine, salt is excluded from the hydrate and therefore the salinity of the remaining brine increases; when hydrate dissociates, freshwater is added to the brine, decreasing its salinity. We plan to directly observe these phenomena by mapping out the variations in salinity in space and time during hydrate formation and dissociation.

Keywords: Methane hydrate, Raman spectrum, Formation

MG
ECG

The 2A Event in 70 Myr Old Oceanic Crust: A Persistent Velocity Contrast?

Dominik Kardell
Kardell, D., UTIG
Christeson, G., UTIG
Reece, R., Texas A&M
Estep, J., Texas A&M
Arnulf, A., UTIG
Carlson, R., Texas A&M

The uppermost igneous layer in oceanic crust, referred to as layer 2A, exhibits seismic velocities rapidly increasing with age and distance from the spreading ridge from 0-10 Ma. This increase in velocity is mainly attributed to hydrothermal alteration by the intrusion and circulation of seawater. At ages >10 Ma layer 2A velocities appear to have little velocity contrast with the underlying layer 2B. However, new seismic reflection data collected during the CREST expedition in the South Atlantic image what appears to be a strong 2A event along the entire length of the transect, which covers crustal ages from 0 to 70 Ma. This implies a persistent strong velocity contrast between layer 2A and layer 2B from 0-70 Ma. In order to explore the nature of the contrast in acoustic impedance causing the observed 2A event, we performed various modeling techniques including traveltime and reflectivity modeling, downward continuation, and tomographic modeling on line 1A, a line segment covering 67 to 70 Ma that exhibits a particularly strong 2A event. This research helps us verify the validity of the imaged event and constrain the unexpectedly layered velocity structure of relatively old upper oceanic crust produced by slow to intermediate seafloor spreading.

Keywords: Layer 2A, South Atlantic, MCS Tomography

ECG-24

MG
ECG

Studying onshore-offshore fault linkages and landslides in Icy Bay and Taan Fiord to assess geohazards in Southeast Alaska

Naoma McCall
McCall, N., Institute for Geophysics, Jackson School of Geosciences, University of Texas, Austin, TX
Walton, M., U.S. Geological Survey, Santa Cruz, CA
Gulick, S., Institute for Geophysics, Jackson School of Geosciences, University of Texas, Austin, TX
Haeussler, P., U.S. Geological Survey, Anchorage, AK
Reece, R., Texas A&M University, Department of Geology and Geophysics, College Station, TX
Saustrup, S., Institute for Geophysics, Jackson School of Geosciences, University of Texas, Austin, TX
Shugar, D., University of Washington, Tacoma WA
Venditti, J., Simon Fraser University, Burnaby BC Canada

Collision of the Yakutat microplate with southeast Alaska has produced large historical earthquakes (i.e., the Mw 8+ 1899 sequence).The active deformation front known as the Pamplona zone as well as the onshore Malaspina fault may have played a role in the September 1899 earthquakes. Onshore and offshore mapping indicates that these structures could connect offshore in Icy Bay.

Recently, on October 17th 2015, nearby Taan Fiord experienced one of the largest non-volcanic landslides recorded in North America. Approximately 200 million metric tons spilled into Taan Fiord creating a tsunami with
~180 m run-up.

In August 2016 we collected high-resolution (300-1200 Hz) seismic reflection and multibeam bathymetry data to search for evidence of faults beneath Icy Bay and to image the Taan landslide in high resolution.

Keywords: Alaska, Yakutat, Earthquake, Seismic, Multibeam, Landslide, tsunami

MG
ECG

Evolution of the Upper Lithosphere in the ENAM Area from 3-D Wide-Angle Seismic Data

Brandon Shuck
Shuck, B., The University of Texas at Austin
Van Avendonk, H., The University of Texas at Austin

Located offshore North Carolina, the ENAM study area contains the geologic record of the rifting episode between North America and Africa that initiated at approximately 200 Ma. In this study we analyze 3-D marine wide-angle seismic data from the ENAM Community Seismic Experiment with the goal of understanding the interaction between mantle melt migration and extension in the lithosphere leading to continental breakup. The East Coast Magnetic Anomaly (ECMA) lies near the continental shelf off the eastern U.S. and is associated with this episode of Mesozoic rifting. However, a puzzling feature of the ENAM area is the Blake Spur Magnetic Anomaly (BSMA) which lies 200 km eastward of the ECMA. The BSMA has no mirror counterpart on the African side, which we would expect if rifting was symmetric in nature. This leads us to formulate two alternative hypotheses: 1) Oceanic crust exists between the ECMA and BSMA, or 2) The ECMA and BSMA form a wide volcanic margin. The first hypothesis would suggest the BSMA represents a sliver of West-African crust that was later transferred to the Atlantic plate by a mid-ocean ridge jump eastward. The second hypothesis would suggest asymmetric rifting accompanied by magmatism offshore North Carolina. Analysis of ENAM seismic refraction data will give insight into how the ECMA and BSMA are related to structure of the crust and mantle. We construct seismic velocity models (P and S-wave) along ENAM lines parallel and perpendicular to the margin to help determine the structural fabrics within the mantle in the ENAM area. We find the seismic compressional velocity is 8% higher parallel to the margin and suggests the BSMA represents a magmatic rifting event which created a shape-preferred orientation of crystals in the upper mantle. The velocity models show the crust in between the ECMA and BSMA is relatively thin and comparable to heterogeneous oceanic crust, and the crust seaward of the BSMA is consistent with normal oceanic crust of similar age. Our preliminary results suggest a spreading center was possibly active between the ECMA and BSMA until a ridge jump eastward occurred at a later time.

Keywords: continental rifting, seismic anisotropy, mantle melt, tomography, crystallographic preferred orientation

MG
ECG

Rapid shut-off and burial of slope channel-levee systems: new imaging and analysis of the Rio Grande submarine fan

John Swartz
Swartz, J., Department of Geological Sciences, The University of Texas at Austin, Austin, TX
Gulick, S., Institute for Geophysics, The University of Texas at Austin, Austin, TX
Mohrig, D., Department of Geological Sciences, The University of Texas at Austin, Austin, TX
Stockli, D., Department of Geological Sciences, The University of Texas at Austin, Austin, TX
Daniller-Varghese, M., Department of Geological Sciences, The University of Texas at Austin, Austin, TX

The continental slope of the western Gulf of Mexico is host to a major depositional system, the Rio Grande Fan. Unlike many submarine fans, the surface of the Rio Grande Fan lacks large submarine channels and associated levees. Prior analysis of continental shelf stratigraphy has identified the presence of past extensive shelf-edge delta systems, when the Rio Grande River system flowed across the modern shelf and delivered high volumes of sediment to the shelf/slope break. A major gap in understanding this system is how large volumes of sediment, particularly sands, are transported from the shelf edge systems down the slope and onto the basin-floor fan without apparent constructional channel-levee systems.

Over 500km of new high-resolution 2D multichannel seismic (MCS) and CHIRP echosounder data were collected over the shelf edge and upper slope of the Rio Grande fan. These new data provide unprecedented imaging of the shelf-edge delta systems and associated slope deposits. Our preliminary observations indicate that the modern seafloor morphology of the fan is dominated by mass-transport deposits, slumps and minor channel systems. However, buried below thick transgressive mud deposits are very large aggradational channels-levee systems and mass transport complexes that have no modern morphologic expression. Transgressive sediments vary in thickness from ~50 meters up to ~500 meters along the shelf edge, and rapidly thin basin-ward. Much of this thickness variation appears to be related to significant variability in subsurface structure, with extensional faulting and large rotational blocks observed. Below the transgressive deposits the main channel-levee systems have channel belts almost 1km wide, with confining levees that approach 8km in width. These channels appear almost entirely constructional, with no apparent canyon formation and minimal incision. The main body of the fan is built from these channel complexes, which appear to aggrade and avulse before either shutting off or being removed by mass wasting.

We document the evolution, from initial channelization to shutoff and failure, of these slope systems. Regional correlation suggests that this episode of channel-levee growth and shutoff occurred during the most recent low-stand and could indicate higher sediment flux through the paleo-Rio Grande River than that of the modern. Our results highlight an example of a slope-channel system that is subject to variations in sediment supply. These results illustrate the potential for the construction of large late Pleistocene submarine fan deposits that can be difficult to recognize in modern seafloor morphology.

Keywords: Submarine channels, continental margins, source-to-sink, marine sedimentology

MG
ECG

Middle-late Miocene siliciclastic influx on the Australian Northwest Shelf: origins and potential links to global events

Gabriel Travassos Tagliaro
Tagliaro, G., University of Texas at Austin, Austin, TX
Fulthorpe, C., Institute for Geophysics, Austin, TX
Lavier, L., University of Texas at Austin, Austin, TX

The Bare Formation in the Northern Carnarvon Basin represents a unique episode of siliciclastic deposition within a carbonate-dominated system. Recent drilling by International Ocean Discovery Program (IODP) Expedition 356, coupled with interpretation of 3D seismic data, provide an opportunity to constrain the sedimentary processes involved in the deposition of these siliciclastics. Two interpretations of the depositional processes responsible for the Bare Fm. have been proposed: 1) shelf and shelf-edge deltas associated with the advance of a fluvial system across the shelf, and 2) a beach barrier system, involving reworking of sediment on the paleo-shelf. We reinterpret the stratigraphy, depositional system, and timing of the Bare Fm. Seismic data are tied to IODP Site U1462, which provides age control and illustrates the relationship of the Bare Fm. to the adjacent carbonate sediments. The Bare Fm. was initiated in the middle/late Miocene and Expedition 356 results do not refine that age because of absence of diagnostic microfossils. However, seismic geomorphology enables us to redefine the Bare Fm. top as Pleistocene in age, younger than the Tortonian age previously assigned. The Bare Fm. comprises two distinct patterns of deposition: strike-oriented sandbodies that suggest deposition by longshore currents in the later Miocene; dip-oriented progradational lobes that are related to a point-based source from the late Miocene to the Pleistocene. Overall, the entire system migrates northeast. The middle to late Miocene was a period when anomalous tectonic and climatic activity led to an abrupt increase in continental-margin sedimentation worldwide. Paleoclimate studies from IODP expedition 356 are suggesting localized wet and arid conditions in the late Miocene of Northern Carnarvon Basin, and the onset and development of the Bare Fm. may constitute the sedimentary response to that transition.

Keywords: seismic stratigraphy, miocene, northern carnarvon basin

PS
ECG

Geochronology of Proposed Ordovician Meteorite Events in North America

Andrew Parisi
Parisi, A., Jackson School of Geosciences
Catlos, E., Jackson School of Geosciences
Brookfield, M., University of Massachusetts, Boston

The Ordovician meteor event was an order of magnitude increase in the amount of extraterrestrial material being delivered to Earth approximately 470 Ma. Previous studies have confirmed impacts from this event in Sweden, China and Oman. It has been suggested that a series of impact structures in the USA and Canada may also be related to this event. The impact structures have been tentatively dated to the Middle Ordovician, but definitive dates have never been obtained. The present study will examine new lines of evidence to determine the impact dates of two of the proposed North American Ordovician impact structures. The impacts to be focused on in this study are the Ames astrobleme in Oklahoma, USA and the Slate Islands in Ontario, Canada. The Ames astrobleme has been dated to ~470 Ma via biostratigraphic means. An attempt to date the site using the 40Ar/39Ar method on impact melt was unsuccessful due to later thermal overprinting. Slate Islands has not been dated by reliable means, and the formation age is suggested based on stratigraphic evidence. The present study will test the viability of performing the 40Ar/39Ar method on felsic minerals within the basement rock of the two impact structures. As part of the impact events, basement rock was shattered and moved into the crater, where it intermixed with sedimentary rock clasts and impact derived melts subsequently forming an impact breccia. The heat from the impact and cooling melt-rock would reset some portion of the potassium/argon ratio within the felsic minerals of the clasts, from which an impact age can be determined. Basement rock samples will be obtained from Ames astrobleme via sampling of drill core which intersects the impact structure. Basement rock at Slate Islands is exposed at the surface and will be collected in the summer of 2017. Samples will also be analyzed for the presence of impact melt zircons, which will be dated using the U/Pb method. If the 40Ar/39Ar method when performed on fractured basement rock proves to be viable, it will provide an additional line of testing which can be utilized to more easily date impact craters. As a concurrent project, surface material of Early to Middle Ordovician age will be collected from the Arbuckle anticline in Oklahoma, USA. The purpose of this is to locate the debris layer from the Ames impact within the sedimentary package. This serves two objectives: it will locate additional material which can be used to date the impact, and will identify an additional marker bed within the Arbuckle anticline. Impact debris layers form nearly instantaneously, and can be used to specify an absolute age. The most famous example of this is the impact layer marking the Cretaceous-Paleogene extinction event. Identifying a debris layer exposed on the surface will allow better correlation of Ordovician age rocks within Oklahoma. All of this information will provide a better understanding of the impacts within the larger geologic context.

Keywords: Geochronology, Meteorite impact, Ames astrobleme, Slate Islands, Ordovician stratigraphy

SETP
ECG

3D Analysis of the Internal Structure of Natural Polycrystalline Diamond Using XCT: Implications for Carbonado History

Scott Eckley
Eckley, S., Department of Geological Sciences, The University of Texas at Austin, Austin, TX
Ketcham, R., Department of Geological Sciences, The University of Texas at Austin, Austin, TX

The origin of the world's hardest natural substances and largest diamonds – carbonados – has remained a geological conundrum for decades. They are an unusual polycrystalline diamond variety found in placer deposits, hypothesized to have been sourced from Mesoproterozoic conglomerates, in the Central African Republic and Brazil. Irregularly shaped and highly porous, these black nodules have never been found in or associated with typical diamondiferous volcanic rocks (*i.e.* kimberlites and lamproites), which has led to a plethora of formation theories. Among natural diamonds, carbonados have a variety of unique traits: (1) where most diamonds are sourced from relatively young volcanic rocks, carbonados have no positively identifiable volcanic origin, and yield ages of 2.6 to 3.8 Ga based off Pb-Pb in quartz, rutile, and clay found in exterior pores and U-Th-Pb from acid leaching of the bulk sample. (2) Carbonado diamonds do not possess the typical inclusion suite that is found in mantle-derived diamonds (*i.e.* pyrope garnet, olivine, chromian spinel, and Mg-ilmenite). Instead, they have three types of inclusions: a seemingly crustal group of minerals (*e.g.* florencite, orthoclase, quartz, and kaolinite) lining the pores spaces that are thought to be a secondary feature that formed during its long residence on the surface. Next, nano-inclusions of highly reduced metals and metal-alloys (*e.g.* Fe, Fe-Ni, Ni-Pt, Si, Ti, Sn, Ag, Cu, and SiC) within the 10-250 μm diamond phenocrysts were discovered with TEM and have been interpreted as primary features. Lastly, with the use of X-ray computed tomography, pseudomorphs taking a pristine, euhedral, rhombic dodecahedral shape have been found and interpreted as macro-scale, primary inclusions, most likely garnet. (3) Typical diamonds span a large range of carbon isotopic compositions (δ13C ~ -45 ‰ to 5 ‰), but carbonados have a relatively narrow range of isotopically light carbon (δ13C -31 ‰ to -24 ‰), whose source in the mantle is still misunderstood. (4) They can grow up to 3167 ct. (> 20 cm in length) with a microporphyritic texture composed of randomly-oriented 10-250 μm diamond phenocrysts sintered together with sub-micron diamond crystals, and also display macro- and microscopic porosity comprising a fully-connected pore network. Because of their polycrystalline nature, studies on carbonados have been limited due to the difficulty of cutting, polishing, and preparing samples. However, by using high-resolution X-ray computed tomography (XCT), this novel study provides the first full characterization of the internal morphology of carbonado diamonds. At least seven samples, ranging from < 1 ct. to 23.45 ct., will be scanned and 3D analysis software will be used to understand the nature of the pore network, which is certainly related to its origin. Preliminary results suggest an alignment of the pores exists. This could be due to a shearing force that led to an elongation and preferential orientation of preexisting pores or from a pervasive, mobile fluid.

Keywords: Diamonds, Porosity, Mantle, X-ray Computed Tomography

SETP
ECG

High-resolution garnet P-T paths for the central Menderes Massif, western Turkey

Thomas Etzel
Etzel, T., The University of Texas at Austin
Lizzadro-McPherson, D., The University of Texas at Austin
Kelly, E., The University of Texas at Austin
Catlos, E., The University of Texas at Austin
Ashley, K., The University of Texas at Austin
Ozerdem, C., Oklahoma State University
Cemen, I., University of Alabama

Garnet-based thermobarometry is often used to develop models for the evolution of the central Menderes Massif, a large-scale metamorphic core complex in western Turkey. Menderes Massif P-T conditions constrain processes that worked to assemble western Turkey and link the massif to core complexes in the Aegean region. Here we report P-T conditions from greenschist- to amphibolite-facies garnet-bearing rocks collected along three transects across the Alasehir detachment, a structure responsible for the exhumation of the central portion the massif. High-resolution BSE images and X-ray Fe, Ca, Mg, Mn, and Y maps were collected from garnets and quantitative compositional data were obtained from garnet and matrix phases to estimate peak P-T conditions using classical thermobarometry. This data suggest that rocks experienced conditions from 575±25°C and 10±1 kbar to 715±55°C and 11.2±2.2 kbar. However, results from adjacent samples are inconsistent, potentially due to disequilibrium among phases and/or the application of barometers to inappropriate (uncalibrated) mineral compositions. Using an alternative G-minimization approach with bulk rock composition estimates and preserved mineral zoning, we obtained garnet core and rim P-T conditions, and high-resolution P-T paths. Garnet core P-T conditions range between 6-9 kbar and 530-630^{o}C and rim conditions range from 6.3-10 kbar and 625-750^{o}C. Most P-T paths show a continuous increase in temperature with pressure, suggesting growth during burial. One sample shows an increase in temperature, but pressure fluctuates from 9.3 kbar (core) to 8.9 kbar (mantle) to ~10 kbar (rim). Interestingly, the final pressure for this rock is 2-3 kbar higher than rocks near-by (<1 km), but thermal conditions are consistent. Th-Pb monazite ages for the samples range from 35.8±3.0 to 20.6±2.4 Ma, and with continuous heating recorded by garnet, suggest the suite of rocks was metamorphosed over a single, 15 m.y. period. Although additional garnet P-T paths are still needed, our findings capture garnet growth related to a single metamorphic event and define some of the most consistent and detailed P-T paths reported for the area. The results differ from recent findings in the southern Menderes Massif that indicate garnet-bearing rocks there record alternations in burial and exhumation.

Keywords: Turkey, garnet, P-T paths, thermodynamic modeling

SETP
ECG

New Geochronometric and Low-Temperature Thermochronometric Insights on the Nature of the Cycladic Basement and Cycladic Blueschist Unit Contact in the Southern Cyclades, Ios Island, Greece: Implications for Aegean Tectonics

Megan Flansburg
Flansburg, M., Department of Geological Sciences, The University of Texas at Austin, Austin, TX
Poulaki, E., Department of Geological Sciences, The University of Texas at Austin, Austin, TX
Stockli, D., Department of Geological Sciences, The University of Texas at Austin, Austin, TX
Soukis, K., Faculty of Geology and Geoenvironment, National and Kapodistrian University of Athens, Athens, Greece

The North Cycladic Detachment System and the West Cycladic Detachment System are both large, single-detachment structures that accommodated exhumation of metamorphic domes in the backarc of the retreating Hellenic subduction zone. However, the nature of the South Cycladic Shear Zone (SCSZ), the heavily sheared contact between the Cycladic Blueschist Unit (CBU) and the underlying Cycladic Basement, has been the center of heated debate for over 30 years. While most previous work on the south Cycladic island of Ios has focused on metamorphic characteristics of the two units, there is a striking lack of robust geochronologic and low-temperature thermochronologic data. Importantly, these metrics can also be used to determine the debated nature of the Cycladic Basement/CBU contact by placing absolute ages on deformation. We hope to determine whether it is a low-angle normal fault, possibly part of a larger-scale detachment system, or whether it is the South Cycladic Thrust.
This question will be tackled through a series of investigations. First, zircon U-Pb ages of the Cycladic Basement and the CBU will determine crystallization ages, maximum depositional ages (MDAs), and provenance. The MDAs of CBU samples will be compared to the neighboring island of Sikinos and to the western Cyclades. Secondly, zircon and apatite (U-Th)/He thermochronometry will time the exhumation of the Cycladic Basement and the CBU (i.e., were they together during exhumation? What was the direction of shear?). Thermochronometric ages and geochronometric metamorphic growth ages will also be correlated with the strain facies identified by Huet et al. (2009) and Mizera and Behrmann (2015). Additionally, in-situ geochronometry of synkinematic minerals will allow us to determine the absolute timing of pervasive top-to-the-north and top-to-the-south deformation on Ios. Data at the time of this submission suggests Carboniferous ages for the crystalline Cycladic Basement (~320 Ma) and a MDA of ~354 Ma for the metasedimentary Carapace overlying the Cycladic Basement. Pan-African ages in a few zircons suggest that Basement granitic plutons were emplaced in Peri-Gondwanan crust. The affinities, provenance, and MDAs of these units have important impact the tectonic history and paleogeography of the Aegean.

Keywords: backarc extension, metamorphic core complex, Cyclades, Aegean Sea, Hellenic Subduction Zone, geochronometry, low-temperature thermochronometry

SETP
ECG

Sediment routing in the Oriente Basin, Ecuador: Detrital zircon and seismic insights into Cenozoic paleodrainage and paleogeography

Evelin Gutiérrez
Gutierrez, E., Jackson School of Geosciences, The University of Texas at Austin, Austin, TX

The Oriente Basin contains the longest record of sedimentation in Ecuador, with Mesozoic to Quaternary accumulation in marine and nonmarine systems. The Cretaceous succession has been studied extensively because of its prolific petroleum source and reservoir units. In contrast, the Cenozoic record is understudied, largely due to insufficient age constraints due to a lack of diagnostic fossils. Nevertheless, the Cenozoic history of sedimentation in the Oriente Basin is critical to understanding the synkinematic response to deformation and exhumation in the Andean fold-thrust belt, hinterland, and magmatic arc of Ecuador. The proposed study will address the Late Cretaceous–Cenozoic (~120 Myr) record of basin evolution using detrital zircon geochronology and seismic stratigraphic analyses with the goal of linking changes in Oriente paleodrainage and paleogeography to shifts in the regional tectonics and basin geodynamics that ultimately are responsible for generating the structural and stratigraphic elements controlling the important hydrocarbon systems.

The Late Cretaceous–Cenozoic evolution of the Oriente Basin is marked by several tectonic events, starting with Campanian-Maastrichtian accretion of an oceanic plateau and affiliated magmatic arc along the western edge of Ecuador (Litherland et al., 1994; Spikings et al., 2001; Vallejo et al., 2006). This event likely induced tectonic inversion and the termination of marine sedimentation in the Oriente Basin, with associated initial uplift in the Andes.

However, little is known about the sedimentary response in the Oriente Basin to Andean uplift and changes in plate geodynamics. This study seeks to answer key questions about the role of Andean uplift and whether crustal deformation was a steady process or occurred in irregular pulses (e.g., Spikings et al., 2001; Christophoul et al., 2002). A critical issue is how the uplift of the Andes impacted the distribution and routes of drainage systems in the Subandean Zone and Oriente Basin, particularly in the Pastaza Depression during Cenozoic basin evolution. Currently, this region has a complex drainage system that bifurcates into two major rivers, the Napo and Pastaza Rivers, which are feeders of the Amazon River. Does the sedimentary record show different drainage pattern with different sources in the past, and if so, when and where were the important changes? These questions are also important for an improved understanding of the impact of the structural evolution of the Subandean Zone on the quality and distribution of hydrocarbon systems. High-quality oil reservoirs, heavy oil reservoirs, or no reservoirs are all possible scenarios, based on structures documented throughout the Subandean Zone. Answers to all these questions are recorded within the Cenozoic stratigraphic record. Therefore, a detailed characterization of sediment provenance and geochronology combined with documentation of surface and subsurface stratigraphic geometries will help elucidate key aspects in the geologic evolution of the Oriente Basin. Ultimately, constraints on sediment sources and sediment routing will provide a better understanding of basin evolution and contribute to reconstructions of paleogeography and paleo-drainage, with implications for improved models of petroleum system that can be based on more precise input data and will thus diminish uncertainties in the exploration and development process

Keywords: Oriente Basin, routing sediment, geochronology, paleodrainage, paleogeography

ECG-33

SETP
ECG

Provenance Analysis of the Late Cretaceous-Paleogene Southwest Texas Sediment Routing System: Detrital Zircon Geochronology from the Tornillo Basin, Big Bend National Park

Cullen Kortyna
Kortyna, C., The Department of Geological Sciences, The University of Texas at Austin, Austin, TX
Stockli, D., The Department of Geological Sciences, The University of Texas at Austin, Austin, TX
Sharman, G., Bureau of Economic Geology, The University of Texas at Austin, Austin, TX
Covault, J., Bureau of Economic Geology, The University of Texas at Austin, Austin, TX

Detrital zircon geochronology is used to determine ancient sediment dispersal pathways, and, along with quantitative stratigraphic analysis, can delineate paleo-catchment areas for ancient river systems. This information is used to understand sediment transfer in source-to-sink systems from catchment headwaters to sedimentary basins, and, ultimately, is useful for relating sediment distribution to various autogenic and allogenic forcings. The Late Cretaceous-Paleogene sediment routing system of the North American Cordillera is one of the better studied continental-scale systems in the world. However, key portions of the system are still poorly constrained. It is largely unknown how the sediment routing system in southwest Texas fits into the larger drainage history of the U.S. and Mexican segments of the Cordillera. Preliminary detrital zircon provenance results from Cretaceous-Paleogene fluvial sediments of the Tornillo Basin in southwest Texas suggest a more extensive paleo-catchment system than previously inferred, potentially sourcing from well within the western U.S. Cordillera. Detrital zircon age modes are consistent with sources in the western U.S. Cordillera, and contain an Early Cretaceous “arc gap” consistent with western U.S. sources and inconsistent with Mexican sources. Further study is required to determine if these river systems drained downstream to the Mexican Difunta group or to the Wilcox group (Rio Bravo/Rio Grande) in south Texas. Improving our understanding of the size, extent, and coastal discharge location of the Tornillo Basin drainage system can improve predictions of sediment supply to the Gulf Coast. In addition, the Tornillo Basin preserves a record of climate change from uppermost Cretaceous to early Eocene time, including the Paleocene-Eocene Thermal Maximum. Further study will elucidate if climatic or tectonic events impacted sedimentation in the drainage system. These results will contribute to oil and gas exploration efforts as better understanding of source terrane lithology and evolution, transport distance, and climatic variation experienced by Texan and north Mexican river systems provides better predictions for reservoir presence, volume, and quality at specific time intervals and river discharge points into the Gulf of Mexico. Better understanding of controls on continental-scale sedimentation can provide improved predictive power to source-to-sink studies in frontier basins worldwide.

Keywords: Detrital Zircon Geochronology, Sediment Routing, Texas, Gulf of Mexico, Wilcox group

SETP
ECG

Attenuation in the African LLSVP Estimated from PcS and PcP Phases

Chujie Liu
Liu, C., The University of Texas at Austin, Austin, TX
Grand, S., The University of Texas at Austin, Austin, TX

The lowermost mantle beneath the African is featured by a broad region with about 3% slower shear velocity, known as the African large-low-shear-velocity province (LLSVP). Recent seismological and geodynamics studies have revealed many details on its elastic properties and geometric features, but its inelastic properties like intrinsic attenuation still need better constrain. Both elastic and inelastic properties are essential to understanding the structure, dynamics, and thermal states of the LLSVP. PcS and PcP are seismic waves that reflected at the core-mantle boundary (CMB) with and without phase transition. One can determine the differential attenuation parameters t* by measuring the spectral ratios of PcS to PcP phases with several reasonable assumptions. In this study, we use high-quality PcS and PcP waves produced by several deep earthquakes in South Sandwich Island region, to constrain the attenuation in African LLSVP. Our preliminary measurements indicate that the estimated average shear wave quality factor Q_β influenced by African LLSVP is 146, which is 50% lower than surrounding “normal” mantle (Dziewonski and Anderson, 1981). Therefore, the African LLSVP is highly attenuated. Our result here can help us better understand the origin of LLSVP and mantle convection processes.

Keywords: Q, LLSVP, Deep Mantle, PcS PcP Waves

SETP
ECG

Interaction of Two, Independent, Pyroclastic Density Currents

Sean O'donnell
O'Donnell, S., Department of Geological Sciences, The University of Texas at Austin, Austin, TX
Gardner, J., Department of Geological Sciences, The University of Texas at Austin, Austin, TX
Andrews, B., Smithsonian Institution National Museum of National History, Washington, DC
Mohrig, D., Department of Geological Sciences, The University of Texas at Austin, Austin, TX
Buttles, J., Department of Geological Sciences, The University of Texas at Austin, Austin, TX

Pyroclastic density currents (PDC) originate during volcanic eruptions from collapse of eruption columns, avalanches from lava domes, or from lateral blasts. PDCs are density driven currents that travel through (mainly) the earth's atmosphere, and are composed of volcanic ash, glass, and other volcanic debris. A PDC begins hotter and denser than the surrounding atmosphere. As the current progresses, it entrains and heats surrounding air, and deposits its sediment load, developing into two distinct layers: a dense, lower current and a dilute, upper current. PDCs may travel many kilometers, at which point they entrain enough air to "lift-off" and create a co-ignimbrite ash plume, which rises adiabatically through the atmosphere. As a consequence of the obvious difficulties in studying active PDCs, research has to be conducted on the deposits, through photographs and video, or through experimental modelling. Prior experiments have been carried out in 2D and 3D settings, with many different combinations of starting mechanisms, particle distributions, and surrounding medium. All of these experiments have focused on the behavior of a single current. However, evidence exists that two or more PDCs can begin at nearly the same time, and interact with each other over the course of their respective runouts. It is possible that during the 1994 and 2010 eruptions of Merapi, Java, Indonesia, and the 1980 eruption of Mt. St. Helens, Washington, USA, two or more independent PDCs interacted with each other. Experiments were run to investigate the impact one current has on the other. The experiments were properly scaled to ensure their behavior is analogous to real PDCs. Heated talc powder was dropped into a tank to create a dilute density current. After allowing the first current to develop, a second current was then released under the same conditions as the first. Temperature data were collected though thermocouples on the floor of the tank, and the currents were monitored with HD video cameras. The data were analyzed to determine the entrainment of air in each current, and test how the behavior of the second current differs from one not preceded by a prior current.

Keywords: pyroclastic density current, entrainment, interaction

SETP
ECG

Path-finding algorithm for stable trace interpolation

Yunzhi Shi
Shi, Y., Bureau of Economic Geology, The University of Texas at Austin, Austin, TX
Fomel, S., Bureau of Economic Geology, The University of Texas at Austin, Austin, TX

Seismic trace correlation provides alignment information between traces and is insensitive to large measurement errors. Similar philosophy has been applied to well-log matching, e.g., using dynamic warping workflow. However, seismic trace data often consist of much more sensors than from well-log; thus, pairwise correlation would be unfeasible. We proposed a reduced form of NP-hard "Traveling Salesman Problem" to find an optimal path that connects each node with a single pass, so that the linear equation for interpolation can be reduced from $O?(N^{?2}?)$ equations to $?O(?N)$ equations. Therefore, it could be possible to adopt such well-log interpolation workflow to seismic data processing.

Keywords: Seismic trace correlation, Traveling Salesman Problem

SETP
ECG

Tectonic History and Rheology of a Subduction Interface Shear Zone, Condrey Mountain Window, Northern California

Carolyn Tewksbury-Christ
Tewksbury-Christle, C., Department of Geological Sciences, The University of Texas at Austin, Austin, TX
Behr, W., Department of Geological Sciences, The University of Texas at Austin, Austin, TX
Helper, M., Department of Geological Sciences, The University of Texas at Austin, Austin, TX

The Condrey Mountain Window (CMW) occupies a subcircular window in the Klamath Mountains of northern California and southern Oregon. The Klamaths consist of a series of eastward dipping, westward younging thrust sheets accreted during Early Paleozoic to Late Jurassic subduction of the Farallon Plate. Previous workers identified two main thrust sheets in the CMW. The upper thrust sheet consists of arc-proximal volcanic and sedimentary protoliths metamorphosed to greenschist facies, whereas the lower thrust sheet consists of pelagic sedimentary, mafic, and ultramafic protoliths metamorphosed to epidote blueschist facies. Prograde deformation, peak metamorphic conditions (6-8 kb, 350-450 °C), and protoliths in the CMW are consistent with subduction and underplating.

Previous work dated emplacement of both sheets at the base of the overriding plate at ~150-156 Ma. Recent detrital zircon work, however, suggest that the upper and lower sheets were not emplaced together and that the lower sheet progressively underplated, based on maximum depositional ages of the lower sheet that young from ~150 to ~136 Ma with increasing structural depth. Appreciable refrigeration of a subduction zone over time should result in emplacement of increasingly colder material. If progressive underplating involves a few thick sheets, I expect to see discontinuities in temperature over the structural thickness. On the other hand, if several thin sheets are involved, I expect a more continuous temperature gradient. I sampled a dense transect of prevalent graphitic mica schist from structurally high to low in the lower sheet and collected graphite-bearing metasediments in the upper sheet. Using graphite crystallinity thermometry determined by Raman spectroscopy, I will map temperature variations across the lower sheet and better constrain peak metamorphic temperatures in both sheets to constrain the nature of progressive underplating. In addition to providing insights into the underplating processes along the subduction channel, these results will also aid comparison of the CMW to modern and ancient subduction zones.

Additionally, I will systematically characterize deformation mechanisms across the range of lithologies in the CMW to inform understanding of steady-state and transient rheology. Amphibole rheology is currently poorly understood, but preliminary work on the CMW blueschist suggests that dislocation creep is the primary steady-state deformation mechanism in amphibole. Through combined microstructural analysis and Electron Backscatter Diffraction, I will determine what slip systems are active in the amphiboles at CMW metamorphic conditions to improve constraints for modeling and interpretation of modern subduction zones. Furthermore, the CMW is exhumed from depths consistent with Episodic Tremor and Slow Slip (ETS) in modern subduction zones. Previous workers attribute ETS to dominantly viscous deformation with transient brittle episodes, and mechanisms consistent with ETS are preserved in the rock record in other exhumed subduction complexes. By investigating deformation mechanisms across the CMW lithologies, I will also characterize the transient rheology in the CMW.

Keywords: subduction, rheology, Raman spectroscopy, microstructures

SETP
ECG

Tracing Environmental Signals from Source to Sink: Zircon (U-Th)/(He-Pb) Double Dating Applied to the Foreland Basins of the South Central Pyrenees, Spain

Kelly Thomson
Thomson, K., Department of Geological Sciences, The University of Texas at Austin, Austin, TX
Odlum, M., Department of Geological Sciences, The University of Texas at Austin, Austin, TX
Stockli, D., Department of Geological Sciences, The University of Texas at Austin, Austin, TX
Findani, A., R&T, Statoil ,Austin, TX
Clark, J., R&T, Statoil, Austin, TX
Puigdefabregas, C., University of Barcelona, Barcelona Spain

The South Central Pyrenean foreland basin system provides an opportunity to investigate sedimentary processes in response to orogenesis during periods of high climatic and eustatic variability. Continuous outcrop exposure allows for investigation of source to sink processes, from fluvial to deep-water environments at high temporal and spatial resolution. Our new data provide insights into the paleogeography of the Pyrenees during the Eocene and how foreland basin source to sink systems respond to climate/tectonic perturbations. The primary aim of this study is to compare detrital zircon (DZ) analyses from the Ripoll, Ager, Tremp-Gras, Ainsa, and Jaca Basins to investigate changes in sediment provenance in response to tectonic and climatic events. The secondary aim of this study is to compare the DZ U-Pb and (U-Th)/He distributions from multiple stratigraphic levels in the South Central Pyrenean foreland basins to investigate how tectonic-induced variations in sediment supply are propagated from fluvial to deep marine and result in the observed stratigraphy. To achieve this we focused on the Eocene Castissent, Guell (lowest Campanue Fm), and Castigaleau sequences, due to their lateral traceability from fluvial to deep marine. U-Pb results indicate that the main sediment source regions were located in the Eastern Pyrenees, Catalan Coastal Ranges and potentially the Ebro Massif from onset of orogenesis through the Eocene. Sediment was delivered via a braided fluvial network flowing parallel to the emergent Pyrenean thrust front into a shallow and deep-marine environment. Results indicate additional sediment contribution from smaller, more restrictive catchments on emergent fold thrust structures (i.e. Montsec thrust). Different DZ signatures from Eocene deposits in the Tremp-Gras basin and Ager basin indicate unique sediment sources suggesting that the Montsec was a topographic barrier between these basins. Axis parallel flow in the Ager and Tremp-Gras systems brought sediment from their respective sources downstream to the west where rivers met and mixed in the area of the Montsec-Peña Montanesa lateral ramp before flowing down submarine canyons into the deep marine basin floor. Our data allow linkage of hinterland and fold thrust belt evolution to the delivery of sediment to the foreland basin.

Keywords: Pyrenees, Tectonics, Detrial Zircons, Source to Sink, Paleogeography, DZDD, Geochronology, Thermochronology

SHP
ECG

Setting the Stage for Levee Building Processes

Hima Hassenruck-Gudipati
Hassenruck-Gudipat, H., The University of Texas at Austin, Austin, TX
Mohrig, D., The University of Texas at Austin, Austin, TX
Passalacqua, P., The University of Texas at Austin, Austin, TX
Mason, J., The University of Texas at Austin, Austin, TX

Levees are built by sediment transported from rivers to floodplains. These floodplains in most levee building models are assumed to be initially flat. Airborne lidar analysis presented here demonstrates the importance of capturing floodplain morphology in order to accurately predict levee growth. We use lidar datasets from 2011 and 2015 to quantify levee characteristics and compare deposition/erosion along 88 km of the lower Trinity River in Texas. This allows us to understand and distinguish spatial trends from local variability. To place constraints on the sediment transport conditions that build levees, we measured the variability of levee width and levee crest elevation. Levee width is relatively constant except for bends with levees that are associated with localized low floodplain elevations (antecedent topography). Levee-crest elevations follow a downstream slope of ~1.5×10^{-4}. Variability in crest-line elevation is low and systematically decreases towards the coastline, corresponding to a decreasing range in river stage driven by a downstream boundary condition of constant sea-level. This boundary condition is also connected to an overall downstream reduction in measured topographic change between 2011 and 2015 on the levee.

Levee characteristics can be used to understand and model how sediments, water, and nutrients are routed onto the floodplain during a flood. To explore different routing mechanisms, a new levee building model should couple water and sediment routing with preexisting topography. A new direction for levee interpretation using ancient records should involve measuring as many as possible levee widths and levee crest elevation in order to infer drainage on the paleo-floodplain, as well as position along the backwater curve.

Keywords: lidar, levees, antecedent topography

SHP
ECG

A First Look at Identifying the Biogeochemical Weathering Front in a Fractured Hillslope at the Eel River Critical Zone Observatory

Alison Tune
Tune, A., Jackson School of Geosciences, The University of Texas at Austin, Austin, TX
Rempe, D., Jackson School of Geosciences, The University of Texas at Austin, Austin, TX

At 'Rivendell' in the Eel River Critical Zone Observatory, previous geophysical studies determined that saprolite is a significant moisture reservoir and transports water through fractures before the wetting front has advanced 1m. While the physical weathering front has been identified, the associated biochemical weathering front has yet to be determined. By utilizing a series of monitors placed with depth in the vadose zone, a structured oxygen and hydrogen stable isotope profile has been discovered at this rapidly eroding location. Ongoing studies will provide insight into the water cycling and biologic interactions at this field site, and future work will focus on identifying what is influencing the biogeochemical weathering front that is possibly generating secondary porosity, altering pore-fluid chemistry, and influencing moisture content fluctuations. Understanding this system has implications for carbon cycling studies, climate models, and watershed studies.

Keywords: ecohydrology, critical zone, weathering front, vadose zone, stable isotopes

SHP
ECG

Towards Developing a Framework for Predicting River Flows on Global Scales

Wen-Ying Wu
Wu, W., Jackson School of Geosciences, The University of Texas at Austin
Yang, Z., Jackson School of Geosciences, The University of Texas at Austin
Lin, P., Jackson School of Geosciences, The University of Texas at Austin
Maidment, D., Department of Civil, Architectural and Environmental Engineering,Cockrell School of Engineering, The University of Texas at Austin

Current approaches to predicting large-scale river flows are limited in many parts of the world, which limits our capacity for flood and drought preparedness in those regions. One of the main reasons for such limitations is due to the lack of high quality river network data in developing countries or the unwillingness to share the data. In the United States, high quality river network data of ~10-m resolution are readily available through the National Hydrograph Dataset Plus (NHDPlus V2), while the river network on the global scale can be derived from Hydrological data and maps based on SHuttle Elevation Derivatives at multiple Scales (HydroSHEDS) which is at approximately 500-m resolution. Launched in August 2016, the National Water Model effectively incorporates weather forecasts to predict river flows for more than 2.7 million rivers across the continental United States (CONUS), which transfers a “synoptic weather map” to a “synoptic river flow map” operationally. It is important to establish a baseline by comparing river flow simulations from the two river networks (NHDPlus versus HydroSHEDS) in the CONUS before expanding the modeling framework to the global scale using the coarse-resolution HydroSHEDS. In this study, we first derive the river network from HydroSHEDS and then connect runoff output from a land surface model to a river routing model (RAPID) to produce river flow. We then compare our river flow simulations with those from using NHDPlus. The results are also compared with observations.

Keywords: hydrology, streamflow simulation, water cycle

CCG
LCMS

Determining the Limiting Factors Controlling Soil Ecosystem Regeneration After a Stand-replacing Wildfire

Sol Cooperdock
Breecker, D., The University of Texas at Austin, Austin, TX

Like all forest disturbances, wildfires remove vegetation, but additionally they can remove or transform soil nutrients through volatilization due to extreme temperatures. As the stability and nutrient source for plants, soils are the key to forest regeneration after disturbances and in order to predict and mitigate damage, it is essential to understand how soils are affected by fires. In this study, soil respiration and temperature were measured in-situ at 20 sites affected by two fires that occurred during September 2011 and October 2015 in Bastrop County, TX. At each site, soil samples were collected from 0-5 cm depth. These samples were incubated in the dark at 25° C and 22% water content to determine respiration rates under controlled environmental conditions. These methods of respiration measurement were performed to distinguish the impact of environmental and chemical factors on soil biological activity. Total C, N, trace element concentrations and pH were measured in each soil sample to determine the effect of fire on soil chemistry and the effect of soil chemistry on soil activity. Regression tests using respiration rates as the response variable show that field-based respiration is highly dependent on whether the soil was burned and what month measurements were taken during. Lab-based respiration rates appear to be mostly driven by organic matter content, however. In addition to burn and month, field respiration was highly dependent on water content, as water contents dropped substantially more during dry months in burned soils than unburned ones.

Keywords: fire, soil

CCG
LCMS

A MULTIPROXY RECORD OF THE TOARCIAN OCEANIC ANOXIC EVENT IN SHALLOW-WATER CARBONATES FROM THE ADRIATIC CARBONATE PLATFORM

Nicholas Ettinger
Ettinger, N., Jackson School of Geosciences, The University of Texas at Austin
Martindale, R., Jackson School of Geosciences, The University of Texas at Austin
Kerans, C., Jackson School of Geosciences & Bureau of Economic Geology, The University of Texas at Austin
Košir, A., Research Center of the Slovenian Academy of Arts and Sciences
Larson, T., Department of Geological Sciences, The University of Texas at Austin
Thibodeau, A., Department of Geological Sciences, Dickinson College

Oceanic anoxic events (OAEs) have been shown to have a close influence on source rock deposition, marine extinctions, and the reorganization of carbonate factories throughout geologic time. The Early Jurassic Toarcian OAE (~183 Ma), in particular, coincides with a marine mass extinction and the deposition of deep-water black shales; the putative cause of the OAE was the emplacement of the Karoo-Ferrar-Chon Aike Large Igneous Province. Although black shales are the hallmark of oceanic anoxic events, the contemporaneous shallow marine response to anoxia and other stresses is subtler and poorly documented by comparison. Nevertheless, being able to recognize the sedimentological and geochemical signals of OAEs in shallow-water carbonates could be a powerful tool in correlating basinal black shales to their shelfal equivalents. This research focuses on characterizing the record of the Toarcian OAE in shallow-water carbonates of the Adriatic Carbonate Platform.

The Adriatic Carbonate Platform provides a key record of the Toarcian OAE as it is one of the few peri-Mediterranean platforms from the Tethys Ocean that experienced nearly continuous sedimentation throughout the Pliensbachian and Toarcian. Geochemical and paleontological data from two sections of the Trnovski Gozd karst plateau are used to assess the timing of volcanism and the response of biotic and abiotic carbonates to environmental changes associated with the OAE. Benthic foraminifera, dasycladacean algae, and oncolitic packstones dominate diverse skeletal assemblages in the Pliensbachian record while the early Toarcian is dominated by crinoidal-oolitic packstones and grainstones, with rare low-diversity skeletal assemblages. A prominent hardground interval separates these two distinct lithofacies and is coincident with a maximum organic carbon isotope excursion of approximately -6‰. This excursion reflects a major global carbon-cycle perturbation. A concomitant mercury enrichment points to a volcanic trigger for the OAE; the effects of which are reflected in nutrient and redox-sensitive element concentrations (Ba, P, Mo, V, Mn, Ni). Together these sedimentological and geochemical changes represent an observable response in the shallow-water carbonates of the Adriatic Carbonate Platform to the Toarcian OAE. Correlation to previously published sections from the platform and adjacent basins shows a shift in the volume and type of carbonate production on the platform coincident with the OAE, suggesting that carbonate platform architecture and development can be significantly influenced by OAEs.

Keywords: Oceanic Anoxic Event, Carbonate Sedimentology, Chemostratigraphy

CCG
LCMS

ARCHITECTURE OF A MID-CRETACEOUS PATCH REEF: HIGH RESOLUTION MAPPING OF FACIES STRUCTURES AND DISTRIBUTION AT PAUL SPUR, BISBEE, ARIZONA

Kelly Hattori
Hattori, K., Jackson School of Geosciences, The University of Texas at Austin, Austin, TX
Martindale, R., Jackson School of Geosciences, The University of Texas at Austin, Austin, TX
Kerans, C., Jackson School of Geosciences, The University of Texas at Austin, Austin, TX

Patch reef complexes are commonly found in the shelf interior of carbonate platforms. These small scattered buildups are potential hydrocarbon targets in the Maverick basin and more broadly within Cretaceous reservoirs in the Middle East. However, three-dimensional facies architecture within patch reefs is difficult to determine using only subsurface data. If cores are available, vertical facies succession can be determined, but lateral variation in facies may be difficult to predict with limited core coverage. Lateral facies distribution and architecture is better assessed in patch reef outcrop analogs. The Paul Spur patch reefs near Bisbee, Arizona are ideally suited for assessing three-dimensional spatial and temporal facies variability. Previous interpretations of this 1.5 km-long exposure of Mural Limestone disagree as to the overall history of the reef with regards to facies relationships and distribution. Early work at Paul Spur attributed spatial facies distribution to biotic zonation of a reef during one period of growth, while later work revisited the depositional history of the locality and concluded that it preserves multiple stages of reef growth with facies succession and variation both spatially and temporally controlled.

This study aims to better resolve the depositional history and biotic composition of the Paul Spur patch reef complex with respect to stratal geometry and both spatial and temporal facies relationships. High-resolution lateral facies mapping of the exposed reef top north of Highway 80 is integrated with three-dimensional digital outcrop modeling techniques to facilitate improved understanding of the history of reef growth and patch reef architecture. New relationships revealed by the high-resolution dataset better elucidate facies architecture throughout the main growth phases of the reef. Multiple generations of reef growth are preserved, and lateral facies variability is extensive and not as well-constrained as initially hypothesized. Reef framework facies exhibit a gradational increase in rudist abundance and decrease in coral abundance moving up-section, reflecting the evolution of reef communities through time. Traditional facies analysis does not fully capture the depositional history of the reef. Here, the use of new techniques reveals readily observable three-dimensional facies architecture that can be integrated into the preexisting depositional model for improved understanding of patch reefs in open shelf moderate energy environments. The model can be used to examine facies architecture from a variety of angles without extrapolation, thus improving the utility of Paul Spur as an outcrop analog for patch reefs identified in the subsurface.

Keywords: Cretaceous, patch reef, facies analysis, photogrammetry

CCG
LCMS

Using central Texas speleothems to identify regional moisture distribution during the last deglaciation

Christina James
James, C., The University of Texas at Austin
Charlton, T., The University of Texas at Austin
Banner, J., The University of Texas at Austin
Koleszar, A., The University of Texas at Austin
James, E., The University of Texas at Austin
Breecker, D., The University of Texas at Austin
Miller, N., The University of Texas at Austin
Edwards, L., The University of Minnesota
Zhang, P., The University of Minnesota

The SW US is a drought-prone and moisture limited region. Understanding the timing and magnitude of changes in moisture source during the last deglaciation, and in particular, abrupt warming (Bolling-Allerod, BA, 14.7 – 12.9 ka) and cooling events (Younger Dryas, YD, 12.9-11.5 ka), can provide insight into how changes in global climate affect moisture distribution in this region. SW US speleothem $\delta^{18}O$ values and growth rates may serve as proxies for source and amount of rainfall. In central Texas, a speleothem $\delta^{18}O$ and growth rate record (sample CWN-4; Feng et al., 2014) appears to predominantly reflect moisture source (e.g. Gulf of Mexico vs. Pacific moisture), and a concomitant increase in rainfall amount, during the BA. This is based on similarities in changes in CWN-4 $\delta^{18}O$ values from Gulf of Mexico (GoM) seawater proxy records before and during the BA. CWN-4 records a hiatus in growth from 12.3 – 10.1 ka, while two speleothem records from a cave in New Mexico and in Arizona (Asmerom et al., 2010; Wagner et al., 2010), also show a cessation in growth near the end of the YD. The consistent cessation in growth between all three records could suggest a more arid climate in the SW US as the climate transitioned from the colder YD to warmer Holocene climate. Here we present speleothem records from two other caves in central Texas (McN-1; IC-2) which grew during the YD and span the CWN-4 growth hiatus interval, extending later into the Holocene. Similar to CWN-4, and the New Mexico and Arizona records, McN-1 has a slower growth rate near the termination of the YD, potentially indicating drier conditions. Consistent decreases in the $\delta^{18}O$ records of ~ -1‰ during the YD in both the GoM seawater and McN-1 and IC-2 records suggest that the speleothem $\delta^{18}O$ records are recording changes in moisture source $\delta^{18}O$ values. Deglacial GoM-sourced moisture was influenced by input from isotopically light meltwater via the Mississippi River drainage system, where $\delta^{18}O$ values from GoM seawater proxy records are suggested to proxy meltwater outflow (Flowers et al., 2004; Williams et al., 2012). These decreases in the $\delta^{18}O$ records could also indicate meltwater outflow into the GoM due to increasing temperatures associated with the end of the YD.

Keywords: speleothem, moisture source, oxygen isotope, paleoclimtate, karst, deglaciation

CCG
LCMS

Sensitivity analysis of Lower Miocene sandstones to CO2 saturation in the inner continental shelf of the Texas Gulf of Mexico

Reinaldo Sabbagh Maciel
Sabbagh, R., The University of Texas at Austin, Austin,TX
Meckel, T., Bureau of Economic Geology, Austin, TX

Time-lapse seismic analysis is the primary method used to monitor CO_2 injected into the subsurface for enhanced oil recovery and permanent storage. The Gulf of Mexico has active CO_2-EOR and great potential for CO_2 storage. Related to storage, few studies attempt to quantify the effects of CO_2 on the seismic response in the saline aquifers that could be used as storage reservoirs. Using well log data from the Lower Miocene section of the inner-shelf, a study was undertaken to understand how the elastic properties of the intended storage reservoirs may be affected by variations in CO_2 saturation. The approach uses rock physics modeling, fluid substitution, amplitude variation with angle (AVA), and statistical classification. The AVA modeling shows a high sensitivity to CO_2 due to the soft frame of the rock. The statistical classification shows that the Vp/Vs and P-impedance is likely to have a higher success probability to discriminate between brine and CO_2

Keywords: CO2 sequestration, seismic monitoring, rock physics

EG
LCMS

Neogene Current-Modified Submarine Fans and Associated Bed Forms in Mexican Deep-water Areas

Luis Enrique Arce Perez
Arce, E., Institute for Geophysics
Snedden, J., Institute for Geophysics
Roberson, R., PGS
Herron, D., PGS

In the southwestern Gulf of Mexico deep-water areas, new and newly reprocessed seismic data have revealed a series of large bed forms, with set thicknesses of 130 to 250 meters. These exhibit hummocky, oblique and shingled to parallel seismic clinoform reflections. This Miocene to Plliocene-age seismic package is interpreted to have been deposited in paleowater depths of 450 meters. Those shingled seismic reflections in offshore east Mexico are interpreted as current-modified submarine fans and associated contourite drift deposits. These bed forms may be related to strong ocean bottom currents that modified submarine fans and transported sediment to the north. Other mechanisms considered are cyclic steps of bed forms related to turbidity flows. These bed forms were identified on older seismic data, but are better imaged and interpreted on new seismic data. Plans are to map out and investigate the origin and extent of fans and contourites that extends over a large area of the Gulf of Mexico.

In the Early Miocene several submarine fans systems were formed by the sediment input related to orogenic activity in Mexico. Submarine fan development persisted into the Middle Miocene due to continued uplift and erosion of the Mexican landmass. Initial contourites are small and close proximity to the deep-water fan. In the Late Miocene time, contourite drift field reached its maximum extent in the Mexican deepwater area, anchored on its southern end by a submarine mound. This mounded submarine fan is located in the offshore northeast Veracruz and can be linked to increased uplift and erosion of the Trans-Mexican volcanic belt. In the Miocene-Pliocene, the large contourite drift field begins to diminish in size and scale and is moribund by the Pliocene, with establishment of oceanic circulation similar to the present day.

This research is important to understand more about the Gulf of Mexico and also for the Miocene timeframe that is a key phase in the earth's history. The role of the changes in bottom water flow during progressive closure of the equatorial seaway separating North and South America will also be discussed

Keywords: Miocene, Deep, waters, gulf, mexico, neogene, submarine, bedforms

EG
LCMS

Integrated Approach to Pressure Prediction at Mad Dog, Gulf of Mexico

Landon Lockhart
Flemings, P., The University of Texas at Austin, Austin, TX
Nikolinakou, M., The University of Texas at Austin, Austin, TX
Heidari, M., The University of Texas at Austin, Austin, TX

We apply a new workflow to predict pressure that integrates sonic velocity data, geomechanical modeling, and a critical state soil model from wellbore data. Specifically, we incorporate the effect of both mean and shear stress in the development of excess pressure. We illustrate this workflow in the deepwater Gulf of Mexico Mad Dog Field, which is associated with an allochthonous salt body. Because of loading from the salt, stresses are not uniaxial; the horizontal stresses are elevated, leading to higher mean and shear stresses. At a control well, we develop a relationship between velocity and an equivalent effective stress in order to account for both the mean and shear stress effect on pore pressure. We obtain this equivalent effective stress using a geomechanical model of the Mad Dog Field. We then apply the calibrated velocity-stress relationship to other wells and demonstrate how our new approach improves pressure prediction in areas near salt where mean and shear stress are different than those measured from the control well. Our methodology and results show that pore pressure is driven by a combination of mean stress and shear stress, and highlight the importance of shear-induced pore pressures. Furthermore, the impact of our study extends beyond salt bodies; the methodology used and insights gained are applicable to geological environments around the world with a complex geologic history, where the stress state is not uniaxial (fault zones, anticlines, synclines, continental margins, etc.)

Keywords: Pore pressure, modeling, Gulf of Mexico, salt

EG
LCMS

Automatic gather flattening for AVO analysis using amplitude-adjusted plane-wave destruction filters

Mason Phillips
Phillips, M., The University of Texas at Austin

I propose a method to efficiently measure regularized non-hyperbolic moveout corrections from seismic offset or angle gathers for AVO analysis using amplitude-adjusted plane- wave destruction filters. Plane-wave destruction filters can efficiently measure shifts of less than a few samples, making this algorithm particularly effective for detecting small time-shifts associated with residual moveout between adjacent seismic traces. Separating the estimation of time-shifts and amplitude variations allows residual moveout associated with complex velocity structures and anisotropy to be measured accurately, even in the presence of class II AVO anomalies. The effectiveness of this algorithm in predicting residual moveout correction is determined by applying it to synthetic and real examples and comparing the results to industry standard correlation based techniques.

Keywords: AVO, seismic data processing, seismic interpretation

EG
LCMS

Pressure and Stress at the Macondo Well

Francis W Pinkston
Pinkston, F., Jackson School Of Geosciences, The University of Texas at Austin, Austin, TX
Flemings, P., Jackson School Of Geosciences, The University of Texas at Austin, Austin, TX

I study pore pressure and stress in the Macondo Well in deepwater Gulf of Mexico (Mississippi Canyon Block 252) with in-situ pressure measurements, log data, leak-off tests (LOT), and the occurrence of kicks and lost mud events during drilling. The average overburden gradient increases from 0.8 psi/ft at 1000 ft $TVD_{sea\ floor}$ to 0.97 psi/ft at the Middle Miocene M56 reservoir sands (13000 ft) as derived by analysis of regional density logs. Our velocity-to-effective stress transform, parameterized with pressure measurements, indicates that pore pressure increases in parallel with the overburden. Normalized overpressure, $\lambda^* = (u-u_h)/(\sigma_v-u_h)$, increases from 0.5 at 4000 ft $TVD_{sea\ floor}$ to 0.78 at 12600 ft, where u= pore pressure, u_h=hydrostatic pressure, and σ_v = overburden stress. From the M57 reservoir at 12600 ft to the M56 at 13000 ft, measured pressures abruptly fall by 1360 psi, causing λ^* to drop from 0.78 to 0.56. Over a similar depth range, the stress ratio, $K = (\sigma_h-u)/(\sigma_v-u)$, decreases from >1 to 0.6, where σ_h = least principal stress. A well in MC 562, 21 miles away, records the same pressure (within 19 psi) within a sand that is mapped as the lateral equivalent to the M56 sand. The hydrocarbon fluid density is also inferred to be identical (0.21 psi/ft). This suggests that the M56 is regionally hydraulically connected and may provide the mechanism for the pore pressure regression encountered at Macondo.

Keywords: pore pressure, fracture gradient, overpressure

LCMS-10

EG
LCMS

Lithofacies, diagenesis and reservoir quality of deepwater unconventional system: Wolfcampian succession, Midland Basin, West Texas

Hualing Zhang
Hualing, Z., Bureau of Economic Geology, The University of Texas at Austin, Austin, TX
Xavier, J., Bureau of Economic Geology, The University of Texas at Austin, Austin, TX
Qilong, F., Bureau of Economic Geology, The University of Texas at Austin, Austin, TX

The Lower Permian Wolfcamp deep-water basinal succession in the Midland Basin has recently become an important target for unconventional reservoirs. However, uncertainty remains for reservoir characterization of the Wolfcamp due to the complexity of lithofacies in this region.

This study combines petrophysical observations from cores, thin sections, and scanning electron microscope cubes with chemostratigraphic data from X-ray fluorescence (XRF) and total organic matter content (TOC).

Lithofacies investigation were made using 4 drilling cores from Counties Glasscock (180 ft), Sterling (110 ft), and Irion (80 ft and 60ft), Texas. Based on core analysis, microscopic observations and XRF data, 4 lithofacies were defined in the Glasscock core representing the Wolfcamp upper calcareous interval: (1) fusulinid bioclast packstone, (2) calcareous mudstone, (3) brecciated mudstone, and (4) laminated skeletal mudstone. While the Wolfcamp lower siliciclastic interval is reflected by 5 lithofacies identified in Sterling and Irion cores as (5) clean litharenite, (8) calcite cemented litharenite, (7) clay-coated litharenite, (8) siltstone, and (9) siliceous mudstone.

The Wolfcamp succession reveals a complex diagenetic history, ranging from compaction, recrystallization, replacement, cementation, and dissolution. Primary pores are rarely preserved due to significant compaction showing concavo-convex grain contact and sedimentary rock fragments as pseudo matrix. Isopachous and blocky carbonate cements further occlude initial pore space, especially in the calcareous interval. However, chlorite coating in lithofacies 7 inhibits further quartz cementation of primary pore space, making it a potential reservoir target.

Measured core plug porosity and permeability suggest moderate porosity up to 10.2%, and very low permeability ranging from 0.001 to 0.197md. The highest porosity and permeability are reported in lithofacies1 and 7. Combining this result with XRF and TOC data, lithofacies7 is expected to have the best reservoir quality since it is more organic-rich and laterally extensive across this region.

Findings in these cores demonstrate variations in lithofacies and complicated diagenesis in the Wolfcamp succession that controls reservoir quality. Future work will incorporate well log correlation for regional reservoir characterization across the Midland Basin.

Keywords: Wolfcampian, Midland Basin, Unconventional resources

LCMS-11

SETP
LCMS

Intra-grain common Pb correction and detrital apatite U-Pb dating via LA-ICPMS depth profiling

Patrick Boyd
Boyd, P., The University of Texas at Austin, Austin, TX
Stockli, D., The University of Texas at Austin, Austin, TX
Galster, F., The University of Texas at Austin, Austin, TX

Apatite is a common accessory phase in igneous and clastic sedimentary rocks. While apatite is widely employed as a low-temperature fission-track and (U-Th)/He thermochronometric tool, it has been increasingly utilized to constrain moderate temperature cooling histories by U-Pb dating. While apatite U-Pb is characterized by a nominal closure temperature of ~450°C, it's closure temperature has been shown to be grain size sensitive and apatite can have a thermal sensitivity window between 375-550°C. This unique temperature window recorded by apatite U-Pb dating and the near-ubiquitous presence of apatite in igneous and clastic sedimentary rocks makes it a powerful tool to complement the high- and low-temperature cooling histories recorded by U-Pb, Ar/Ar, fission-track, and (U-Th)/He dating methods and to illuminate mid-crustal tectono-thermal processes. Apatite, unlike zircon, incorporates only modest amounts of U and Th (1-10s of ppm). Hence a major hurdle for apatite U-Pb dating is the incorporation of non-radiogenic "common" Pb during formation, limiting the application and utilization of the technique. In bedrock samples, common Pb concentration in apatite can be corrected for by the measurement of common Pb in cogenetic mineral phases (e.g., feldspar) that do not incorporate U, or possibly through multi-aliquot mixing lines in Tera-Wasserburg Concordia space. While these traditional methods for common Pb correction in apatite can work for igneous samples due to the presence of a U-free cogenetic phase, this is not possible for detrital apatite in sedimentary rocks with variable common Pb composition and no cogenetic phases. This obstacle has hindered the application of detrital apatite U-Pb dating in provenance studies, despite the fact that the obvious power of apatite U-Pb dating in detrital provenance studies has been widely recognized. The lower chemical and mechanical durability of apatite means that apatite found in a sedimentary rock are more often first-cycle detritus, whereas high-durability zircons often endure weathering and abrasion and undergo multiple recycling episodes. Secondly, apatite are present in a wide spectrum of magmatic rock types, while zircon form mainly in felsic plutonic rocks and zircon fertility is biased by source lithology. Thirdly, the 375-500°C temperature window allows access to thermal histories of mid- to lower-crustal processes in the interior of orogenic belts and experience minimized burial resetting. This study presents an exciting new method for the *in situ* correction of common Pb in apatite through the utilization of novel LA-ICP-MS (Laser Ablation-Inductively Coupled Plasma-Mass Spectrometry) depth profiling that can recover U/Pb ratios at high spatial resolution (<1 micron) during progressive ablation of euhedral grains. Due to common intra-grain U variability in apatite, depth profiled U-Pb analysis allows for the reconstruction of intra-grain radiogenic-common Pb mixing lines in Tera-Wasserburg space. This mixing line allows for determination of both the common Pb corrected U-Pb age and the common Pb composition of individual detrital apatite. This novel method allows for effective correction of common Pb in detrital apatite despite the lack of a cogenetic phase, making it feasible to conduct detrital apatite U-Pb dating in provenance and source-to-sink studies.

Keywords: Apatite U-Pb, Provenance, Detrital

This abstract has been withdrawn

LCMS-12

SETP
LCMS

Structural diagenesis of a sub-salt fractured carbonate reservoir analog, NE Brazil

Elizabeth McKinnon
McKinnon, E., Jackson School of Geosciences, The University of Texas at Austin, Austin, TX
Marrett, R., Jackson School of Geosciences, The University of Texas at Austin, Austin, TX

This study presents a microstructural and outcrop analysis of the Crato Formation, NE Brazil. The Crato Formation is an Aptian fractured limestone that has been considered an analog to low-permeability laminated facies of pre-salt offshore carbonate reservoirs of Brazil. Fractures are the most prominent structures and are the most important features for potential fluid storage and flow in the subsurface tight reservoirs. Horizontal gypsum veins present in the study region indicate that the Crato Fm. may have experienced periods of localized fluid overpressure that resulted in the formation of bedding parallel opening mode fractures.

This study aims to describe the microstructural characteristics of these horizontal veins and examine their context in relation to other structures of the formation in order to understand the structural diagenesis of the formation. Structures in the study area include horizontal gypsum veins, vertical to subvertical gypsum veins, horizontal stylolites, steeply dipping shear fractures, vertical calcite veins and vertical stylolites. Cross-cutting relationships indicate that horizontal gypsum veins and shear fractures were the earliest structures to form, indicating early tectonism and possible fluid overpressure during diagenesis. Vertical gypsum veins are also an early feature and are the largest structures found in the formation. These structures continue into the muddy beds that overlie the laminated limestones and show evidence of reactivation and jointing. Horizontal gypsum veins and matrix rocks are host to horizontal stylolites, features created by pressure solution likely due to increased overburden with burial. Vertical stylolites, due to their short lengths, rarely cut other features. Finally, thin, vertical calcite veins cut every other feature and were among the last structures to form.

The current work presents SEM images of horizontal fractures and structural maps in regions where they are both abundant and absent in order place them in context of other, more ubiquitous structures. The ultimate goal of the study is to determine the opening mechanisms of the horizontal gypsum veins, their relationship with vertical gypsum and calcite veins and the potential for fluid flow and overpressure in the Crato Fm. at the time of diagenesis.

Keywords: carbonate, limestone, structure, tectonics, gypsum, overpressure, aptian, brazil

LCMS-13

SETP
LCMS

Holocene Geologic Slip Rate for the Mission Creek Strand of the southern San Andreas fault, Indio Hills, CA

Juan Munoz
Munoz, J., The University of Texas at Austin
Behr, W., The University of Texas at Austin
Gold, P., The University of Texas at Austin
Fryer, R., The University of Texas at Austin
Sharp, W., Berkeley Geochronology Center

Slip on the southern San Andreas fault in the northwestern Coachella Valley in Southern California is partitioned between three strands, the Mission Creek, Garnet Hill, and Banning strands. In the vicinity of the Indio Hills, the NW striking Mission Creek strand extends from the Indio Hills into the San Bernardino Mountains, whereas the Banning and Garnet Hill strands strike WNW and transfer slip into the San Gorgonio Pass region. Together, these three faults accommodate ~20 mm/yr of right-lateral motion. Determining which strand accommodates the majority of fault slip and how slip rates on these strands have varied during the Quaternary is critical to seismic hazard assessment for the southern California region. Here we present a new Holocene geologic slip rate from an alluvial fan offset along the Mission Creek strand at the Three Palms site in the Indio Hills. Field mapping and remote sensing using the B4 LiDAR data indicates that the Three Palms fan is offset ~53 +4/-6 meters. U-series dating on pedogenic carbonate rinds collected at 25-100 cm depth within the fan deposit constrain the minimum depositional age to 3.49 +/- 0.92 ka (2σ error), yielding a maximum slip rate of 15.1 +1.2/-1.8 mm/yr. This Holocene maximum slip rate overlaps within errors with a previously published late Pleistocene slip rate of 12-22 mm/yr measured at Biskra Palms, a few kilometers to the south. Cosmogenic 10Be surface exposure samples were also collected from the fan surface to bracket the maximum depositional age.The samples yielded a scattered dataset with high apparent inheritance and a mean age of 13.1 +7.5/-6.1 ka (1σ error). However, the minimum sample age of 5.2 ± 0.5 ka (1σ error) was taken as the maximum depositional age for the fan (assuming zero inheritance). This age, along with the preferred offset, yields a minimum slip rate of 10.2 +0.9/-2.0 mm/yr. We therefore propose a range of Holocene geologic slip rates of10.2-15.1 mm/yr.

Keywords: geologic slip rate, neotectonics, San Andreas fault, cosmogenic, LiDAR, tectonic geomorphology

SETP
LCMS

Provenance of the Cycladic Blueschist Unit and Basement in the Southern Cyclades and Cooling and Exhumation History of the Metamorphic Core Complex in the Aegean Domain, Sikinos Island, Cyclades, Greece

Eirini Poulaki
Poulaki, E., Department of Geological Sciences, The University of Texas at Austin, Austin, TX
Flansburg, M., Department of Geological Sciences, The University of Texas at Austin, Austin, TX
Stockli, D., Department of Geological Sciences, The University of Texas at Austin, Austin, TX
Soukis, K., National and Kapodistrian University of Athens, Greece

The Hellenic subduction complex, exposed in the Cyclades Island of Greece, has a unique assemblage of metamorphic units that record both early Cenozoic subduction-related metamorphism and subduction-channel exhumation as well as late Cenozoic back-arc extension and formation of domal metamorphic core complex formation during slab rollback. During early Cenozoic times, during subduction the CBU experienced high-pressure-low temperature metamorphism during the subduction of Gondwana-derived continental fragments and the associated trench fill underneath Variscan Europe (Pelagonia). The Cycladic Islands can be subdivided into two major tectonic domains, the Sub-Pelagonian Upper Unit and the Cycladic Blueschist Unit (CBU) and its associated crystalline Cycladic Basement. The CBU and its crystalline basement complex were exhumed in a two-stage fashion. The first stage took place during the subduction, under eclogite and blueschist facies conditions, while the second stage occurred under greenschist facies during the Oligocene-Miocene large-magnitude, back-arc extension. While most Cycladic islands only exposed limited extents of Cycladic Basement, the islands of Sikinos and Ios exposes greenschist-facies CBU marbles and schist with preserved blueschist-facies relicts and the lithologically variable Cycladic Basement. The Cycladic Basement complex comprises a wide variety of deformed felsic plutonic rocks as well as metasedimentary country rocks, known as the Cycladic Basement Carapace, dominated by garnet mica schists.

In this study, detrital zircon U/Pb geochronometry will be used to determine the sedimentary provenance and maximum depositional ages of the different metasedimentary CBU and CBU Basement units on Sikinos and the northern part of Ios. In addition, zircon U-Pb dating will be employed to constrain the igneous intrusion ages and the timing of metamorphism of the CBU Basement units on Sikinos. Zircon U-Pb) dating is being carried out by laser-ablation split-stream ICP-MS analysis in order to simultaneously determine U-Pb ages and trace element compositions and hence to distinguish between magmatic and metamorhic zircon ages. This is critical for determining both maximum depositional ages (youngest magmatic zircon) and the age of metamorphism in the CBU. Preliminary zircon U-Pb results from the CBU Basement Carapace and the igneous CBU Basement in Sikinos indicate that the Carapace is only slightly older(~325Ma) than the intrusions (~268Ma), but both are Carbonifeous in age. In contrast, the CBU exhibits a spread of detrital zircon U-Pb ages ranging from ~100 Ma to 2000 Ma with enigmatic metamorphic cores of ~26 Ma that would imply the youngest reported HP-LT metamorphism in the Cyclades. In order to constrain the late Cenozoic core-complex formation and put this into a regional context, zircon and apatite (U-Th)/He thermochronometry are used to determine the cooling and exhumation history of the islands. Importantly this will also clarify the nature of the tectonic contact between the two units and allow the comparison with nearby islands, such as Naxos or Paros. The conclusions of the study will have broad implications for the paleogeographic evolution of the northern margin of Gondwana and the subduction interaction with the Eurasian plate, the evolution of the Hellenic subduction zone, the timing of slab rollback, and the multi-stage exhumation history of the CBU in the Aegean core complexes.

Keywords: Hellenic subduction zone, Aegean metamorphic core complex, Geothermochronology, Sikinos, Ios,

LCMS-15

SETP
LCMS

Structural Controls on Fluid Flow and Stable Isotope Transport during Skarn Formation

Evan Ramos
Ramos, E., Department of Geological Sciences, The University of Texas at Austin
Hesse, M., Department of Geological Sciences, The University of Texas at Austin
Jordan, J., Department of Geological Sciences, The University of Texas at Austin
Barnes, J., Department of Geological Sciences, The University of Texas at Austin

Fluid flow during skarn formation is responsible for massive fluxes of CO_2 and the deposition of ore metals. Commonly, it is thought that most skarns form from an initial pulse of magmatic fluid and later incorporate surface-derived meteoric fluids and host rock-derived metamorphic fluids (e.g., Meinert et al., 2005). However, geochemical observations at Empire Mountain in the Sierra Nevada Batholith suggest the opposite trend. The oxygen isotope composition of skarn garnets reveals meteoric water input at the onset of skarn formation with magmatic fluids entering the system later (D'Errico et al., 2012). This, in addition to large and rapid fluctuations in garnet's oxygen isotope composition during growth, is argued to be evidence for brecciation of the surrounding rock via fluid overpressurization: a process which forms high-permeability pathways that can enhance flow of meteoric water to skarn-forming depths. Our study tests this hypothesis by numerically modeling two dimensional fluid flow, heat transport, and stable isotope transport during skarn formation. The models allow us to observe spatial and temporal changes in a fluid's oxygen isotope composition. Different crustal permeability structures and their influence on stable isotope transport are explored in detail.

Preliminary models reveal two ways in which fluid with meteoric oxygen isotope compositions can exist at skarn-forming depths: (1) flow along pre-existing high permeability pathways, such a high angle normal faults or vertically-dipping metarhyolitic units or (2) the existence of meteoric fluid that is isotopically out of equilibrium with the surrounding rock prior to skarn formation. Both ways illustrate that fluid flow in high-permeability regions operates faster than solid-fluid isotope exchange and heat transfer, thus allowing fluids with meteoric oxygen isotope compositions to retain their original compositions. The models further reveal that brecciation does not need to be invoked to cause rapid and large fluctuations in fluid oxygen isotope composition. In models with vertically dipping metarhyolitic units, areas adjacent to the magmatic body and up-flow of the regional flow system experience > 10 ‰ fluctuations in $\delta^{18}O$ values, on par with observations of skarn garnets at Empire Mountain. The modeled fluctuations occur due to the competition between heat transfer and fluid advection during isotope transport and not due to changes in fluid source during skarn formation. Future geochemical measurements of oxygen isotopes in more distal skarn rocks and the surrounding country rock will better elucidate the fluid source evolution during the formation of the Empire Mountain skarn. Nevertheless, this study underscores the influence that physical properties of the medium have on stable isotope transport during skarn formation.

Keywords: oxygen isotopes, skarn, garnet, carbon dioxide, numerical modeling, hydrothermal

SETP
LCMS

Correlating Cu-sulfide and Au mineralization in the Ertsberg-Grasberg District using LA-ICP-MS and HRXCT: Is There a Genetic Connection?

Kylie Wright
Wright, K., Department of Geological Sciences, The University of Texas at Austin, Austin, TX
Miller, N., Department of Geological Sciences, The University of Texas at Austin, Austin, TX
Ketcham, R., Department of Geological Sciences, The University of Texas at Austin, Austin, TX
Kyle, J., Department of Geological Sciences, The University of Texas at Austin, Austin, TX

The Ertsberg-Grasberg district in Papua, Indonesia, hosts two of the largest intrusion-related Cu-Au deposits in the world: the Ertsberg Intrusive System and the Grasberg Igneous Complex. Cu mineralization within the Grasberg porphyry and Ertsberg skarn systems is primarily found as bornite and chalcopyrite. Au is commonly found in association with Cu mineralization where gold occurs as inclusions within or along the boundaries and edges of Cu-sulfide minerals. The traditional model for gold deposition in large scale porphyry and skarn systems relies primarily on hydrothermal fluid pulses and does not take into account potential gold contributions from Cu-sulfides. At hydrothermal ore-forming temperatures, approximately 400° to 700° C, bornite and chalcopyrite can host up to 1800 ppm Au within the Cu-sulfide lattice. However, upon retrograde cooling of the hydrothermal system, the ability of bornite and chalcopyrite to host Au decreases significantly to about 10 ppm, indicating that the Au could be expulsed from the sulfide lattice. Given the close association of gold and Cu-sulfide concentrations, it is possible that gold grains along the boundaries of Cu-sulfides form as the gold passively migrates out of the sulfides and collects to form a grain. We use HRXCT to construct 3D Voronoi regions of potential Au “diffusional drainage” from within the Cu-sulfides, where the expectation is a positive correlation between Au grain size and modified Voronoi polyhedron volume, defined as the volume of sulfide closer to that grain than any other via a connected path through sulfide. Modified Voronoi polyhedra will provide a minimum correlation between Cu-sulfides and proximal gold grains. In this study, we use LA-ICP-MS to evaluate trace element contents of porphyry and skarn Cu-sulfides, as well as determine spatial variations of elemental concentrations near gold grains within Cu-sulfide minerals. Initial LA-ICP-MS data do not show clear spatial variation in concentrations, though this will be improved in future scans using a smaller laser spot size and slower scan rate during analyses.

Keywords: Computed tomography, LA-ICP-MS, ore, gold, copper

SHP
LCMS

Isolating lithologic controls on landscape morphology in the Guadalupe Mountains

Emily Bradshaw
Marino, E., The University of Texas at Austin
Johnson, J., The University of Texas at Austin

Qualitatively, lithologic control on topography is apparent in many landscapes. This is perhaps most notably evident in dryland settings with horizontal stratigraphy, where the contrasting geomorphic expression of “cliff formers” and “slope formers” is common. However, in many geomorphic studies, lithologic contrasts are often acknowledged as important, but are otherwise ignored in attempts to determine tectonic forcing or climatic control. Tectonic inactivity and relatively little spatial variability in climate make the Guadalupe Mountains of Texas and New Mexico an ideal site to investigate the effects of lithology on topography. To determine the effects of lithology, channel steepness will be compared to lithologic units across the region. Steepness indices were calculated for approximately 1200 channels in the Guadalupe Mountains and surrounding area using elevation data extracted from USGS 10m Digital Elevation Models. Individual steepness indices were fitted for distinctive segments along each longitudinal stream profile in order to capture the variability as streams cross potential lithologic contacts. These indices were then grouped per 23 discrete lithologic units, including abundant limestone and dolomite with some sandstone and shale. Preliminary datasets were compared using the Kruskal-Wallis method for hypothesis testing and results show that significant differences exist between the lithologic groups, suggesting potential correlation among the variables. With additional analysis, we expect to find statistically significant differences in steepness among the lithologic units, indicating some effect of lithology on landscape morphology within this environment.

Keywords: Geomorphology, Channel Steepness, Lithology, Digital Elevation Models

LCMS-18

SHP
LCMS

Geomorphic and Incision History of the Northern Rio Grande Gorge near Questa, New Mexico

Travis Clow
Clow, T., Jackson School of Geosciences, The University of Texas at Austin, Austin, TX
Behr, W., Jackson School of Geosciences, The University of Texas at Austin, Austin, TX
Helper, M., Jackson School of Geosciences, The University of Texas at Austin, Austin, TX
Stockli, D., Jackson School of Geosciences, The University of Texas at Austin, Austin, TX

We investigate relationships between river incision, aggradation, and widening in a ~5 km stretch of the northern Rio Grande River Gorge near the confluence with the Red River in New Mexico using detailed geomorphic mapping and cosmogenic ^{3}He surface exposure dating. This wide and deep stretch of the river exhibits a unique set of cohesive, stacked toreva blocks, incoherent landslides, rockfalls, and slumps developed within ~3-5 Ma Servilleta basalts and intercalated Pliocene Santa Fe Group gravels. Toreva blocks of paired upper and lower Servilleta basalt are best developed along the eastern side of the river—they exhibit coherently-dipping, patinated tops that can be reconstructed to the gorge walls, but with toes that are truncated or buried by later deposits. Located below these landslide features is a flight of fill and fill-cut terraces spanning 5 levels at elevations of 49, 39, 29, 22, and 7 m above the modern river grade. Terraces at 29 m can be correlated across and along the river axis, whereas others are more locally developed. All terraces exhibit well-defined boulder levees and risers, and rounded and sculpted basalt clasts.

A preliminary ^{3}He surface exposure age of ~62 ka was obtained from the uppermost terrace tread (Qt5); additionally, a ^{10}Be exposure age of ~28ka was obtained from the Qt2 terrace tread, with more dating in progress. If initiation of gorge incision was coeval with capture of the San Luis Valley of southern Colorado at ~440-389 ka, average incision rates prior to the formation of Qt5 were .5-.6 mm/yr. This incision was likely coincident with toreva block formation and substantial gorge widening, as the toreva blocks and large-scale uncohesive landslide deposits predate terrace development. Average incision from ~62 ka to present day appears to have been faster, with minimum rates of .8 mm/yr. Gorge narrowing is observed during this time period, with only minor widening accommodated by slumping and incoherent landsliding that post-date terrace treads. This period of incision was punctuated by aggradational events that may correlate with late Pleistocene MIS climate cycles and/or regional climatic events, with terraces incised into and abandoned during transitions from glacial to interglacial climate. These increasingly rapid incision rates mirror the phenomena seen in other western US river systems since the Pliocene.

Keywords: geomorphology, terraces, cosmogenic, geochemistry, surface, exposure, dating, landslides, gorge, river, fluvial, climate, tectonics, MIS, pleistocene, incision, interaction

CCG
LCPHD

Speleothem chronology with sub-annual resolution in a near-entrance cave setting

Peter Carlson
Carlson, P., Department of Geological Sciences, The University of Texas at Austin, Austin, TX
Miller, N., Department of Geological Sciences, The University of Texas at Austin, Austin, TX
Banner, J., Department of Geological Sciences, The University of Texas at Austin, Austin, TX
Breecker, D., Department of Geological Sciences, The University of Texas at Austin, Austin, TX

Speleothems that grow in well-ventilated zones of caves are typically avoided when selecting specimens for paleoclimate reconstruction, due to concerns about evaporation and kinetic isotope effects. Near-entrance cave environments are characterized by near ambient CO_2 concentrations year-round and are influenced by surface temperature fluctuations. At Westcave Preserve (Westcave), a shallow, well-ventilated cave in central Texas, we have found seasonal temperature differences recorded in both the oxygen isotope and trace element compositions of speleothem calcite. The seasonal nature of these records has been confirmed by monitoring the chemical composition of drip water and substrate calcite since 2009 (Feng et al., 2014; Casteel and Banner, 2015). We present an ultra-high-resolution (weekly to monthly) record of $\delta^{18}O$, Mg, Sr, and Ba in Westcave stalagmite WC-3, as well as monthly measurements of drip water geochemistry. We find drip water $\delta^{18}O$ and Mg/Ca are essentially invariant, while seasonal variations in stalagmite calcite $\delta^{18}O$ and Mg compositions are in good agreement with predicted temperature-dependent fractionation between water and calcite. Both drip water and speleothem calcite Sr and Ba vary seasonally, which we hypothesize is due to changing moisture conditions in the epikarst. We use each of these annual geochemical cycles as independent chronological controls in order to develop a single age model for the stalagmite. These independent chronological counts are consistent with each other, and with ^{14}C bomb-peak and U-series evidence. We argue that the potential for this kind of multi-proxy, seasonally-resolved dating in near-entrance stalagmites makes them especially valuable paleoclimate archives that should not be ignored in speleothem studies.

Keywords: near-entrance stalagmites, multi-proxy records, stalagmite chronology, oxygen isotopes, trace elements

CCG
LCPHD

Why Grow Armor After the Predators Are Gone? Late Ontogenetic Development of Crocodilian Osteoderms with Behavioral Implications

Lauren English
English, L., Department of Geology, The University of Texas at Austin, Austin, TX

All extant, and most extinct, crocodilians possess bony carapaces made up of articulating osteoderms. These carapaces are most commonly described as defensive structures against predators. However, qualitative observations in the literature have suggested that the carapace of extant crocodilians does not fully mature into a completely imbricated structure until well after the hatchling stage, which is when the risk of predation is greatest. If osteoderms primarily serve a defensive function they may be expected to experience strong selection to appear earlier in ontogeny. However, many aspects of crocodilian locomotor, social, and feeding behavior are known to change markedly throughout ontogeny and would be expected to exert different kinds of selective pressures on crocodilians as they grow. Alternative hypotheses of osteoderm function can be tested in part by looking to see which of the aforementioned selective pressures shift at the same time as the osteoderm carapace fully develops. I examined CT scans of juveniles and adults of eight species of extant crocodilians including two particularly well-sampled ontogenetic series of *Crocodylus niloticus* and *Caiman yacare*. Specimens were coded for total body length and degree of imbrication of osteoderms. Osteoderms were considered to have mature morphology when all nuchal and dorsal osteoderms were rectangular and fully articulated mediolaterally and overlapping craniocaudally. I found that a complete carapace is indeed only fully developed after the hatchling stage and different regions of the body develop osteoderms at different times. I then compared the timing of osteoderm initial growth and maturation with expectations derived from four hypotheses of function and development: (1) osteoderms assist in thermoregulation in larger individuals; (2) their development is constrained by diet; (3) hatchlings are protected by adults and predator self-defense is only necessary later in life; (4) they act as armor in intraspecific conflicts over resources. The absolute body length at the time of carapace maturation varied by species due to species differences in maximum body length, but generally corresponded to a stage when individuals begin competing with adults for territories and resources, shortly before sexual maturity. Thus, the observed pattern is more consistent with osteoderms acting as defensive structures against conspecifics than any other proposed hypothesis.

Keywords: crocodilians, biology, paleontology

CCG
LCPHD

Prediction of Gross Primary Production during the Drought and Normal Years over the US Using Solar-Induced Chlorophyll Fluorescence

Maryia Halubok
Halubok, M., The University of Texas at Austin, Austin, TX
Yang, Z., The University of Texas at Austin, TX

This study investigates how gross primary production (GPP) estimates can be improved with the use of solar-induced chlorophyll fluorescence (SIF) and presents an effort to produce GPP predictions based on the interdependence between SIF, precipitation, soil moisture and GPP using Global Ozone Monitoring Experiment-2 (GOME-2), Tropical Rainfall Measuring Mission (TRMM), European Space Agency Climate Change Initiative Soil Moisture (ESA CCI SM) datasets and FLUXNET observations.

We found that considering the relationships between SIF, precipitation and soil moisture, isolating SIF-GPP relationships for different plant functional types (PFTs), and using precipitation and soil moisture conditions pertinent to the continental US provides the most accurate GPP estimates over the Great Plains and Texas. We found that there exists a lag between a precipitation event and corresponding fluorescence levels, ranging from about 2 weeks for grasses to a month for crops. Using these lead-lag relationships, we estimate GPP using SIF, precipitation and soil moisture data for two different PFTs (C3 non-arctic grass and crop) over the US applying the multiple linear regression technique. GPP values estimated from our lead-lag based SIF show the closest possible match with the observational data from the FLUXNET stations. During the drought 2011 year over Texas, our GPP values show a decrease by 100 gC/m^2/month as compared to the reference year of 2007. In 2012 (drought year over the Great Plains), we observe significant decrease in GPP, especially in the area of high production (>500 gC/m^2/month) that is reduced in July and August 2012. Hence, estimating GPP using specific SIF-GPP relationships, considering the differences in biomes and their interactions with precipitation and soil moisture pertinent to a certain region can detect the drought trends and produce reasonable GPP estimates. Thus, this simple and computationally efficient method based on derived linear equations can be used to obtain GPP predictions.

Keywords: solar-induced chlorophyll fluorescence, plant productivity, drought

CCG
LCPHD

Macroevolutionary patterns in North American mosasaurs: a study system for understanding evolution in a greenhouse world

Joshua Lively
Lively, J., Department of Geological Sciences, The University of Texas at Austin, Austin, TX

I examine the evolutionary dynamics of mosasaurs, marine squamates that filled numerous niches within the marine ecosystems of the Late Cretaceous. The Late Cretaceous was a time of greenhouse climate, with higher temperatures and a reduced latitudinal thermal gradient. Recent authors demonstrated that some evolutionary responses to environmental shifts were different under greenhouse conditions than under Quaternary icehouse conditions. Because of their high diversity and exceptional fossil record, mosasaurs are an ideal study system for understanding evolution during greenhouse conditions. To elucidate accomplish that, I collected discrete osteological character data from over 250 mosasaur specimens, sampling the known taxonomic diversity from the Cretaceous of North America. In addition to traditional phylogenetic analyses, I performed a pair-wise dissimilarity analysis to understand disparity, or anatomical diversity, in mosasaurs through the Late Cretaceous. I found that basal mosasaurines, traditionally referred to *Clidastes*, exhibited higher intraspecific variation than taxa from other major mosasaur clades, such as tylosaurines or plioplatecarpines. Later mosasaurine taxa exhibited higher diversity and disparity compared to any other clade of mosasaurs. That increase in taxonomic and anatomical diversity occurred sometime prior to 81 million years ago, during the early Campanian. That was a time of sea level highstand and decreasing sea surface temperatures. It is unclear what selective pressures drove the diversification of mosasaurine mosasaurs. I hypothesize that the high taxonomic diversity and disparity observed in Campanian – Maastrichtian members of this clade resulted from selection acting upon the high variability expressed by basal mosasaurines.

Keywords: Cretaceous, mosasaurs, evolution, global change

EG
LCPHD

Dispersion in Sonic Wave Modes Caused by Global and Local Flow

Elliot Dahl
Dahl, J., Department of Geological Sciences, Jackson School of Geosciences
Spikes, T., Department of Geological Sciences, Jackson School of Geosciences

To better understand the effect of fluid dispersion mechanisms on acoustic wave propagation we combine Chapman's squirt flow model with Biot's poroelastic theory. Chapman's model assumes the porous media to have interconnected stiff and compliant (soft) pores. At sonic frequencies the compliant pores appear to be the main cause of dispersion and attenuation. It is therefore of importance to investigate the contribution of squirt flow on acoustic wave modes considering that the sampled subsurface formations of interest in exploration usually are fluid saturated and have heterogeneous pore space. We apply the unified theory to a slow and fast formation with a permeable borehole wall containing different amounts of compliant pores which are compared to a formation with no soft pores. The wave fields are generated using the discrete wavenumber summation method with a monopole source in which we can detect four different receiver wave modes, the P-, S-, Stonely and pseudo-Rayleigh waves. The analytical expression for dispersion for the P-, S- and Stoneley wave modes are compared with the weighted spectral semblance (WSS) dispersion received from the waveforms. We find the WSS P-wave and Stoneley wave dispersion to agree well with the analytical results in both slow and fast formations. The WSS S-wave dispersion however does not correlate as well with its respective analytical expression. Both the P- and S- waves phase velocity are significantly affected by soft pores, while the Stoneley wave is shown to be less sensitive in fast then slow formations.

Keywords: sonic log, dispersion, global and local flow

EG
LCPHD

Sub-Permafrost Injection of Combustion Power Plant Effluent as a Solid-Phase Carbon Dioxide Storage Strategy

Kristopher Darnell
Darnell, K., Department of Geological Sciences & Institute for Geophysics, The University of Texas at Austin, Austin, TX
Flemings, P., Department of Geological Sciences & Institute for Geophysics, The University of Texas at Austin, Austin, TX
DiCarlo, D., Department of Petroleum and Geosystems Engineering, The University of Texas at Austin, Austin, TX

Long-term geological storage of carbon dioxide may be essential for greenhouse gas mitigation, yet most proposed storage strategies suffer feasibility issues, such as fluid leakage through fractures, or economic issues, unless there is a recoverable by-product such as in enhanced oil recovery. Recent work shows that injection of combustion power plant effluent, a carbon dioxide and nitrogen mixture, into methane hydrate-bearing reservoirs provides an ideal blend of carbon dioxide storage with simultaneous methane production where the carbon dioxide is stored in hydrate, an immobile, solid compound. This strategy creates economic value from the methane production, reduces the pre-injection complexity since costly carbon dioxide separation from nitrogen is circumvented, and limits leakage since the hydrate is immobile. Here, we explore the phase behavior of these types of injections and describe the individual roles of water, carbon dioxide, methane, and nitrogen as these components partition into aqueous, vapor, hydrate, and liquid carbon dioxide phases. Our results show that the volatile component, nitrogen, induces a three-phase equilibrium state that facilitates an exchange of methane for carbon dioxide within the hydrate phase. Without nitrogen, such as in pure carbon dioxide injection, excessive hydrate formation limits the carbon dioxide storage potential of the reservoir. This work fundamentally explains the success of laboratory experiments and the Ignik Sikumi field test located on Alaska's northern slope that blended simultaneous carbon dioxide storage with methane production. We present a graphical framework akin to those used in enhanced oil recovery that serves as a basis for future dynamic modeling.

Keywords: hydrates, carbon dioxide storage, methane production

EG
LCPHD

3D simulation of seismic wave propagation in fractured media using an integral method accommodating irregular geometries

Han Liu
Liu, H., Department of Geological Sciences, The University of Texas at Austin, Austin, TX
Sen, M., Institute for Geophysics, The University of Texas at Austin, Austin, TX
Spikes, K., Department of Geological Sciences, The University of Texas at Austin, Austin, TX

Fractures play an important role in most carbonate and unconventional reservoirs. Precise identi- fication of fractures and their associated properties from seismic data have a significant impact on reservoir management and hydrocarbon recovery. Traditional seismic methods for fracture identi- fication and characterization, such as shear birefringence and amplitude variations with offset and azimuth, are based on equivalent medium theory with the assumption that fracture dimensions and spacing are small relative to the seismic wavelength. Hence, the overall population of fractures is equivalent to a homogeneous anisotropic medium. Large fractures with spacing on the order of the seismic wavelength can be more interesting because they are crucial for enhanced oil recovery, and they scatter seismic waves. Instead of equivalent medium theory, characterizing discrete fractures us- ing scattered seismic energy can aid in the understanding of wave patterns observed on seismograms and can provide crucial guidance for seismic interpretation. Here, we model seismic wave propagation in a fractured medium using an integral method with tetrahedral grid cells. The integral approach is derived from finite element and finite difference methods in heterogeneous media. It is flexible in modeling irregular interfaces and surface topography. It also has low computational cost and memory requirements compared to a conventional finite difference or finite element method, which is essential for 3D simulations. The fractures are explicitly treated as interfaces with displacement discontinuities using the linear slip model. We implemented the 3D explicit interface scheme using an irregular mesh. Our numerical examples demonstrate the effects of varying fracture height, spacing and width on the seismic response. The wave scattering caused by the fracture is one of the key features. Diagnostic features observed in our simulation can be used for characterizing realistic fractures. We use the scattering index method to quantify this feature by establishing a correlation between the scattering index and fracture spacing. Such an approach can be used to estimate fracture spacing with given fracture compliance and orientation.

Keywords: fracture, wave propagation, scattering

LCPHD-8

EG
LCPHD

Double path-summation diffraction imaging workflow for velocity estimation in azimuthally anisotropic media

Dmitrii Merzlikin
Merzlikin, D., Bureau of Economic Geology, The University of Texas at Austin, Austin, TX
Fomel, S., Bureau of Economic Geology, The University of Texas at Austin, Austin, TX

We propose a workflow for wave-propagation parameters' estimation in azimuthally anisotropic media based on double-path summation migration diffraction imaging approach. Double path-summation migration workflow has successfully been applied to synthetic and real data examples within the isotropic media approximation for both conventional and diffraction imaging. Double path-summation migration allows for automatic migration velocity extraction based on the asymptotic evaluation of path integral weighted by the corresponding velocity. We extend the approach to azimuthally anisotropic media and apply it to separated from full-wavefield diffraction component. As opposed to conventional velocity estimation techniques double-path summation migration allows for simultaneous anisotropic parameter estimation. The effectiveness of the approach is illustrated by synthetic data example.

Keywords: Diffraction imaging, azimuthal anisotropy, path summation

EG
LCPHD

Muir-Dellinger parameters for analysis of anisotropic signatures

Yanadet Sripanich
Sripanich, Y., Bureau of Economic Geology, The University of Texas at Austin, Austin, TX
Fomel, S., Bureau of Economic Geology, The University of Texas at Austin, Austin, TX
Fowler, P., Fowler Geophysical Consulting
Stovas, A., Norwegian University of Science and Technology (NTNU)
Spikes, K., Department of Geological Sciences, The University of Texas at Austin, Austin, TX

Seismic anisotropy is often described using a set of anisotropic parameters instead of the stiffness coefficients because of the conciseness of the resulting expressions and their abilities to describe physically meaningful quantities. We consider one such parameterization, namely the Muir-Dellinger (MD) parameters, discuss their characteristics, and point out their advantages for analysis of anisotropic signatures. We also analyze an empirically observed strong linear relationship between two anelliptic parameters q_1 and q_3 in MD parameterization that govern the second-order change of qP phase velocity squared with respect to phase angle when the horizontal or vertical axis is considered. This empirical relationship is confirmed by laboratory measurements on many different rock samples from various geographical locations and depths. It provides a constructive means to reduce the total number of parameters for anisotropic signatures analysis from four to three in trans- versely isotropic (TI) media and from nine to six in orthorhombic media. Further analysis shows that it can possibly also provide more insights towards distinguishing types of sub- surface lithologies and pore fluids from surface-seismic data. We use the self-consistent rock physics modeling and the Backus averaging theory to provide some supportive evidence of the observed linear dependence.

Keywords: Anisotropy, shales, rock physics, unconventional

EG
LCPHD

Machine Learning and Digital Rock Physics

David Tang
Tang, D., Department of Geological Sciences, The University of Texas at Austin, Austin, TX
Spikes, K., Department of Geological Sciences, The University of Texas at Austin, Austin, TX

In this work, I solve for displacements in a shale sample using a digital rock physics approach. Solving for displacements allows for the calculation of the overall elastic properties of a complex heterogeneous material. Predicting the elastic response represents the forward modeling portion of the problem we normally wish to solve in rock physics (inverting for elastic properties). The digital rock physics workflow starts with obtaining and segmenting a scanning electron microscope image. Traditionally, this step is done through amplitude thresholding. Here, a new approach is taken that uses machine learning methods to identify minerals. Material properties are then assigned to every pixel in the image. A strain is applied to the digital sample, and the displacements themselves are approximated by using the finite element method. Elastic properties of the sample are then calculated.

Keywords: Machine learning, Digital, Rock Physics, SEM

LCPHD-11

EG
LCPHD

Predictive painting with constraints for seismic interpretation

Zhiguang Xue
Xue, Z., Bureau of Economic Geology, The University of Texas at Austin, Austin, TX
Wu, X., Bureau of Economic Geology, The University of Texas at Austin, Austin, TX
Fomel, S., Bureau of Economic Geology, The University of Texas at Austin, Austin, TX

Structural information is the most important content of seismic images. Predictive painting can be used to accomplish some interpretation tasks such as automatic flattening and horizon picking. It is a numerical algorithm for automatic spreading of information in 3-D seismic volumes according to the local structure of seismic events. Currently, it just requires the local dip as its input. We propose to add more constraints to make predictive painting more reliable when dealing with complicated seismic images, which may contain faults and unconformaties. The constraints can be control points or fault slips. Synthetic and field data tests demonstrate that the predictive painting with constraints preforms much better for seismic interpretation.
.

Keywords: Seismic interpretation, Horizon picking, Predictive painting, Constraints, Local structure

LCPHD-12

MG
LCPHD

Methane Hydrate Formation in Coarse-Grained, Brine-Saturated Samples Through the Induction of a Propagating Gas Front

Dylan Meyer
You, K., Jackson School of Geosciences, The University of Texas at Austin, Austin, TX
Phillips, S., Jackson School of Geosciences, The University of Texas at Austin, Austin, TX
Flemings, P., Jackson School of Geosciences, The University of Texas at Austin, Austin, TX
DiCarlo, D., Petroleum and Geosystems Engineering Department, The University of Texas at Austin, Austin, TX
Kneafsey, T., Lawrence Berkely National Laboratory, Berkeley, CA

We generate methane hydrate in coarse-grained, brine-saturated, vertically-oriented samples through gas injection at a range of flow rates. The volumetric fraction of gas injected that is converted into hydrate is inversely proportional to the brine drainage rate. The presence of temporary outlet pressure excursions suggests that hydrate formation in the pore space can temporarily eliminate sample permeability, but that flow can be restored through the development of a differential pressure ranging from 0.01 – 1 MPa. Computed-tomography data collected throughout an experiment performed at the highest flow rate show a low density front that propagates down the sample at a velocity of approximately 2 cm/day, with flow concentrated preferentially in the higher porosity regions of the sample. This study shows that hydrate can form to high saturations during gas injection and that continuously flow and propagation of the gas front is possible with the development of a pressure differential across the hydrate boundary.

Each sample consists of an industrial, fine sand mixed with a 0.5 wt% fraction of natural, smectitic clay from the Eugene Island region in the Gulf of Mexico (5.08cm diameter, 11.79cm length). The sample is initially saturated with a 7 wt% sodium chloride brine, pressurized to 12.24 MPa, and cooled to 1 degree Celsius, to bring the sample into the hydrate stability zone. Syringe pumps filled with methane gas and brine are connected to the top and bottom of the sample, respectively, to control fluid flow. We withdraw from the base of the sample at a constant rate between 3 to 0.5 μL/min and inject methane to maintain a constant pressure, initiating hydrate formation. We analyze these experiments using mass balance and computed-tomography scans to investigate the fundamental formation behavior of hydrate in gas-rich, coarse-grained reservoirs during gas injection

Keywords: Methane hydrate, formation mechanisms, free gas migration, computed-tomography analysis

LCPHD-13

SETP
LCPHD

Linkages between orogenic plateau build-up, fold-thrust shortening, and foreland basin evolution in the Cenozoic Zagros (Iran-Iraq)

Douglas Barber
Barber, D., Department of Geological Sciences, Jackson School of Geosciences, University of Texas at Austin, Austin, TX
Stockli, D., Department of Geological Sciences, Jackson School of Geosciences, University of Texas at Austin, Austin, TX 78712, USA

The Iranian Plateau is a thickened, low-relief morphotectonic province of diffuse deformation that formed due to Cenozoic collision of the Arabian and Eurasian plates, and may serve as a younger analogue for the more mature Tibetan Plateau. Despite a detailed geophysical understanding of the Iranian Plateau, it's long-term geologic evolution remains poorly understood with respect to its deformation history and relationship to Zagros fold-thrust belt development and peripheral foreland basin evolution. This study presents new structural and thermochronologic data from a transect across the internal and external Zagros collisional belt to constrain models of orogenic plateau build-up and quantify the timing of lateral and cross-strike migration and patterns of deformation. Kinematic models are tested against synthetic thermochronometric data derived from a series of restored cross-sections in FETKIN (Finite Element Temperature and KINematics), which in turn are compared to the observed data. In addition, these results are augmented by detrital zircon U-Pb provenance data from the Cenozoic Zagros foreland basin, which record the timing of exhumation of various hinterland source terranes.

Low-temperature thermochronometric data from the internal and external Zagros in the Lorestan province of Iran document a two-phase outward expansion of the Iranian Plateau and Zagros fold-thrust belt since earliest Oligocene time, tightly coupled to distinct phases of basin evolution and provenance shift in the Zagros foreland. Zircon (U-Th)/He ages from plutonic and metamorphic basement rocks in the Sanandaj-Sirjan Zone (SSZ) record initial upper-plate exhumation by ~32 Ma. Deformation continued to migrate southwestward through the SSZ until late Oligocene time. This phase of initial deformation triggered flexural subsidence and a transition to marine sedimentation in the Zagros foreland. Overlapping apatite fission-track and (U-Th)/He ages in the SSZ indicate that by early-middle Miocene time (~16-19 Ma) the internal Zagros underwent a secondary phase of rapid exhumation interpreted as internal crustal thickening within the SSZ, coincident with rejuvenation of foreland basin subsidence and onset of clastic deposition in the Zagros foreland. Detrital zircon U-Pb data indicate that foreland basin sediments during this time were primarily sourced from Eurasian (upper plate) terranes, including the Eocene Gaveh Rud volcanics and SSZ. Major shortening and exhumation within the Arabian plate occurred by Late Miocene time as indicated by apatite (U-Th)/He ages from the Zagros imbricate zone and fold belt as well as a shift in sediment provenance to dominantly Arabian-derived detritus and is coincident with the onset of rapid facies progradation in the Zagros foreland.

In contrast to previous work, these results show that deformation in the SSZ of the Iranian Plateau occurred in two distinct phases, with significant plateau expansion postdating the timing of collision by up to ~15 m.y., perhaps as a result of rapid lower-crustal injection during continental suturing. The distinct transfer of deformation from the SSZ to the Zagros imbricate zone and fold belt following the final major phase of plateau exhumation shows the decoupled behavior of deformation in the upper and lower plate during continent collision. Lastly, the tight temporal linkage between SSZ exhumation and Zagros basin stratigraphy highlights the importance of upper crustal processes on foreland dynamics.

Keywords: orogenic plateau, tectonics, Zagros, fold-and-thrust belt, foreland basin, thermochronology, detrital zircon geochronology

SETP
LCPHD

Constraints from naturally deformed peridotites on controls on olivine lattice preferred orientation

Rachel Bernard
Bernard, R., Department of Geological Sciences, The University of Texas at Austin, Austin, TX
Behr, W., Department of Geological Sciences, The University of Texas at Austin, Austin, TX

Seismic anisotropy in the upper mantle is produced primarily by lattice preferred orientations (LPO) in olivine formed during viscous deformation. Because seismic anisotropy is one of the principal means of characterizing upper mantle flow directions, it is critical to understand how LPO is affected by deformation conditions. Laboratory experiments suggest that water content and stress magnitude each play key roles in the development of LPO in olivine under experimental conditions, but it is unclear to what extent these results apply to natural conditions. We use peridotite xenoliths from a wide range of tectonic settings (Lunar Craters, Geronimo, and San Carlos volcanic fields in the Basin and Range; Cima and Deadman Lake volcanic fields in the Mojave; the Navajo Volcanic field in the Colorado Plateau; and the Potrillo volcanic field in the Rio Grande Rift region) to investigate correlations between water content, stress, and olivine LPO in natural rocks. Water contents were measured using Secondary Ion Mass Spectrometry, stress magnitudes using paleopiezometry, and LPOs using electron backscatter diffraction. The samples examined exhibit a range of fabric types, including A-, B-, C-, and E-type LPOs. Mojave xenoliths show no difference in water content between A- and E-type LPO; instead, differences in fabric type appear to reflect variations in strain magnitude. Samples from the Navajo volcanic field do show a correlation between water influx and stress magnitude as they exhibit abundant hydrous minerals and high water contents, stress magnitudes greater than 250 MPa and B-type olivine LPOs.

Keywords: olivine, deformation, lattice

SETP
LCPHD

Fracture toughness and subcritical fracture indices in damaged and hydrothermally altered rocks, Dixie Valley, NV: implications for fault conduit development in geothermal systems

Owen Callahan
Callahan, O., Bureau of Economic Geology, The University of Texas at Austin, Austin, TX
Eichhubl, P., Bureau of Economic Geology, The University of Texas at Austin, Austin, TX
Olson, J., Department of Petroleum and Geosystems Engineering, The University of Texas at Austin, Austin, TX
Davatzes, N., Earth and Environmental Science, Temple University, Philadelphia, PA

Hydrothermal alteration resulting from enhanced fluid-rock interaction in hydrothermal systems changes the textural and mineralogical composition of the host rocks, affecting the mechanical properties of fault-fracture meshes and the development of hydrothermal convection cells. To characterize the impact of alteration on fracture mechanical properties, we integrate: (1) double-torsion load relaxation tests under ambient air conditions that measure the mode-I fracture toughness (K_{IC}) and subcritical fracture growth index (SCI), (2) uniaxial testing to measure elastic parameters, and (3) XRD and petrographic analysis to characterize the mineralogy and texture of rock samples. By comparing a variety of distinct hydrothermal alteration assemblages preserved in the footwall of the Dixie Valley Fault, NV, we can infer the relative changes in mechanical properties during progressive deformation and chemical alteration.

Our tests indicate that alteration influences both rock and fracture mechanical properties to varying extent. Silicification is associated with high K_{IC}, SCI, unconfined compressive strength (UCS), and Young's modulus, and low Poisson's ratios. Disseminated calcification correlates with moderate increases in K_{IC} and UCS, while albitized and chloritized samples contain unhealed damage and are mechanically weaker. We conclude that changes in mechanical properties are related to the dominant alteration mechanism rather than the degree of alteration. A key control on relative strength of altered rocks is the prevalence of existing damage, in the form of microcracks or dissolution, versus mineral precipitation and healing.

Spatial variation in dominant alteration mechanisms across hydrothermal systems likely produces systematic changes in the mechanical properties of fault-fracture conduits and adjacent host rock. Based on the alteration assemblages that we sampled, the mechanical contrast between fault zone and host appears to reverse between deep and shallow portions of the system: precipitation in shallow portions of the system may seal and strengthen fault-fracture conduits, while damage and dissolution at depth may contribute to mechanical localization of fault-fracture conduits.

Keywords: faults, fractures, hydrothermal, alteration, fracture mechanics, rock mechanics

LCPHD-16

SETP
LCPHD

Neoproterozoic-Paleozoic tectonics and paleogeography of the west-central South America convergent margin as revealed by detrital zircon geochronology

Amanda Calle
Calle, A., Department of Geological Sciences and Institute for Geophysics, The University of Texas at Austin, Austin, TX
Horton, B., Department of Geological Sciences and Institute for Geophysics, The University of Texas at Austin, Austin, TX
Garcia, R., Instituto de Investigaciones Geologicas y del Medio Ambiente, Universidad Mayor de San Andres, La Paz, Bolivia

The long-lived proto-Pacific convergent plate margin modulated regional tectonics, sediment transport, and basin evolution during Rodinia supercontinent dispersal to Gondwana amalgamation. Detrital zircon U-Pb geochronological results for 17 sandstones from a >15 km-thick Neoproterozoic-Carboniferous sedimentary archive in the Andes of southern Bolivia highlight the spatial configuration of eroding sediment source regions and governing subsidence patterns during marine and nonmarine deposition along the proto-convergent margin of western South America. Young zircon populations indicate deposition during Cambrian–Ordovician (505-456 Ma) magmatism, and Devonian–Carboniferous orogenesis and renewal of continental arc magmatism (383 and 340 Ma, respectively). Neoproterozoic–Cambrian (0.75-0.51 Ga) U-Pb ages preserved in Neoproterozoic–middle Ordovician subduction complexes and marginal basins demonstrate a primary eastern source region from the Braziliano-Pampean orogenic system, the product of eastward subduction of the Pampia terrane beneath the Amazon, Rio Apa, and Rio de la Plata cratons. Substantial Famatina and Ocloyic age zircons (0.50-0.42 Ga) in middle Ordovician–Devonian backarc, remnant ocean, and collisional retroforeland deposits chronicle the establishment of a western “Protocordillera”, the possible result of Ordovician trench roll-back and later arc-continental collision of the Arequipa-Antofalla terrane against the Famatina arc. Renewed Pampean-Braziliano (0.75-0.51 Ga) zircon populations in the Silurian and Carboniferous retroforeland settings suggest high-frequency glaciation guiding sediment influx from inboard segments of the eastern-southeastern Pampean-Braziliano orogens and Rio de la Plata craton (2.2-2.0 Ga).

Detrital zircon U-Pb syntheses combined with independent geologic records of Neoproterozoic-Carboniferous basins from northwestern Argentina to southern Peru suggest sediment derivation from two regional eroding source areas adjacent to west-migrating accretionary systems. The large-scale, eastern Pampia-Braziliano source area is evidenced by sustained input of Neoproterozoic-early Cambrian (0.75-0.61 Ga) and subordinate Precambrian (1.30-0.95 Ga) zircons in Paleozoic inboard strata. In turn, the Protocordillera provided Famatina (0.50-0.46 Ga), Pampean-Braziliano (0.65-0.75 Ga), and subordinate Ocloyic (0.46-0.42 Ga) detritus to Ordovician–Carboniferous basins. Variable proportions of Paleozoic (0.50-0.42 Ma) and Precambrian zircons (2.00-0.95 Ga) along the western Paleozoic basin margin document an interplay between drainage system reorganization during Ordovician-Carboniferous sea level fall and heterogeneous source area compositions along the convergent margin.

Keywords: proto-Pacific convergent system, pre-Andes tectonics, sediment provenance

LCPHD-17

SETP
LCPHD

Neogene foreland basin evolution during a shift to flat-slab subduction in Argentina (30.5°S)

Tomas Capaldi
Capaldi, T., Department of Geological Sciences, Jackson School of Geosciences, University of Texas at Austin, TX, USA
Horton, B., Department of Geological Sciences and Institute for Geophysics, Jackson School of Geosciences, University of Texas at Austin, TX, USA
McKenzie, R., Department of Earth Sciences, University of Hong Kong, Hong Kong, China
Stockli, D., Department of Geological Sciences, Jackson School of Geosciences, University of Texas at Austin, TX, USA

New geochronological constraints on upper crustal exhumation in southern central Andes of western Argentina (30.5°S) characterize changes in Neogene foreland/hinterland basin deposystems, provenance, paleodrainage, and sedimentation rates as the foreland was structurally partitioned by various Andean ranges before and during slab flattening. Detrital zircon U-Pb age signatures from western Calingasta hinterland basin, central Talacasto wedge-top basin, and eastern Bermejo foreland basin of western Argentina records sequential unroofing of multiple Andean ranges. Initial shortening 25-20 Ma in the Principal Cordillera is represented by accumulation of distal eolian facies with Principal Cordillera derived detrital zircons in Talacasto basin. Calingasta basin records Frontal Cordillera shortening that lasted ~18-10 Ma marked by upward coarsening trend fluvial and alluvial facies with prolonged Permian-Triassic zircon age component. Precordillera exhumation 12-5 Ma shutoffs Calingasta and Talacasto foreland basin deposition and migrates foreland depocenter to the Mogna section. Depocenter migration generates increased sedimentation rates and rise in Precordilleran derived Paleozoic zircon age populations and concurrent decrease in Frontal Cordilleran derived Permian-Triassic zircon age component. Progressive unroofing from Principal Cordillera (25-20 Ma) to Frontal Cordillera (18-10 Ma) to Precordillera (12-5 Ma) is perturbed during 12- 10Ma with drastic change in depocenter location, provenance trends, and accumulation rates, which coincides with initiation of flat-slab subduction below South America at these latitudes. Suggesting initiation of middle Neogene shallow subduction increases plate coupling at the continental margin, which migrated foreland deformation and caused wholesale exhumation along Precordilleran structural domain.

Keywords: flat-slabs

LCPHD-18

SETP
LCPHD

Mechanics of fold-and-thrust belt systems based on geomechanical modeling

Baiyuan Gao
Gao, B., Institute for Geophysics, The University of Texas at Austin, Austin, TX
Flemings, P., Institute for Geophysics, The University of Texas at Austin, Austin, TX
Saffer, D., Penn State University
Maria, N., Bureau of Economic Geology, The University of Texas at Austin, Austin, TX
Heidari, M., Bureau of Economic Geology, The University of Texas at Austin, Austin, TX

Active fold-and-thrust belt systems are the source of many of the largest earthquakes in the world. Despite the fact that the slip behaviors of the major faults in these systems are closely linked to both of the in-situ stress and the sediment compression conditions, the spatial variation and the evolution of the stress and porosity behaviors are not well studied. We use large-strain, drained, poro-elasto-plastic models to investigate the evolution of stress and compression behaviors in fold-and-thrust belt systems. Based on the result of the characteristic relative shear stress pattern, we recognize 4 distinctive stress regimes in typical thin-skinned fold-and-thrust belts, including (I) critical state wedge, (II) transition, (III) far-field geostatic, and (IV) footwall regimes. We find the mean and shear stress inside the wedge increase significantly and reaches critical state condition. As a result, the sediment porosity in the wedge decreases dramatically and shows a much lower porosity than that of the footwall sediment. We show about 33% of the porosity loss in the wedge results from tectonic shear-induced compression. Different from the traditional views that consider the sediment compression in the footwall is nearly complete decoupled from the wedge sediment, we find the footwall sediment is sensitive to the basal friction coefficient. As the basal friction coefficient increases from 0.1 to 0.3, the principal stress ratio σ_1/σ_3 of the footwall sediment increases from 1.4 to 1.9, the σ_1 dip angle decreases from 72^0 to 55^0, and the porosity of the footwall sediment decreases. The change of basal friction coefficient does not impact the wedge porosity. We also find that the increase of internal friction decreases the porosity in the wedge, but does not impact the footwall porosity. Using the relative shear stress ratio pattern, we present a set of porosity-depth trends by taking into account the varied degree of shear compression in FTB systems. Our quantitatively mechanical analysis on FTB from this study will be instructive in predicting more accurate physical properties in tectonic compressional fields including stress, pore pressure, strength, permeability and seismic architecture.

Keywords: fold-and-thrust belt, stress, porosity, compression, geomechanics

LCPHD-19

SETP
LCPHD

Miocene basin evolution in Ecuador: Implications for the growth of topographic barriers linking the Northern and Central Andes

Sarah George
George, S., Jackson School of Geosciences, The University of Texas at Austin, Austin, TX
Horton, B., Jackson School of Geosciences, The University of Texas at Austin, Austin, TX
Gutierrez, G., Jackson School of Geosciences, The University of Texas at Austin, Austin, TX
Jackson, L., Jackson School of Geosciences, The University of Texas at Austin, Austin, TX

Establishment of the Eastern Cordillera of Ecuador as a topographic barrier during the Neogene caused significant drainage reorganization, perhaps even as dramatic as the reversal of the Amazon River. Situated between the Eastern and Western Cordilleras of Ecuador, a series of Miocene intermontane basins (Cuenca, Giron-Santa Isabel, Nabon, Loja and Vilcabamba) offer a unique opportunity to constrain the development of the Eastern Cordillera as a contiguous drainage divide in the Northern Andes. Detrital zircon geochronology yields regional up-section trends through Miocene sections marked by: (1) Middle Miocene samples containing a strong syndepositional age peak derived from the Western Cordillera, with a complementary Eocene-Oligocene peak from the basement of the basins, and subsidiary low intensity Mesozoic-Neoproterozoic age peaks derived from low-lying crystalline basement exposures in the nascent Eastern Cordillera. By the Late Miocene, samples either: (2a) maintain similar trends to that of the Middle Miocene, or (2b) show a dramatic shutoff of most Cenozoic populations and a switch to Mesozoic-Neoproterozoic zircons from the growing Eastern Cordillera, as seen in Nabon and Loja basins. These trends will be compared to age equivalent strata in the Oriente and Santiago foreland basins for a regional evaluation of the along-and across-strike development of the Eastern Cordillera.

Keywords: Andes, basin analysis, detrital zircon geochronology, Miocene, Oriente Basin, Santiago Basin, Cuenca Basin

LCPHD-20

SETP
LCPHD

U-Pb Geochronology of Grandite Skarn Garnet: Case Studies From the Mesozoic Cordilleran Arcs.

Michelle Gevedon
Gevedon, M., University of Texas at Austin, Austin, TX
Seman, S., Pennsylvania State University, State College, PA
Barnes, J., University of Texas at Austin, Austin, TX
Stockli, D., University of Texas at Austin, Austin, TX
Lackey,, J., Pomona College, Claremont, CA

We present 4 case studies using a new method for U-Pb dating grossular-andradite (grandite) skarn garnet via LA-ICP-MS (Seman et al., *in prep*). Grandite is commonly rich in U, with high Fe^{3+} contents generally correlating with higher U concentrations. Micron-scale non-radiogenic Pb heterogeneities allow for regression of age data using Tera-Wasserberg concordia. Although others have dated accessory skarn minerals, garnet U-Pb ages are powerful because garnet grows early and is nearly ubiquitous in skarns, resists alteration, and provides a formation age independent of that of the causative pluton.
The Darwin stock (Argus range, eastern CA) was likely a short-lived, single pulse of magmatism, genetically related to the Darwin skarn. A robust skarn garnet U-Pb age of 176.8 ± 1.3 Ma agrees well with the pluton U-Pb zircon age of 175 Ma (Chen and Moore, 1982). Furthermore, zircon separated from, and in textural equilibrium with, exoskarn garnetite yields a U-Pb age of 176.8 ± 1 Ma. Such agreement between plutonic and skarn zircon ages with a skarn garnet age in a geologically simple field area is the ideal scenario for establishing grandite U-Pb as a viable tool for directly dating skarns.
The Black Rock skarn (BRS; eastern CA) is more complex: multiple plutons and ambiguous field relations complicate determination of a causative pluton. A skarn garnet U-Pb age of 172.0 ± 3 Ma confirms a middle Jurassic BRS formation age. Investigation of 4 local plutons yield zircon U-Pb ages of 222 ± 3 Ma, 213 ± 4 Ma, 207 ± 4 Ma and 176.2 ± 2 Ma. Comparison of the skarn garnet U-Pb and pluton ages suggest the BRS is genetically related to the youngest pluton, providing basis for further field and geochemical investigation.
The Sidewinder skarns (WS; Mojave Desert, CA) lie in an important region for studying the changing tectono-magmatic regime of the Jurassic North American Cordillera; basin fill suggests a tectonically-controlled oscillating regional shoreline (Busby, 2012). Values of $\delta^{18}O$ of WS garnet are strongly negative, —9.8‰ to 1.2‰, and can only be the result of access to meteoric water. Grandite U-Pb ages have been obtained for 2 skarns, the Whitehorse skarn and the Sidewinder skarn yield ages of 154.1 ± 4 Ma and 162.3 ± 2 Ma respectively, and require the region of the Sidewinder mountains not be submerged below the sea at this time. Future work coupling grandite U-Pb and $\delta^{18}O$ may be vital in establishing the timing of Jurassic Cordilleran tectonic changes in the Mojave Desert.

Keywords: skarn, andradite, garnet, U-Pb, laser ablation, Mojave desert, Cordilleran arcs

LCPHD-21

SETP
LCPHD

Late Quaternary slip history of the Agua Blanca Fault, northern Baja California, Mexico

Peter Gold
Behr, W., University of Texas, Austin
Rockwell, T., San Diego State University
Fletcher, J., Centro de Investigacion Cientifica y de Educacion Superior de Ensenada

Pacific-North American plate boundary slip is transferred across northern Baja California by the right-lateral Agua Blanca Fault, a subsidiary of the San Andreas Fault system. Slip rates and earthquake timing estimates for this fault are critical to hazard estimates and active fault studies for two important reasons. First, slip from the Agua Blanca Fault is absorbed to the west by a network of poorly understood offshore faults that present both seismic and tsunami hazard to the west coast of northern Baja California and southern California. Second, the Agua Blanca Fault is a prime example of a segmented fault system, thus resolving its slip history will lead to insights into how strain is accommodated by geometrically and structurally complex faults. Earlier slip rate and paleoseismic earthquake timing estimates for the Agua Blanca Fault are based on qualitative soil age estimates calibrated to only 5 radiocarbon samples. We have combined topographic surveys, quantitative Quaternary geochronologic dating methods, paleoseismic trench excavations and field mapping to measure the first well-constrained late Pleistocene-early Holocene slip history for the Agua Blanca Fault. Offset alluvial and fluvial landforms dated with ^{10}Be exposure dating and optically stimulated luminescence dating record slip rates of 2-4 mm/yr along the Agua Blanca Fault over the past ~20 ka at three sites. At one site, successive displacements of a channel fill deposit record ~2.5 m of slip in each of the last two earthquakes. Radiocarbon dating of ~80 charcoal samples will constrain the timing of 4 surface ruptures observed in two paleoseismic trench excavations. Combined, these new slip rate, slip-per-event and earthquake timing measurements are the first new quantitative constraints on the recent slip history of the Agua Blanca Fault and provide key information for regional earthquake hazard estimates.

Keywords: Agua Blanca Fault, San Andreas Fault, slip rate, earthquake recurrence, seismic hazard

LCPHD-22

SETP
LCPHD

Unraveling alteration histories in serpentinites and associated ultramafic rocks with magnetite (U-Th)/He geochronology

Emily Hernandez Goldstein
Cooperdock, E., Department of Geosciences, The University of Texas at Austin, Austin, TX
Stockli, D., Department of Geosciences, The University of Texas at Austin, Austin, TX

Serpentinization, hydration of peridotite, has a profound effect on fundamental tectonic processes such as deformation of the lithosphere, fluid-mobile element cycling and deep earth carbon cycling. Though numerous studies have investigated the petrology, structure and geochemistry of serpentinites, the absolute chronology of serpentinization remains elusive due to a lack of common accessory minerals which can be dated using established techniques. Magnetite [Fe_3O_4] forms as a common secondary mineral in serpentinites from the fluid-induced breakdown reactions of primary minerals. Magnetite (U-Th)/He chronometry provides the potential to directly date the cooling of exhumed ultramafic bodies and the low-temperature fluid alteration of serpentinites. We present the first application of magnetite (U-Th)/He chronometry to date stages of alteration in ultramafic rocks from the Kampos mélange belt, a high-pressure low-temperature (HPLT) subduction complex that experienced exhumation in the Miocene on the island of Syros, Greece. Two generations of magnetite are distinguishable by grain size, magnetite trace element geochemistry and (U-Th)/He age. Large magnetite grains from a chlorite schist and a serpentinite schist have geochemical signatures indicative of formation during blackwall-related fluid alteration and record Mid-Miocene exhumation-related cooling ages. Smaller grains from the serpentinite schist lack blackwall-related fluid and signatures record post-exhumation mineral formation associated with Pliocene normal faulting. These results reveal evidence for multiple episodes of fluid-rock alteration, which has implications for the cooling history and local geochemical exchanges of this HPLT terrane. This new tool that may be expanded to investigate the processes and timescales of serpentinization, as it allows direct dating of magnetite formation in response to low-temperature alteration and tectonic shearing in serpentinites. Given the fundamental impact of serpentinizaton on a vast array of tectonic, petrological, and geochemical processes, the ability to differentiate and date these alteration events can be used to address significant questions related to serpentinization in exhumed subduction complexes, continental margins, or obducted ophiolites.

Keywords: serpentinization, Syros, magnetite, geochronology, trace elements

This abstract has been withdrawn

LCPHD-23

SETP
LCPHD

DETRITAL ZIRCON U-PB GEOCHRONOLOGY OF LATE MIOCENE–EARLY PLIOCENE HINTERLAND BASIN DEVELOPMENT IN THE ANDES OF NORTHERN PERU

Lily Jackson
Jackson, L., Department of Geological Sciences, UT Austin
Horton, B., Department of Geological Sciences, UT Austin

Andean hinterland basins preserved within the Marañon fold-thrust belt in the Western Cordillera of northern Peru contain Neogene nonmarine deposits (up to 1 km thick) resting in angular unconformity on principally Jurassic-Cretaceous marine strata. The Cajabamba and San Marcos hinterland basins are positioned along the Cajamarca Deflection, a prominent tectonic feature defining the transition from the central to northern Andes and marked by a sharp change in the regional structural grain. Resolving the poorly constrained timing and mode of hinterland basin genesis, associated structures, and possible tectonic (vertical-axis) rotations is fundamental to understanding the contrasting tectonic histories of the northern and central Andes. We use detrital zircon U-Pb geochronology, basin analysis, and sedimentology to more precisely define the chronostratigraphic and tectonic history of basin development and associated sediment provenance. New detrital zircon U-Pb age distributions from Mesozoic and Cenozoic sandstones show that Neogene basin sedimentation had commenced by the late Miocene (~11 Ma) and was dominated by syndepositional volcanic input that persisted to the early Pliocene (~5.2 Ma). In contrast, the uppermost levels of the basin-fill successions show an increase in Jurassic-Cretaceous age peaks and Proterozoic age peaks (recycled from Mesozoic strata) and an absence of Pliocene-age zircons, suggesting cessation of volcanism, changes in sediment routing, and further unroofing of adjacent Mesozoic units. This shift in detrital zircon age populations is coincident with a change from lacustrine conditions to coarse-grained fluvial to alluvial fan sedimentation in upper stratigraphic levels. Further efforts will evaluate the potential competing roles of previously proposed late Miocene to Quaternary shortening, extension, and strike-slip deformation.

Keywords: Detrital zircon geochronology, Basin analysis, northern Peru, hinterland basin

SETP
LCPHD

On circular reasoning in mantle chromatography

Jacob Jordan
Jordan, J., Department of Geological Sciences, University of Texas at Austin, Austin, TX
Hesse, M., Department of Geological Sciences, University of Texas at Austin, Austin, TX
Rudge, J., Department of Earth Sciences, University of Cambridge, Cambridge, UK

Partial melting of the mantle leads to a percolating melt network that allows for the segregation of melt by porous flow at very low porosities. The geochemical diversity of oceanic basalts requires partial melting of a lithologically heterogeneous mantle source. Partial melting of fertile heterogeneities will produce local increases in porosity with distinct geochemical signatures. Any such region of increased porosity, migrates upwards as a porosity wave, driven by the buoyancy of the melt at a velocity greater than that of melt in the ambient mantle. During migration, these regions of increased porosity evolve into solitary waves that propagate at constant velocity without change in shape, referred to as porosity waves below.

The concept of porosity waves leads to a paradox in our current understanding of melt migration: it is believed that porosity waves cannot transport the geochemical signatures of the heterogeneities that produced them. The melting of a fertile heterogeneity locally increases the porosity and the concentration of a tracer in the melt, that is associated with the source heterogeneity. Given current understanding of porosity waves in one dimension, the region of elevated porosity and trace element signature are initially co-located, but become separated during melt migration.

As the trace element signatures abandoned by the porosity wave slowly migrate upwards, the continuous exchange between the melt and solid separates tracers according to their compatibility. This process is analogous to a chromatographic column. The combination of fast moving porosity waves and chromatographic separations during melt transport, should eliminate any distinct geochemical signatures from partial melting of fertile heterogeneities. Such model predictions are difficult to reconcile with the sampling of signals derived from the partial melting of heterogeneities observed in erupted basalts.

It is well known that one-dimensional porosity waves are unstable in two and three dimensions and break up into sets of circular or spherical waves. However, our current understanding of melt and tracer transport with porosity waves, is still based upon one-dimensional models similar to models published by Barcilon et al. 1989 and Watson 1994 and references therein. Here we show that tracer transport in higher dimensional porosity waves is dramatically different.

Keywords: melt transport, magma, mid ocean ridge basalt, solitary wave

LCPHD-25

SETP
LCPHD

Metamorphic heterogeneity and transient rheology of the deep subduction interface: Insights from meta-mafic blueschists and eclogites exposed on Syros Island, Greece

Alissa Kotowski
Kotowski, A., The University of Texas at Austin
Behr, W., The University of Texas at Austin
Ashley, K., The University of Texas at Austin
Stockli, D., The University of Texas at Austin

The rheological properties of rocks that occupy the plate interface in subduction zones control many aspects of subduction dynamics, including the magnitude and depth of coupling between the slab and overriding lithosphere, the rates and amounts of exhumation of subducted material, and the depths and styles of seismicity. We investigate the rheological properties of the deep subduction interface using exhumed blueschists and eclogites exposed on Syros Island, Greece. Syros rocks were subducted to ~60 km in the Eocene, were exhumed part way along the top of the subducting slab, and were ultimately exhumed beneath Miocene detachment faults. The PT conditions (450-550?C, 12-16 kbar) of these fabrics are comparable to conditions of episodic tremor and slow slip (ETS) observed in several modern subduction zones.

We combine structural and petrologic evidence that rocks from Kini Beach, Syros, preserve fabrics representative of prograde subduction. Garnet-epidote blueschists are isoclinally folded parallel to the dominant foliation and are locally crenulated. Quartz inclusion barometry, Si-in-phengite barometry, and mineral zonations suggest blueschists formed during prograde subduction and preserve peak P ~16 kbar. Eclogites (cm- to m-scale) are present in the blueschist matrix as massive pods with abundant brittle veining, foliated pods rotated with respect to the blueschist matrix, and attenuated and/or folded foliation-parallel lenses. Apatite and quartz inclusion barometry, mineral zonations, and Gnt-Cpx thermometry indicate eclogites are also prograde and preserve PT conditions 12-14 kbar, 550-600?C. Blueschists and foliated eclogites appear to deform by dynamic recrystallization accommodated by dislocation creep, whereas veined, massive eclogite pods do not show evidence of viscous deformation. Together, eclogites and blueschists produce a rheologically heterogeneous shear zone along the deep subduction interface. Brittle shear in eclogites transitioning to ductile deformation in blueschists may produce an ETS-type signal as observed in active subduction zones. The long-term steady state rheology of the deep subduction interface appears to be a composite, non-Newtonian function of the rheologies and relative proportions of eclogites and blueschists.

Keywords: blueschist, eclogite, subduction, Episodic Tremor and Slow Slip

LCPHD-26

SETP
LCPHD

Lower Mantle S-wave Velocity Model under the Western United States

Peter Nelson
Nelson, P., The University of Texas at Austin, Austin, TX
Grand, S., The University of Texas at Austin, Austin, TX

Deep mantle plumes created by thermal instabilities at the core-mantle boundary has been an explanation for intraplate volcanism since the 1970s. Recently, broad slow velocity conduits in the lower mantle underneath some hotspots have been observed (French and Romanowicz, 2015), however the direct detection of a classical thin mantle plume using seismic tomography has remained elusive (Anderson and Natland, 2014). Herein, we present a seismic tomography technique designed to image a deep mantle plume under the Yellowstone Hotspot located in the western United States utilizing SKS in conjunction with finite frequency tomography (Dahlen et al., 2000). Synthetic resolution tests show the technique can resolve a 235 km diameter lower mantle plume with a -2% Gaussian velocity perturbation even if a realistic amount of random noise is added to the data. The Yellowstone Hotspot presents a unique opportunity to image a thin plume because it is the only hotspot with a purported deep origin that has a large enough aperture and density of seismometers to accurately sample the lower mantle at the length scales required to image a plume. Previous regional tomography studies largely based on S wave data have imaged a cylindrically shaped slow anomaly extending down to 900km under the hotspot, however they could not resolve it any deeper (Schmandt et al., 2012). To test if the anomaly extends deeper, we measured and inverted over 20,000 SKS travel times measured at 10-100s recorded at ~1700 stations deployed during 2005-2012. We present two models, one with TX2016 as the starting model and another where we have averaged the results from using different starting models (Ritsema et al., 2011; French and Romanowicz, 2014; Schmandt and Lin, 2014; Lu and Grand 2016). Our preliminary models show a continuous narrow slow velocity extending from a depth of 2500km up toward the anomaly previously imaged under Yellowstone. The slow anomaly is located in the lower mantle near the Utah-Nevada border and is deflected toward the hotspot at around 1000km deep.

Keywords: Mantle Plume, Yellowstone, Tomography, Hotspot, Western United States, SKS, Lower Mantle

LCPHD-27

SETP
LCPHD

Detrital zircon (U-Th)/(He-Pb) double dating of Southern Pyrenees foreland basin fill: implications for sediment routing during tectonic inversion and orogenesis

Margaret Odlum
Odlum, M., University of Texas at Austin
Stockli, D., University of Texas at Austin
Thomson, K., University of Texas at Austin
Fildani, A., Statoil Research Center, Austin
Clark, J., Statoil Research Center, Austin
Puigdefabregas, C., University of Barcelona

New detrital zircon (DZ) U-Pb and (U-Th)/He double dating from exceptionally preserved extensional and contractional basin stratigraphy shows changes in drainage and provenance that elucidate the dynamics among pre-orogenic rift basins, the orogenic hinterland, and foreland basins during tectonic inversion and orogenesis in the Pyrenees.

Flysch deposits of the Vallcarga Fm. represent the initiation of foreland basin deposition during the Late Cretaceous in response to tectonic inversion of the hyperextended Iberian-Eurasian margin. DZ U-Pb data from Vallcarga flysch indicate sediment sources derived from recycling of syn-rift sediments. DZ U-Pb data from the Paleocene Tremp Fm. suggest continued recycling of Early Cretaceous-Triassic sediments sourced from the north and east with input from S-SE sources in the Catalan Coastal Ranges and/or Iberian basement blocks. Eocene sandstones from the Ripoll Basin suggest primary sediment sources from the eastern Axial Zone with minor input from the Catalan Coastal Ranges. Ripoll Basin DZ data show a systematic up section decrease in grains derived from the Catalan Coastal Ranges compensated by an increase in grains from the Axial Zone as the orogen started to develop significant topography exhuming and eroding Paleozoic basement rocks.

The Pyrenees are ideally suited to use DZ double-dating to study foreland basin evolution and sediment routing during orogenesis. New double-dated DZ data allow for a more detailed understanding of the provenance evolution of the foreland basin fill during tectonic inversion. The earliest foreland basin deposits after the onset of convergence ~83 Ma are sourced from both north and eastern recycled syn-rift basin fill and southern sources which persisted for ~20 myrs as the highly-attenuated crust thickened. Eocene deposits record the initiation of the basement-involved Axial Zone shortening and progressive orogenic unroofing during convergence. These results demonstrate that recycling of early Mesozoic syn-rift deposits was the primary sediment source of the early foreland basins from Late Cretaceous- mid-Eocene. The dominant control on the evolution of sediment routing during initial foreland basin evolution is the inherited extensional structures and discontinuous syn-rift basin fill.

Keywords: inversion, foreland basin, detrital zircon double-dating

LCPHD-28

SETP
LCPHD

Comparison of Olivine Grain Growth during Dynamic Recrystallization and Post-deformation Annealing

Pamela Speciale
Speciale, P., The University of Texas at Austin, Austin, TX
Behr, W., The University of Texas at Austin, Austin, TX
Hirth, G., Brown University, Providence, RI
Tokle, L., Brown University, Providence, RI

Strain localization is associated with dynamic recrystallization in shear zones. However, whether localization persists to form long-lived plate boundaries is debated because of the possible counteracting effects of grain growth. We deformed Balsam Gap dunite, a natural olivine aggregate, under axial compression to examine the relative contributions of strain energy and surface energy in facilitating grain boundary migration (GBM) and grain growth. Experiments were conducted at 1100-1200°C, 10^{-4}-10^{-5} s^{-1}, and 1300 MPa confining pressure. Samples that were allowed to recover after deformation show abundant evidence of surface energy-driven GBM, but average grain size does not increase significantly compared to that in samples quenched prior to annealing. In contrast, samples that continued to deform at a reduced strain rate (for the same time as the annealed samples) show both strain energy- and surface energy-driven GBM, and an increased grain size. These observations suggest that growth is enhanced by continued deformation at low stress. More sluggish grain growth in deformed samples that annealed under static conditions may result from continued recrystallization during stress relaxation, grain boundary pinning by accessory chromite, or melt along grain boundaries and at triple junctions. To facilitate comparison of our results to published grain growth laws for olivine, we also conducted a hydrostatic grain growth experiment on 10-20 μm powders of Balsam Gap dunite and San Carlos olivine separated by a Pt disc and annealed for ~24 hours at 1100°C. A similar experiment was run at 1000°C for ~10 minutes to constrain the initial grain size before annealing. Both powdered materials exhibit grain growth after 24 hours. However, although they had the same starting grain size, the annealed San Carlos olivine is slightly coarser than the annealed Balsam Gap dunite, which suggests that grain growth is inhibited in the dunite.

Keywords: experimental deformation, olivine, stress relaxation, strain localization, Griggs rig

SETP
LCPHD

Connecting the Seismic Cycle to the Long-Term Topographic Evolution at Convergent Margins

Xinyue Tong
Tong, X., UTIG, The University of Texas at Austin, Austin, TX
Lavier, L., UTIG, The University of Texas at Austin, Austin, TX

ubduction zones produce the largest earthquakes. However, our understanding of the connections between earthquakes' spatial-temporal occurrence and long-term tectonic deformation at convergent margin is limited. Subduction zone earthquake cycles is usually interpreted in three stages: Interseismic - superposition of steady elastic strain accumulation and occasional short duration aseismic strain release, Coseismic – rapid opposite-direction release of accumulated elastic strain, and Postseismic – superposition of afterslips and viscoelastic flow in mantle wedge and lower crust. However, the way strain accumulates interseismically which may be related to the generation of long-term deformation and uplift in the forearc region is still a matter of debate. Moreover, when integrated over time, coseismic uplift poorly matches the longer-term vertical deformation in most convergent margins. To better understand these relationships, we investigate numerically how coseismic slip and long-term deformation accumulate and interact at subduction zones by using a robust, adaptive, multi-dimensional, finite element method solver, Dynearthsol3D, on a 2D continuum visco-elasto-plastic (VEP) model. To simulate stick-slip instabilities and subsequent healing, we integrated a strongly rate and state dependent friction coefficient into this VEP model with a dynamic time stepping technique. We set the conditions in this model to a realistic convergent margin setting that resembles Sumatra region. Our results show that we can simulate tectonic dynamics (long-term deformation) problem while not losing resolution during seismic (short-term deformation) events. Moreover, we also find out that earthquake occurrence, magnitude, and fault slip behaviors (locking, stick-slip, or creeping) are highly dependent on parameters like static friction coefficient and pore fluid pressure. By introducing bathymetric features on subducting interface, our approach can also explore mechanisms that could explain how strain accumulation in space and time is modified by the presence of large asperities at the subducting interface.

Keywords: Seismic Cycle, Geodynamics

LCPHD-30

SETP
LCPHD

Andradite Garnet U-Pb Geochronology of the Big Gossan Skarn, Ertsberg-Grasberg Mining District, Indonesia

Stephanie Wafforn
Wafforn, S., Jackson School of Geosciences, University of Texas at Austin, Austin, TX
Seman, S., Jackson School of Geosciences, University of Texas at Austin, Austin, TX
Kyle, R., Jackson School of Geosciences, University of Texas at Austin, Austin, TX
Stockli, D., Jackson School of Geosciences, University of Texas at Austin, Austin, TX
Cloos, M., Jackson School of Geosciences, University of Texas at Austin, Austin, TX

The Big Gossan skarn is located in the prolific Ertsberg-Grasberg mining district, on the island of New Guinea in Indonesia. Despite its relatively small size, Big Gossan has the highest ore grades in the district (71 million tonnes at 2.39 wt% Cu and 0.91 ppm Au, assuming a 1 wt% Cu cutoff grade). Big Gossan was emplaced into the steeply upturned southern limb of the Yellow Valley Syncline near the conformable contact between the Ekmai sandstone and Waripi dolomitic limestone. Previous attempts to constrain the timing and duration of ore formation at Big Gossan have been limited to two phlogopite $^{40}Ar/^{39}Ar$ cooling ages. A novel technique developed at UT Austin directly dates andradite garnet using the LA-ICP-MS method. Seven garnet samples were selected for analysis, and the results show that the Big Gossan skarn formed at 2.8 ± 0.1 Ma. The BG240W-06 sample was dated three times over a six month period, and the age consistently overlapped at 2.75 ± 0.03 Ma (n=150 spots) (lower intercept age, Tera-Wasserburg concordia). This precision was achievable due to the high U contents (10-100 ppm) and consistent common Pb composition of Big Gossan garnets. These ages are compatible with the district-wide zircon U/Pb geochronology and the phlogopite $^{40}Ar/^{39}Ar$ ages. The new garnet ages show that Big Gossan was one of the last ore-forming events in the Ertsberg-Grasberg district, and the maximum duration of skarn formation was 100 - 200 kyr.

Keywords: Garnet U/Pb Geochronology, Big Gossan, Ertsberg-Grasberg Mining District, Hydrothermal Skarn

LCPHD-31

SHP
LCPHD

Carbonate Platform Evolution During The Oligocene-Miocene, Offshore East Java, Indonesia

Reynaldy Fifariz
Fifariz, R., Department of Geological Sciences, The University of Texas at Austin, Austin, TX
Janson, X., Bureau of Economic Geology, The University of Texas at Austin, Austin, TX
Kerans, C., Department of Geological Sciences, The University of Texas at Austin, Austin, TX

The Oligocene-Miocene carbonates of the Kujung Formation offshore East Java, Indonesia is a well-known reservoir, hosting a significant hydrocarbon reserves. Despite its economic importance, the entire succession (2,500-3,000 feet thick) is only divided into three intervals based on the order of carbonate lithology penetrated during drilling operation (Kujung-1, Kujung-2, and Kujung-3). The complexity of this succession that documents the evolution of a carbonate platform remains poorly understood.

Based on core, well-logs, and cuttings lithology, we divided the Kujung Formation into a mixed siliciclastic-carbonate system (MSCS) in the lower part (Rupelian – Chattian) and a carbonate-dominated system (CDS) in the upper part (Aquitanian). The topography that precedes the Kujung Formation deposition is a fault-block (the JS-1 Ridge) that was diachronously transgressed by marine conditions during the Eocene. This marine transgression is driven by eustasy and is happened in the context of decreasing subsidence associated with the syn-rift to post-rift transition. Existing paleogeographic reconstruction depict the Kujung Formation deposited over a rifted fault-block bordered at both sides by deep-water conditions. Current interpretation of regional 2D seismic lines combined with 1200 km^2 3D seismic volume suggests that previous interpretation may be oversimplified.

Lithofacies of the Kujung Formation described from the core data consist of *shale-siltstone, silty mudstone-wackestone*, *packstone-grainstone*, *floatstone-rudstone,* and *bindstone-framestone*. Main carbonate-grain constituents are *Large Benthic Foraminifera* (LBF), *Corals*, *Red Algae*, *Echinoids*, and *Molluscs*. We grouped the lithofacies into three main facies associations (FA), which are siliciclastic-influenced shelf facies association (SIFA), open carbonate shelf facies association (OCFA), and reefal-buildups facies association (RBFA). Lithology proportion based on Gamma Ray log and cuttings shows abrupt decrease of siliciclastic influx around the Oligocene-Miocene boundary. The Kujung Formation was deposited over about 13.5 My duration according to $^{87}Sr/^{86}Sr$ isotope age constraints. A transgressive event near the Oligocene-Miocene boundary (~23 Ma) together with the initial collision between Sundaland and Australia possibly pushed the siliciclastic source landward resulting in a significantly less turbid, shallower water, and higher energy environment for the carbonate-dominated system during Aquitanian. A major exposure event related to eustatic sea-level fall near the end of Aquitanian (~20 Ma) is marked by the presence of *paleosol* and *karst-breccia* in several core sample. Subsequent transgression marked the end of the depositional episode of the Kujung Formation.

This study aims at proposing a framework for the stratigraphic architecture that will offer a better understanding of the spatio-temporal distribution of the MSCS and the CDS. This study will also allow us to assess the main controls on carbonate platform evolution and the distribution of potential reservoir within the Oligocene-Miocene succession of the East Java Sea. The results of this study will provide valuable insights for other Oligocene-Miocene carbonate reservoirs and plays in SE Asia, Caribbean, and Mediterranean region.

Keywords: oligocene-miocene, lithofacies, stratigraphic architecture, strontium, controls on carbonate platform evolution

LCPHD-32

SHP
LCPHD

PRODUCTION of COUPLED SAND-and-MUD DEPOSITS by REMOBILIZATION in SUBAQUEOUS TRANSITIONAL FLOWS

Woong Mo Koo
Koo, W., Jackson School of Geosciences, The University of Texas at Austin, Austin, TX
Mohrig, D., Jackson School of Geosciences, The University of Texas at Austin, Austin, TX
Buttles, J., Jackson School of Geosciences, The University of Texas at Austin, Austin, TX
Sturmer, D., Jackson School of Geosciences, The University of Texas at Austin, Austin, TX
Pontén, A., Statoil ASA, Trondheim, Norway
Messina, C., Statoil ASA, Oslo, Norway

Turbidite-debrite couplets have been interpreted as the product of deposition from spatially separated turbidity currents and debris flows or a current transitioning from turbulent to laminar flow over significant time and space. We present results from 3D laboratory experiments demonstrating that a single sediment-gravity flow can also develop turbidite-debrite-like couplets by early-stage remobilization sediments that are still in the process of being deposited. This remobilization appears common to flows composed of mixtures of sand and mud with viscosities and strengths measurably greater than water, but not so high as to fully suppress the settling of sand through the depositional current. The dewatering of the early sand deposit acts to lubricate the basal portion of the increasingly muddy cap of the flow, causing it to accelerate downslope, triggering a secondary flow with a sediment composition distinct from the primary mixture. While remobilization of an upper muddier interval by dewatering of a basal sand deposit is the primary autogenic process observed, minor flow acceleration of the uppermost muddy cap is triggered where its thickness exceeds its strength. The flow, sedimentation, and remobilization processes are all imaged using ultrasonic transceivers. After all transport ceases the final deposit is also acoustically imaged. This 3D imaging is supported by an extensive coring and sediment sampling scheme. The collected cores and grain-size data show sand-mud couplets that in 2D section are qualitatively similar to interpreted turbidite-debrite couplets in natural systems. Recent advances in visualization techniques have enabled mapping of seismic geomorphology on ultrasonic data cubes and reveal unprecedented deposit patterns. Sediment deposition and remobilization by a single-event flow produces various sedimentologic patterns including clean, structureless basal sands, structureless sandy muds, thin sand-mud bands, and reverse grading in the muddy capping layer. We interpret the composite internal deposit morphology to reflect the spatial heterogeneity occurring within a vertically segregated flow where divisions with different rheological properties interact during both transport and deposition of sediment. This work highlights the presence and complex spatial organization of argillaceous and clean sands in subaqueous lobes, and contributes to a better understanding of palaeoenvironments and property distributions in these settings.

Keywords: subaqueous transitional flow, remobilization, turbidite-debrite couplet, 3-D laboratory acoustic survey

SHP
LCPHD

Hydrological response to the 2012 7.6 Mw Costa Rican Earthquake

Kimberly McCormack
McCormack, K., The University of Texas at Austin
Hesse, M., The University of Texas at Austin

Remote sensing and geodetic measurements are providing a new wealth of spatially distributed, time-series data that have the ability to improve our understanding of co-seismic rupture and post-seismic processes in subduction zones. Following a large earthquake, large-scale deformation is influenced by a myriad of post-seismic processes occurring on different spatial and temporal scales. These include continued slip on the fault plane (after-slip), a poroelastic response due to the movement of over-pressurized groundwater and viscoelastic relaxation of the underlying mantle. Often, the only means of observing these phenomena are through surface deformation measurements - either GPS or InSAR. Such tools measure the combined result of all these processes, which makes studying the effects of any single process difficult.

For the 2012 Mw 7.6 Costa Rica Earthquake, we formulate a Bayesian inverse problem to infer the slip distribution on the plate interface using an elastic finite element model and GPS surface deformation measurements. From this study we identify a horseshoe-shaped rupture area surrounding a locked patch that is likely to release stress in the future. The results of our inversion are then used as an initial condition in a coupled poroelastic forward model to investigate the role of poroelastic effects on post-seismic deformation and stress transfer. We model the co-seismic pore pressure change as well as the pressure evolution and resulting deformation in the months after the earthquake. The surface permeability field is constrained by pump-test data from 526 groundwater wells throughout the study area. The results of the forward model indicate that earthquake-induced pore pressure changes dissipate quickly in most areas near the surface, resulting in relaxation of the surface in the seven to twenty days following the earthquake. Near the subducting slab interface, pore pressure changes can be an order of magnitude larger and may persist for many months after the earthquake. Dissipation of earthquake-induced pore pressure in deeper, low permeability areas manifests as surface deformation over a much longer timescale - on the order of months - which may influence the interpretation of longer timescale post-seismic deformation as purely viscoelastic relaxation.

Keywords: hydrology, earthquakes, post-seismic

SHP
LCPHD

The illusive constant pH experiment: Couling salinity and acidity transport

Colin McNeece
McNeece, C., Department of Geological Sciences, The University of Texas at Austin, Austin, TX
Hesse, M., Department of Geological Sciences, The University of Texas at Austin, Austin, TX

Salinity in aqueous systems governs electrostatic behavior of dissolved ions and charged surfaces. These phenomenon are well understood in batch settings, yet their influence on transport behavior is not. Of primary concern is the coupling of salinity and acidity through reactive surfaces. Saline intrusion is often modeled with ion exchange, yet changes in pH are seldom reported and a full analysis of the role of surface chemistry models has not been presented. To gain insight we extend chromatographic theory to the salinity-acidity system including including the most common surface chemistry models. Transport predictions are then compared against a systematic set of column experiments through silica sand. The analysis shows salinity can induce an order of magnitude change in acidity, even in the absence of salt sorption. The direction and magnitude of this change is only captured when both the Helmholtz and diffuse layer components of the surface electrostatic model are considered. The ion exchange model is therefore a poor representation of the underlying physical phenomenon in such systems and a full surface complexation model is needed.

Keywords: sea-water intrusion, low salinity water flooding, chromatography, diffuse double layer

SHP
LCPHD

Diurnal stream temperature effects on nitrogen cycling in hyporheic zones

Lizhi Zheng
Zheng, L., Department of Geological Sciences, The University of Texas at Austin

Stream temperature naturally varies diurnally and seasonally. These variations in turn propagate into hyporheic zones (HZs), resulting in their dynamic and non-uniform thermal patterns. This complex thermal distribution could create potential hotspots and hot moments for temperature-dependent HZ biogeochemical reactions. Yet, how diurnal temperature variations affect HZ biogeochemistry remains unknown. We thus conducted a series of multiphysics numerical simulations of non-isothermal fluid flow and multi-component reactive solute transport to investigate this problem. We assumed a sinusoidally varying stream temperature representing diurnal warming and cooling and then studied the effects of different temperature means and amplitudes on HZ nitrate removal efficiency. The results showed that the time-variable nitrification, denitrification and nitrate removal efficiency responded differently to the diurnal stream temperature signal. The temporal variation of spatially-averaged nitrification rate tracks the stream temperature signal, whereas the spatially-averaged denitrification variation pattern has a more complex connection to temperature. We observed a persistent hotspot where significant denitrification rates are present over the 24-hour period. We further evaluated and estimated the bulk removal efficiency calculated by time integration of spatially-averaged reaction rates over a day. The bulk nitrate removal efficiency for cases with dynamic stream temperature was effectively the same as those with constant and equivalent temperature for denitrification-dominant systems. Therefore, a diurnally dynamic system can be represented by an equivalent steady system with respect to bulk removal efficiency. However, since large instantaneous variations in various rates and metrics were observed, results from randomly timed measurements are unlikely to be representative. This has implications on both past and future synoptic observational studies.

Keywords: hyporheic zone, denitrification, temperature, reactive transport, nitrogen, bedform

U

Lessons learned from an International Researperience from the underrepresented student perspective

Kimberly Aguilera
Yin, Z., The University of Texas at Austin, Austin, TX
Tandon, S., The University of Texas at Austin, Austin, TX
Aguilera, K., The University of Texas at Austin, Austin, TX
Etzel, T., The University of Texas at Austin, Austin, TX
Catlos, E., The University of Texas at Austin, Austin, TX
Elliot, B., Bureau of Economic Geology, The University of Texas at Austin, Austin, TX
Kyle, J., The University of Texas at Austin, Austin, TX

International Research Experience for Students (IRES) is a NSF-funded program designed to provide underrepresented, globally-engaged U.S. science students exposure to field research in an international setting. Three U.S. undergraduate geoscience students were chosen to participate and, under the guidance of three faculty members, they partnered with Slovak researchers from Comenius University and the Slovak Academy of Sciences to conduct a 3-week field season in Slovakia in the summer of 2016 aimed at bolstering their understanding of processes related to the formation of the Western Carpathians. The students returned to the U.S. with an increased understanding of key geologic concepts and rock samples for analysis. Each student then formulated an individual research project with the goal of producing novel and relevant scientific contributions which are in progress and will be submitted for presentation at future research symposiums.

Students felt that the most beneficial aspects of the program included the degree of autonomy that they were allowed in selecting and executing research projects and in learning how fieldwork is conducted internationally. They felt that their influence over research topics and approach granted them a valuable “seat at the table” and that they benefited from learning about the processes involved firsthand: from applying for funding to formulating and publishing research. They experienced the challenges of international field work and, thus, benefited from having a graduate student mentor to whom they could ask questions in a low stakes environment. The international setting also allowed them to compare diversity in the geosciences across disparate cultures. It is the recommendation of the students involved that the productive aspects of their program be incorporated into other projects aiming to broaden diversity in the geosciences.

Keywords: diversity, Slovakia, field research

CCG
U

A new Assemblage of Mosasaurs from the Upper Cretaceous Savoy Pit, Austin Chalk, North Texas

Blake Chapman
Chapman, B., Jackson School of Geosciences, The University of Texas at Austin, Austin, TX
Lively, J., DGS, Jackson School of Geosciences, The University of Texas at Austin, Austin, TX

We describe an assemblage of mosasaurs from the Savoy Pit of Fannin County, in northeastern Texas. The site was excavated in 1940 by the Works Progress Administration (WPA) in conjunction with The University of Texas Bureau of Economic Geology. Based on field notes from the WPA, specimens were recovered from the Upper Cretaceous (Coniacian) Austin Chalk, approximately 7 m above the contact with the Eagle Ford Shale. Previously published taxa from the site include *Ichthyornis* and fish such as *Belonostomus* and *Laminospondylus*. Other fossils that were discovered at the site include crustaceans and asteroids. Additionally, the Savoy Pit yielded several specimens of mosasaurs. Those specimens include both isolated elements and associated skeletons that have yet to be described.

We scored material from the Savoy Pit using a combination of published and novel morphological characters and compared our results to over 200 other mosasaur specimens. We then ran a phylogenetic analysis to hypothesize the taxonomic composition of the assemblage. We identified at least three mosasaur taxa from the Savoy Pit assemblage, including *Tylosaurus nepaeolicus*, a russellosaurine identified from a frontal similar to that of *Russellosaurus coheni*, and an undetermined basal mosasaurine. The latter taxon is exemplified by an associated, partial skeleton that includes a quadrate, maxilla, and vertebrae. That specimen exhibits a unique combination of characters that include synapomorphies of Mosasaurinae (e.g., dorsally constricted suprastapedial process and a striated tympanic rim on the quadrate) and character states observed in russellosaurines (e.g., an elongate stapedial pit).

The presence of *Tylosaurus nepaeolicus* extends the temporal distribution of this species into the Early Coniacian whereas the russellosaurine similar to *Russellosaurus coheni* signifies a potential range extension of that lineage into the Coniacian. The basal mosasaurine fills a stratigraphic gap in the record of that clade between *Dallasaurus* in the Turonian and *Clidastes liodontus* higher in the Coniacian. Our study not only presents new data that are critical to understanding the distribution and evolution of mosasaurs, but also highlights the continued importance of WPA excavations during the Great Depression to our understanding of the fossil record, particularly in Texas.

Keywords: mosasaur, Savoy Pit, 1940, morphological characters, Tylosaurus, russellosaurine, basal mosasaurine, range extension, Coniacian, fills gap

CCG
U

The cranial osteology of a rare species of gerrhonotine lizard, Elgaria panamintina

David Ledesma
Ledesma, D., Jackson School of Geosciences, University of Texas
Scarpetta, S., Jackson School of Geosciences, University of Texas

The clade Gerrhonotinae, commonly known as alligator lizards, represents a number of genera and species that inhabit regions that range from western North America to localities in Central America. I investigate the cranial osteology of the rare species, *Elgaria panamintina*, which is exclusively native to the great basin expanse of California including areas in the Inyo and Nelson Mountains. This species was first discovered in the Panamint Mountains and is geographically separated from all other species of *Elgaria*. Little information is present for this species of lizard and there have been no osteological studies for the species. I used x-ray computed tomography (CT) to scan alcohol preserved specimens from museum collections in order to examine the cranial osteology of *Elgaria panamintina*. I provide novel osteological descriptions for this species as well as a comparison with the better studied species, *Elgaria multicinata*. Comparisons utilizing skeletal material of *Elgaria multicarinata* as well as digital CT data of *Elgaria panamintina* has granted me the ability to document interspecific variation and identify characters unique to individual extant species. Description of the cranial osteology of *Elgaria panamintina* is necessary when assessing the taxonomic classification of fossil specimens assigned to Gerrhonotinae. My description of the cranial osteology of this rare species will greatly assist in the classification of a fossil skull collected in Anza-Borrego Desert State Park.

Keywords: cranial osteology, gerrhonotine lizard, California, CT, Elgaria panamintina

CCG
U

Timing of Ocean Acidification at the Latest Permian: Evidence from Fossils

Maria Reistroffer
Reistroffer, M., Jackson School of Geosciences, The University of Texas at Austin, Austin, TX
Foster, W., Jackson School of Geosciences, The University of Texas at Austin, Austin, TX
Martindale, R., Jackson School of Geosciences, The University of Texas at Austin, Austin, TX
Twitchett, R., The Natural History Museum, London, United Kingdom

The most catastrophic mass extinction in Earth's history, the latest Permian mass extinction (252 million years ago) resulted in the loss of approximately 81% of all species on Earth. Currently, the explanation favoured by most researchers is that the cause of this extinction event in the oceans was a combination of ocean anoxia, high sea surface temperatures, and ocean acidification. Nevertheless, despite several provocative studies, there is no robust evidence as to whether ocean acidification was a contributing factor. To test for evidence of acidification at the latest Permian mass extinction, this research seeks to identify dissolution and repair marks on post-extinction fossils, which would indicate shell growth in acidic conditions. An exceptionally well-preserved fossil assemblage collected from the Permian/Triassic boundary in Svalbard (Arctic Norway) provides the opportunity to assess both shell dissolution and repair, and thus investigate whether ocean acidification was present at the extinction event. Because ocean acidification events are rapid (typically less than 20 kyr), the samples collected from horizons closest to the latest Permian extinction are expected to show dissolution scars and repairs, caused by an acidified water column, while those after the hypothesized acidification interval, i.e. at the Permian/Triassic boundary, would not. Samples from the hypothesised ocean acidification pulse are dominated by lingulids, but very little else. Lingulids would not have been affected by the undersaturation of calcium carbonate because of their organophosphatic shell and use of hemerythrin. Samples collected from the strata deposited immediately after the expected ocean acidification pulse contain gastropods, bivalves, lingulids, and sponge spicules. This composition change, therefore, may suggest the presence of acidification during the extinction as recovery occurs rapidly following the theoretical return to supersaturation. The lack of dissolution and repair marks in the well-preserved mollusks at the Permian/Triassic boundary (11.9 and 12.6 m and roughly 60 kyrs above the extinction horizon) clearly demonstrates that neither the planktic nor benthic habitats were affected by the ocean acidification at this time, contrary to some geochemical evidence from other sections.

Keywords: Acidification, Ocean Anoxia, Permian, Triassic, Paleontology, Extinction

CCG
U

Database analysis of coral population distributions in the Caribbean, 200 ka to Present

Walker Wiese
Wiese, W., Jackson School of Geosciences, The University of Texas at Austin, Austin, TX
Martindale, R., Jackson School of Geosciences, The University of Texas at Austin, Austin, TX

Concern for the future of coral reef ecosystems has motivated scientists to examine the fossil record to predict changes in coral distributions and population health. Specifically, in regions of concern, such as the Caribbean, long-term records of coral reef health and change during climate perturbations are particularly useful. The Caribbean coral reef record through the last 200,000 years (Pleistocene and Holocene) provides a good indicator of general reef construction. This research has compiled a database of dominant reef corals across the Caribbean from 200 ka to present, which documents how species have responded to different rates of sea-level rise and climatic changes. The habitat of different coral species around the Caribbean and their changes over time can indicate both dominant morphological preferences and environmental controls on species distribution. Here, we found that the three main reef builders, *Acropora palmata, Acropora cervicornis*, and *Montastraea* "*annularis*", have distinct location on the reef and distribution throughout the Pleistocene and Holocene. Changes from these typical distributions, like a contraction of the *A. palmata* during the marine isotopic stage 5 (125,000 ka), show an influence of a cold, northern sea surface temperature and rapid sea level rise on *A. palmata* production. A species turnover from *Montastraea nanyci* to *M.* "*annularis*" reflects reef zone shift during an extinction of *M. nanyci* around 82,000 ka. These changes in reef location show these modern *M. "annularis"* respond to niche absences through morphological changes. The recent history of coral responses to climatic changes provides the best understanding for how reefs will adapt to future alterations in pCO_2 and sea-level. Knowing what changes to expect in the composition and structure of reef ecosystems will be a critical tool to help dampen large scale ecosystem collapse of coral reefs in the future.

Keywords: Holocene, Pleistocene, Caribbean coral, climate change, Acropora

EG
U

Matching and Merging High-Resolution and Legacy Seismic Data

Sarah Greer
Greer, S., Bureau of Economic Geology, The University of Texas at Austin, Austin, TX
Fomel, S., Bureau of Economic Geology, The University of Texas at Austin, Austin, TX

Modern high-resolution seismic acquisition systems, such as P-cable, can produce detailed images of the subsurface at shallow depths. These data often need to be matched with those previously produced from legacy data using conventional seismic acquisition. In comparison with high-resolution data, conventional data have generally lower frequency content and correspondingly lower depth resolution, but better signal content with depth. In order to reconcile the differences between the two types of data sets, they need to be properly matched.

We consider the problem of matching data sets obtained with different resolution. Using techniques borrowed from multicomponent image processing, we propose a multistep approach. First, the two data sets are balanced in amplitude and frequency content. As a result, the resolution of the high-resolution data is degraded. Next, we measure and correct for shifts between the data sets using local similarity scanning. Finally, when the data sets are aligned and matched, we create a blended data set using least-squares inversion.

The resultant merged data set effectively combines the best features of the two initial data sets: the broader frequency bandwidth of the high-resolution data with the reflection continuity and deeper coverage of the legacy data. Successful results were achieved in application of the proposed workflow to data from the Gulf of Mexico.

Keywords: seismic, high-resolution, P-cable, Gulf of Mexico, merge

EG
U

Architectural Elements Within the Northern Taranaki Basin and a Closer Look to Better Understand Controlling Processes of Deposition and Preservation

Jeffrey Hensley
Hensley, J., Bureau of Economic Geology, The University of Texas at Austin, Austin, TX

Seismic interpretation is essential for evaluating the architectural elements of submarine fans. Using a high resolution seismic volume in the Northern Taranaki Basin, New Zealand various channel characteristics were analyzed with respect to the controlling processes of deposition and preservation. During the development of submarine fans, sand and mud are both supplied to the system. The sand is generally concentrated within the channel margins, while the mud is aggregated on the banks of the channels. The placement of sand and other architectural elements within channel systems is of upmost importance for the petroleum industry. By analyzing the lateral continuity and vertical connectivity of the sand bodies, depositional and erosional characteristics can be inferred. Within the Northern Taranaki Basin there is a prograding clinoform set that is a host for several channel and gully systems. The gullies in this region have a relatively high degree of sinuosity which can be influential in the development of cut-offs. These cut-offs are important when describing reservoir quality and can lead to interpretations of depositional setting. Furthermore, characterization of these channels will help describe various parameters that influence the deposition and stratigraphic preservation in the Northern Taranaki Basin.

Keywords: Architectural elements, vertical connectivity, sub-marine channel, reservoir quality, deposition environment

EG
U

Seismic Stratigraphic Analysis of the Yoakum/Lavaca Canyon System ,South Texas, USA

Colin White
White, C., Institute for Geophysics, The University of Texas
Snedden, J., Institute for Geophysics, The University of Texas
Gulick, S., Institute for Geophysics, The University of Texas

The Yoakum/Lavaca canyon system is composed of two ancient, superimposed submarine canyons located in the subsurface of Lavaca and DeWitt counties, Texas. The Yoakum/Lavaca canyon system's initial formation was described previously as a response to sudden interruption of incoming sediment supply from the lower Wilcox Rockdale delta system, followed by a period of rapid transgression causing instability and slope failure at the time of Upper Wilcox deposition during the Late Eocene. Analysis of stratigraphic relationships from well data and morphology of the Yoakum/Lavaca canyon system in two dimensional (2D) seismic reflection data has provided an opportunity to propose a new explanation for the initiation of slope failure that excavated the base of the canyon system. The Chicxulub impact event is linked to the CretaceousPaleogene (KPg) mass extinction and is believed to have induced massive slope failures across the Yucatan platform and surrounding continental margins. This study considers the possibility that initiation of the Lavaca canyon system, the older canyon system, was a result of the induced seismicity from the Chicxulub impact event ~66 Ma. Structure of the Yoakum/Lavaca canyon system is easily identified on 2D high-resolution seismic reflection data. The Lavaca Canyon is interpreted to incise through an underlying Albian age carbonate platform. Seismic data reveals the Cretaceous-Paleogene boundary as a high amplitude, continuous reflection that truncates seismic reflectors below . Other stratal terminations, found at the base of the canyon system, suggest that slope failure of the final Cretaceous carbonate platform resulted in the initial canyon excavation. Interpretation of seismic stratigraphic relationships and well penetrations of the canyon system has provided robust constraints on timing of excavation and fill of the entire Yoakum/Lavaca canyon system. This work provides the first comprehensive depositional synthesis of the canyon complex utilizing both subsurface seismic and well log data .

Keywords: Seismic Stratigraphy, Wireline Analysis, Seismic-Core Integration

MG
U

Late Quaternary Paleochannel Systems of the East Texas Inner Continental Shelf

Cole Speed
Speed, C., Institute for Geophysics, The University of Texas at Austin, Austin, TX
Gulick, S., Institute for Geophysics, The University of Texas at Austin, Austin, TX
Goff, J., Institute for Geophysics, The University of Texas at Austin, Austin, TX
Swartz, J., Institute for Geophysics, The University of Texas at Austin, Austin, TX
Fernandez, R., Institute for Geophysics, The University of Texas at Austin, Austin, TX

The northern Gulf of Mexico continental shelf plays host to a variety of buried incised valley and paleochannel systems. The formation of these incisional features is due in part to Quaternary eustatic sea level oscillations, thought largely to represent fluctuations in global ice volume. However, a complex interplay exists between the role of climate, eustasy, and autogenic sedimentary processes in the formation and evolution of paleochannel systems throughout geologic time. These elaborate channel networks act not only as a conduit for sediment transport to the outer shelf and deep sea, but also as a location for sediment storage during subsequent transgressions. Understanding the timing of incision and the internal sedimentary architecture of buried channel systems provides insight into the formational processes of the paleochannel system and the role it played in sediment transport and storage.

Over 300 kilometers of ultra-high-resolution (0.7-12 kHz) CHIRP sub-bottom profile and high-resolution (40-450 Hz) two-dimensional multichannel seismic (MCS) data were collected on the inner continental shelf south of Freeport, TX during the 2015 and 2016 University of Texas south Institute for Geophysics Marine Geology and Geophysics summer field courses. The survey focused on imaging the Late Quaternary formation and evolution of the incised valley and channel system associated with the paleo-Brazos River. CHIRP data provide decimeter-scale vertical resolution imaging the upper 15-50 meters of the subsurface, while high-resolution MCS data provide vertical resolution of 1-3 meters and penetration on the order of hundreds of meters. These complementary datasets allow for an integrated stratigraphic analysis of multiple generations of Pleistocene to Holocene-aged paleochannels and key comparisons of various channel-forming processes, sediment transport mechanisms, and storage potential on the northern Gulf of Mexico continental shelf.

Keywords: Marine geology, sedimentary processes, allogenic, autogenic

PS
U

3He/22Ne Variations among Ocean Island, Mid-Ocean Ridge, and Backarc Basalts

Jesse Gu
Gu, J., Department of Geological Sciences, The University of Texas at Austin, Austin, TX
Dygert, N., Department of Geological Sciences, The University of Texas at Austin, Austin, TX

^{3}He and ^{22}Ne are primordial isotopes inherited from Earth's accretion. Neither isotope is produced in the mantle or fractionated by partial melting. It has been observed that mid-ocean ridge basalts (MORBs) have relatively high ^{3}He/^{22}Ne (typically 4 - 10) compared to ocean island basalts (OIBs), whose ^{3}He/^{22}Ne approach solar nebula and chondritic values (< 2). This discrepancy reflects the existence of a heterogeneous mantle with distinct reservoirs for MORBs and OIBs. Because Earth formed from precursor materials with low, chondritic or solar nebula-like ^{3}He/^{22}Ne, a mechanism for producing a high ^{3}He/^{22}Ne MORB source is required. Fractionation of He from Ne has been attributed to the effects of multiple giant impacts which led to outgassing of liquid magma oceans. However, the discrepancy in ^{3}He/^{22}Ne can also be modeled by plate tectonic cycling and diffusion between dunite channels and surrounding harzburgite wallrock. We compiled data from papers which recorded isotopic compositions for basalt samples from mid-ocean ridges, hotspots, and back-arc basins. In addition to differences in ^{3}He/^{22}Ne between MORBs and OIBs, we identify discrepancies in the distribution of ^{3}He/^{22}Ne in OIBs from various localities. While the distributions from Tristian, Reunion Island, and Iceland reflect the expected low ^{3}He/^{22}Ne (~2-5), those from Hawaii, the Shona Ridge and the Azores Archipelago display higher average ^{3}He/^{22}Ne (~4-6). Proximity of the Shona Ridge and the Azores Archipelago to the Mid-Atlantic Ridge could result in interactions between mantle plume and the MORB source, leading to a net elevated ^{3}He/^{22}Ne source. Alternatively, among themselves, OIBs may source distinct mantle reservoirs with variable ^{3}He/^{22}Ne as suggested by radiogenic isotopes. The current kinetic fractionation model predicts that mantle sources which experienced extensive or repeated melting should have high ^{3}He/^{22}Ne. This is supported by our observations from highly depleted basalts from the Manus backarc basin, which are unusually higher in ^{3}He/^{22}Ne than MORBs, as well as positive correlations of ^{3}He/^{22}Ne with radiogenic isotope indices of depletion.

Keywords: noble gases, ocean island basalts, fractionation, mantle convection

SETP
U

Investigating Magma Chamber Evolution using Mafic Enclaves and Plagioclase Zoning: Grasberg Igneous Complex, Papua, Indonesia

Emilie Bowman
Bowman, E., Jackson School of Geosciences, University of Texas at Austin, Austin, TX
Cloos, M., Jackson School of Geosciences, University of Texas at Austin, Austin, TX

The Grasberg Igneous Complex (GIC), located in the Ertsberg Mining District in the province of Papua, Indonesia and host to the supergiant Grasberg porphyry Cu-Au deposit, provides a natural laboratory to study porphyry copper deposit genesis. This study strives to better understand the magma chamber evolution of the GIC in order to further investigate magmatic processes related to ore formation. Twenty-nine enclaves in the Kali Dikes unit have been collected from a ~270m-long section of the AM96-35-1 horizontal core that runs through the center of the GIC. Mafic enclaves make up less than ~0.01% of the Kali phase, are commonly ellipsoidal with varying degrees of elongation, and have diameters on the order of mms to a few cms. Based on their igneous textures and mineralogies, the enclaves have been separated into three petrogenetic groups: 1) twenty-three enclaves have equigranular to porphyritic igneous textures defined by plagioclase, biotite, oxides, ±amphibole, ±clinopyroxene. They often contain acicular apatite formed during quenching and hybrid rims that record mass exchange, disequilibrium, and/or metasomatism at the boundary between the two magmas. These mafic enclaves are pieces of magma that recharged and crystallized in contact with a more felsic magma chamber; 2) two enclaves contain plagioclase, oxides, biotite, and sillimanite. The presence of sillimanite suggests that these enclaves are pieces of sedimentary wall rock incorporated during magmatic ascent; and 3) three enclaves are characterized by randomly-oriented, coarse-grained euhedral amphibole surrounded by intercumulus plagioclase. Amphibole crystals show little evidence of disequilibrium, implying that these clots are aggregates of ferro-magnesian minerals that crystallized along the chamber sidewalls while in equilibrium with the host magma. Additionally, plagioclase phenocrysts in the host rocks of the same twenty-nine samples from the Kali Dikes display sieve zoning and patchy zoning, both of which represent resorption of plagioclase crystals due to disequilibrium caused by mixing between two compositionally distinct magmas of different temperatures. Oscillatory zoning is also observed and may be related to decompression, repeated magma recharge, or convection. These textures formed when mafic magma recharge caused heating, resulting in resorption of plagioclase grains within the host magma. Pieces of mafic melt from the recharging magma became entrained in the host, and convective dispersal most likely caused sidewall magma to dislodge and enclaves to break into smaller pieces.

Keywords: magma, recharge, mafic enclaves, plagioclase

SETP
U

Trace Elements and Oxygen Isotope Zoning of the Sidewinder Skarn

Cody Draper
Draper, C., The University of Texas at Austin, Austin, TX
Gevedon, M., The University of Texas at Austin, Austin, TX
Barnes, J., The University of Texas at Austin, Austin, TX
Lackey, J., Pomona College, Claremont, CA
Jiang, H., Rice University, Houston, TX
Lee, C., Rice University, Houston, TX

Skarns of the Verde Antique Quarry and White Horse Mountain areas of the Sidewinder Range give insight into the paleohydrothermal systems operating in California's Jurassic arc in the Southwestern Mojave Desert. Garnet from these skarns are iron rich: Xand= 55–100. Laser fluorination measurements show oxygen isotope (δ18O) compositions of garnet crystals and crystals domains have large ranges: –3.1‰ to +4.4‰ and –8.9‰ to +3.4‰, respectively. In general, the garnet cores have more negative δ18O values than rims, although oscillations are present. Negative values have been interpreted as influx of meteoric fluid and positive values as increased magmatic input. Here we report major and trace element concentrations for core to rim Sidewinder garnet transects. REEs concentrations are low in all crystals, with total REE concentrations ranging from 0.710 ppm to 33.7 ppm, values that are lower than Cretaceous skarn garnets in the Sierra Nevada in the White Chief and Empire Mt skarns. Such low concentrations are likely due to the higher fraction of meteoric fluids during formation of the Sidewinder skarns. REE concentrations decrease from core to rim (REE core average=12.2ppm, REE rim average=7.21ppm). This is slightly more pronounced in the LREEs than in the HREEs (LaN/YbN core average= 10.9; rim average= 9.73, normalized to Chondrite). Xand tends to decrease core to rim in the Verde Antique skarn, whereas, Xand of the White Horse skarn does not correlate with distance from core. A large positive Eu anomaly (Eu/Eu* = 3–30) in garnet from both skarns suggests oxidizing fluid conditions. Oxygen isotope data from garnet in these same skarns show periods of time with increased proportion of magmatic derived fluids in the total fluid budget. However, there is no corresponding widespread increase in total REE concentrations. Other studies of skarns from the western Sierra Nevadan arc (White Chief and Empire Mountain) observe complete decoupling of d18O values and trace element compositions. Future modeling should consider modal abundance of fluid soluble minerals in cooling and altering plutons to probe the REE budget.

Keywords: Skarn, Garnet, Metasomatism, Cordillera, Oxygen, Trace Elements

SETP
U

Rock Record of Seismic Nucleation and Decay

Daniel Ortega-Arroyo
Ortega-Arroyo, D., Department of Geologic Sciences, The University of Texas at Austin, Austin, TX
Behr, W., Department of Geologic Sciences, The University of Texas at Austin, Austin, TX

Studies of natural pseudotachylyte-bearing samples from the Whipple Detachment Fault (WDF) were performed to better constrain the dynamic weakening mechanisms that lead to nucleation of seismic slip, the conditions at which they operate, and the processes associated with the decay of slip.
We analyzed cross-cutting relationships within the host rock and the pseudotachylyte veins using field observations and microstructural analyses, and identified two main types of pseudotachylytes: veins with a cataclastic precursor and veins with no cataclastic precursor.
Some of the veins with no cataclastic precursor were found in association with SC fabrics in feldspar-rich regions of the mylonite host rock, while others were found at lithological boundaries between feldspar-rich dikes and the mylonite host rock. Furthermore, we found narrow splays of dynamically recrystallized grains (DRX) originating along the margins of the veins and oblique to the host mylonitc foliation. On the other hand, some of the veins with cataclastic precursors were found along the slip surface of larger splays of the WDF and late high angle normal faults. All samples had an asymmetric deformation intensity gradient leading to the pseudotachylyte.
Along deeper sections of brittle to ductile transition zone, small variations in composition and grain size can cause large enough stress concentrations to surpass the fracture strength of the material, and localize the slip in zones where the rigid phases are more abundant.
As the slip decays, the strain rates and higher temperatures imparted by friction would make it more favorable for the rock next to the slip surface to deform through ductile means rather than brittle mechanisms.

Keywords: pseudotachylyte, seismic, slip, disequilibrium, friciton, melting

This abstract has been withdrawn

U-14

SETP
U

New Geochemical and Thermochronologic Constraints on the Tectonic Affinity, Cooling History, and Timing of Obduction of the Spongtang Ophiolite, Northwest India

Emily Pease
Pease, E., Jackson School of Geosciences, The University of Texas at Austin, Austin, TX
Dygert, N., Department of Geological Sciences, University of Texas at Austin, Austin, TX
Catlos, E., Department of Geological Sciences, University of Texas at Austin, Austin, TX
Brookfield, M., School for the Environment, University of Massachusetts Boston, Boston, MA

The Spongtang ophiolite, located in northwest India, is a fragment of oceanic lithosphere emplaced during a collision between the Indian and Asian plates. The structure was previously sampled and studied by Reuber, who argued that Spongtang formed at a slow spreading center near a transform fault. Here, we report new major and trace element data for a peridotite (SPO-25) and a sample from the metamorphic sole (SPO-26). Our objectives are to gather insights into the tectonic setting in which the structure formed, and to characterize the ophiolite's cooling history and the timing of its formation and emplacement. Amphibole, clinopyroxene, olivine, and spinel mineral compositions were measured using an Electron Microprobe. SPO-26 amphibole is zoned hornblende, with relatively Al2O3 rich, FeO poor rims and flat REE patterns (~35 × chondrite). SPO-25 is a spinel harzburgite. Spinel Cr# [100×(Cr/(Cr+Al)), in moles] provides information regarding the degree of partial melting experienced by a sample and is a useful proxy for tectonic setting. With a spinel Cr# of 30 and an olivine Mg# of 90 [100×(Mg/(Mg+Fe)), in moles], the sample falls within the range of abyssal peridotites and ophiolites with mid-ocean ridge affinity, consistent with the structural interpretations of Reuber. Clinopyroxene are depleted in light rare earth elements and have flat mid-heavy chondrite normalized REE patterns. Abundances range from 0.1×chondrite for Sm to 4×chondrite for mid-heavy REEs. Using the REE-in-two-pyroxene thermometer of Liang et al. (2013), a temperature of 1060ºC was calculated and from the major element based two-pyroxene thermometer of Brey and Köhler (1990), a temperature of 876ºC was calculated. The temperature discrepancy suggests the ophiolite cooled slowly, on the order of 10s of degrees / Myr. Additional work is underway to determine ages of zircons from the metamorphic sole and a diabase dike that cross cut the ophiolite. Using an SEM, zircon crystals have been located which will be analyzed by SIMS to constrain the timing of metamorphism and/or emplacement. The timing and sequence of plate- and arc-collisional events from the ophiolite will significantly improve our understanding of the paleogeography of the Neo-Tethyan Ocean and the formation of the Himalayan Mountains.

Keywords: Tectonics/Tectonophysics Petrology, Igneous Geochemistry, Himalayan Geology

SETP
U

MINERLIZATION IN THE KALI PHASE OF THE GRASBERG IGNEOUS COMPLEX, PAPUA, INDONEISA

Chase Svoboda
Svoboda, C., The University of Texas at Austin, Austin, TX
Cloos, M., The University of Texas at Austin, Austin, TX

The super-giant Grasberg porphyry copper deposit is situated in the Ertsberg mining district in Papua, Indonesia and once produced 6% of the world's new copper supply. The copper gold ore body is hosted in the Grasberg Igneous Complex (GIC), which consists of three primary phases: the Dalam, the Main Grasberg Intrusion (MGI), and the Kali. The Late Kali Intrusion (LKI), part of the Kali phase of dikes, cuts through the Main Grasberg Intrusion and parts of the Dalam. While the chronology of intrusions in the GIC is well constrained, there are still questions surrounding the relative timing of high-grade copper mineralization: it has been proposed that high grade mineralization either pre- or post-dates the Kali Dikes.
In order to evaluate the timing of mineralization in the GIC, a horizontal drill core that trends NW through the intrusions in the GIC was evaluated petrographically. Cored logging showed that the majority of the ore grade copper and gold material in the LKI is located along the Dalam and LKI contacts and the LKI and MGI contacts. Hand sample and thin section observations showed that the majority of the ore grade copper resides in veins as chalcopyrite. The Dalam and LKI contacts show 61 of 119 chalcopyrite veins are associated with magnetite. The LKI and MGI contact show 46 of 86 chalcopyrite veins are associated with quartz. Geochemistry will be used to evaluate the contacts and the middle of the LKI, with the goal of determining whether chalcopyrite in the LKI is from hydrothermal fluids or from the magma. Collectively the results of this study will determine whether ore grade mineralization in the LKI formed prior to intrusion and was remobilized into the edges of the dike, or whether mineralization occurred post-LKI intrusion.

Keywords: Grasberg, Kali, copper, gold

SETP
U

Characterizing the Structure, Mineralogy, and Paragenetic Sequence of Sheeted Quartz Veins in the Ertsberg East Skarn System, Papua, Indonesia

Daniel Young
Young, D., The University of Texas at Austin, Austin, TX
Ledvina, M., The University of Texas at Austin, Austin, TX
Kyle, J., The University of Texas at Austin, Austin, TX

The Ertsberg East Skarn System (EESS), a 3-Gt orebody at 0.59% Cu and 0.49 ppm Au, is located in the Ertsberg-Grasberg district in the highlands of Papua, Indonesia. Subduction of the Australian plate beneath the Pacific plate ca. 12 Ma uplifted and deformed a succession of Upper Cretaceous siliciclastic to Paleogene carbonate strata into which ca. 3 Ma magmatism and episodic hydrothermal fluid flow created stockwork- and skarn-hosted Cu-Au orebodies. The EESS is located on the northern margin of the Ertsberg pluton at its contact with steeply dipping strata forming the southern limb of the Yellow Valley Syncline. The mineralized zone extends from surface exposures at ~4300-m to below 2000-m, forming one of the world's largest skarn Cu-Au systems.

A NW-SE-trending zone of sub-vertical sheeted quartz veins up to 30-m wide has been intercepted in at least 11 drill holes and can be traced for at least 150 m along strike through the ErtsbergDiorite ~100 m inboard of the irregular diorite-wallrock contact. The sheeted vein structure appears to be parallel to major district NW-SE faults and extends at least from the 2550- to 2700-m elevations, with all limits poorly constrained by current drilling information. Modeling of the drill intercepts of the sheeted veins indicates that the structure is planar. Composite images of photographed core from these drill holes were analyzed and suggest an average quartz vein width of ~1 cm, but many individual veins record multiple opening events. Cu sulfide mineralization is irregularly distributed through the sheeted vein zone and overprints the main stage of quartz vein formation.

Thin sections of individual quartz veins were made for petrographic study and to analyze selvage alteration. Individual SEM-CL images were stitched into composite maps that reveal zonation textures that record changes in P-T-X conditions and crystal growth rates. The eight textures identified in more than one image were used to construct a paragenetic sequence of EESS quartz-sulfide vein architecture as it varies by elevation and host lithology. The CL textures observed are consistent with other Cu-Au porphyry systems, including the nearby Grasberg intrusive system. The sheeted vein zone may record a major early hydrothermal fluid pathway, but appears to have limited significance towards focusing later Cu-Au mineralization.

Keywords: Ertsberg, Paragenesis, Sheeted Veins

SHP
U

Exploring Better Methods for Deriving Qv and How It Relates to Surface Conduction

Danny Anderson
Anderson, D., The University of Texas at Austin, Austin, TX
Robinson, J., Rutgers University Newark, Newark, NJ
Ntarlagiannis, D., Rutgers University Newark, Newark, NJ
Falzone, S., Rutgers University Newark, Newark, NJ
Slater, L., Rutgers University Newark, Newark, NJ
Keating, K., Rutgers University Newark, Newark, NJ
Seleznev, N., Schlumberger-Doll Research Center Cambridge

Improving understanding of the relationship between the cation exchange capacity (CEC), normalized surface area to pore volume (S_{por}) and imaginary conductivity may improve estimates of surface conduction. S_{por}, a physical property, has been shown in several studies to be linearly correlated with imaginary conductivity. CEC has long been recognized as an important parameter controlling surface conductivity, but is difficult to measure relative to other laboratory techniques, such as specific surface area. Measuring cation exchange capacity per unit pore volume (Q_v), a value closely related to CEC, has historically been challenging, requiring destruction of samples, time-consuming tests, and inaccurate results, as sample pulverization can break bonds and affect readings. A membrane potential method, measured with self potential, proposed in the 1970s and successfully implemented in this experiment offers a substantial improvement on Qv estimates. Subcores remain intact, tests are shorter, and results are repeatable. Using the data collected from these methods, we analyze whether the CEC is a better indicator of surface conduction (quantified from imaginary conductivity) versus S_{por} in these formations. This study was done on eighteen different sandstone subcores cut from four separate boreholes from two lithological formations. S_{por} data were acquired using the nitrogen BET gas adsorption method. Self potential measurements were acquired using nonpolarizing Ag-AgCl electrodes. Within these samples, correlations between both S_{por} and CEC to imaginary conductivity fall within one order of magnitude. However, CEC is more strongly correlated with imaginary conductivity, indicating that CEC is better related to imaginary conductivity than S_{por}.

Keywords: cation exchange capacity, surface conduction, imaginary conductivity, Qv, near surface geophysics

SHP
U

Investigating the Relationship of Late Pleistocene Terrace Formation and Channel Dynamics within the Texas Gulf Coastal Plain

Thaddeus Ellis
Ellis, T., Jackson School of Geosciences, The University of Texas at Austin, Austin, TX
Hassenruck-Gudipati, H., Jackson School of Geosciences, The University of Texas at Austin, Austin, TX
Mohrig, D., Jackson School of Geosciences, The University of Texas at Austin, Austin, TX
Goudge, T., Jackson School of Geosciences, The University of Texas at Austin, Austin, TX

Terrace formation along coastal rivers is often assumed to be a direct result of punctuated sea-level fall. However, it has been experimentally shown that terraces commonly form under conditions of constant base level fall. In addition, it has been demonstrated that migrating channels in a bedrock system with steady state rock uplift can produce similar looking terraces. The lower Trinity River, in East Texas, is an ideal location to study allogenic (punctuated external forcing) versus autogenic terrace-building mechanisms using lidar measurements and OSL depositional age constraints (Gavin, 2005). To understand paleochannel influence on terrace construction, we measured channel characteristics for 27 preserved segments of paleochannels that are late Pleistocene in age and associated with 27 of 34 measured terraces along about 90 km of the modern river. There is no clear clustering of terrace elevation that might be tied to distinct sea level change events. Rather, the range of mean terrace elevations is indicative of a more constant system transformation. Based on lidar measurements, all paleochannels are larger than the modern channel, suggesting a wetter climate or larger watershed. Channel width measurements are used to quantify these changes in paleoflow discharge. Paleochannel width, radius of curvature and terrace slope measurements are used to characterize the movement of an incising channel. Based upon OSL terrace dates (Gavin, 2005), known global climate variations can be compared to discharge estimates and investigated as a predictor of terrace formation. If terrace formation occurred during distinct intervals of sea level fall, terraces with similar calculated paleoflow discharges are expected to plot along specific downstream elevation profiles. Assuming avulsion-driven terrace formation occurs at locations of higher channel sinuosity, the sinuosity of paleochannels on terraces is compared to the sinuosity of the modern river. Higher paleo-sinuosity would indicate preferential terrace formation at avulsion prone channel bends. Many factors may contribute to terrace formation during sea level fall and as such, we seek correlations between paleochannel morphology and terrace characteristics to distinguish between different terrace forming mechanisms.

Keywords: Terraces, Paleochannels, Paleoclimate, Forming Mechanisms

SHP
U

Caves, Carbonates and Climate: Karst Landscape Development through Environmental Forcing, Little Cayman Island

Scarlette Hsia
Hsia, S., The University of Texas at Austin
Ouellette, G., Louisiana State University
Manfrino, C., Central Caribbean Marine Institute

The Cayman Islands are situated in the west-central Caribbean Sea, between Cuba and the Yucatan Peninsula. Little Cayman Island (LCI) is relatively underdeveloped and understudied in comparison to its sister islands, Grand Cayman and Cayman Brac, and hosts less than 200 permanent residents over a 30 square kilometer area. However, like its sister islands, LCI is a small carbonate platform derived from reef building during the Oligocene, Miocene, and Quaternary. The shared geologic history of the Cayman Islands along with minimal human disturbance makes LCI an ideal site to study an island karst landscape. Conduction of field surveys and stratigraphic comparisons between primary lithologic formations and compilation of a geospatial inventory of karst features and lithology of LCI using GIS revealed novel insights into landscape evolution on LCI. In addition to surface karst surveys, several caves on the island were mapped. Cave morphologies suggest that evolution of LCI karst features have been driven by both hydroclimate, as well as salt and freshwater mixing, modulated by sea level fluctuations. These findings are mirrored in the lithology of partially dolomitized Miocene carbonates, which contain paleo-karst fill features and reveal hydroclimate influence, as well as enhanced resistance to dissolution in the present day, ostensibly from submersion in Mg-rich sea waters prior to the Quaternary. These findings shed light on the complex relationship of climate, geology, and karst landscape development on this particular carbonate island. This information is critical in anticipating structural and hydrogeological integrity on LCI under future climate change scenarios and serves as an example of the interplay linking climate and geologic processes to karst landscape development on small carbonate islands.

Keywords: Caribbean, Cayman Islands, Karst, Caves

SHP
U

Thermal and hydraulic properties of active-layer soils in the McMurdo Dry Valleys, Antarctica

Logan Schmidt
Schmidt, L., Department of geophysics
Levy, J., University of Texas institute of geophysics

Spatial variability in the hydraulic, physical, and thermal properties of active layer soils may reflect the fluvial and climatic history of cold-desert regions. In this study we measured the constant-head saturated hydraulic conductivity and grain-size-distribution of sixty-five soil samples taken from Taylor Valley, as well as the thermal diffusivity of twelve soil samples taken from met stations throughout the McMurdo Dry Valleys, Antarctica.
Both the hydraulic conductivity and grain size distribution of soils are spatially organized within Taylor valley. Soils collected down-valley near McMurdo Sound have a higher percentage of fine-sized sediments (silt, clay) and lower hydraulic conductivities than soils collected up-valley near Taylor Glacier. Soils collected mid-valley have intermediate amounts of fines and conductivity values consistent with a hydrogeologic gradient spanning the valley. Soil hydraulic conductivity is strongly dependent on the presence of fines, with lower conductivities associated with soils containing a higher percentage of fines. The spatial organization of these soil properties within the valley suggests an active fluvial history in which glacier-fed channels, perhaps aided by water tracks, have flushed fine sediments down into lake basins. Three samples taken from neighboring Garwood Valley by contrast have very low conductivities, perhaps reflecting the less active fluvial history in that region that has left till un-eroded resulting in a soil column clogged with fines throughout the valley.
Thermal diffusivity curves were created by measuring the thermal conductivity and heat capacity of soils collected from near Long Term Ecological Research project met stations. Soil thermal properties were measured over a range of water contents to provide a basis for interpreting the thermal history of Dry Valley soils and their stability under changing temperature and precipitation conditions. Three qualitative soil groups emerged from this analysis: soils with low diffusivities at all water contents, soils that slowly increase in diffusivity with increasing water content, and soils that exhibit high thermal diffusivity at low water contents. The first two groups are spatially correlated with ground ice, while the latter group is associated with thermokarst features.

Keywords: Surface geology, hydrology, soil physics, cryisphere, permafrost, thermokarst

SHP
U

Understanding variations in grain size distributions in Wax Lake Delta, Louisiana

Zehao Xue
Xue, Z., Jackson School of Geosciences, The University of Texas at Austin, Austin, TX
Mohrig, D., Jackson School of Geosciences, The University of Texas at Austin, Austin, TX

Wax Lake Delta is a modern delta system formed by deposition of sediments transported from the Atchafalaya River through the Wax Lake outlet artificial channel. Since its creation, the Wax Lake delta has been studied extensively for delta formation. Cores taken from previous research displayed variations in grain size distributions consisting of clean, well sorted sand deposits and mud-rich, poorly sorted sand deposits. As sorting of sandstones has a strong control on their porosity and permeability, understanding the deposition and erosion mechanisms is crucial. Preliminary analysis of core x-ray images and core sample grain sizes suggest clean sands depositing in the distal regions of mouth bars. Current hypothesis suggests wave reworking as a significant cause to the disparity. 8 additional cores and additional samples were taken in October 2016 along the distributary channel, Gadwall Pass, to test this hypothesis. Grain size analysis of the new and existing samples are expected to further understanding of the deposition mechanism of sands and muds in Wax Lake Delta.

Keywords: wax lake delta, sedimentology, deposition pattern